

S.S.ALTINTAŞ

ATTENUATION RELATIONSHIP FOR PEAK GROUND VELOCITY
BASED ON STRONG GROUND MOTION DATA
RECORDED IN TURKEY

SÜLEYMAN SERKAN ALTINTAŞ

METU
2006

DECEMBER 2006

ATTENUATION RELATIONSHIP FOR PEAK GROUND VELOCITY
BASED ON STRONG GROUND MOTION DATA
RECORDED IN TURKEY

A THESIS SUBMITTED TO
THE GRADUATE SCHOOL OF NATURAL AND APPLIED SCIENCES
OF
MIDDLE EAST TECHNICAL UNIVERSITY

BY

SÜLEYMAN SERKAN ALTINTAŞ

IN PARTIAL FULFILLMENT OF THE REQUIREMENTS
FOR
THE DEGREE OF MASTER OF SCIENCE
IN
CIVIL ENGINEERING

DECEMBER 2006

Approval of the Graduate School of Natural and Applied Sciences

Prof. Dr. Canan Özgen
Director

I certify that this thesis satisfies all the requirements as a thesis for the degree of Master of Science

Prof.Dr. Güney Özcebe
Head of Department

This is to certify that we have read this thesis and that in our opinion it is fully adequate, in scope and quality, as a thesis for the degree of Master of Science

Prof.Dr. Polat Gülkan
Supervisor

Examining Committee Members

Prof. Dr. Haluk Sucuoğlu (METU,CE) _____

Prof. Dr. Polat Gülkan (METU,CE) _____

Assoc. Prof. Dr. Ahmet Yakut (METU,CE) _____

Assoc. Prof. Dr. Sinan Akkar (METU,CE) _____

Assoc. Prof. Dr. Zülfü Aşık (METU,ES) _____

I hereby declare that all information in this document has been obtained and presented in accordance with academic rules and ethical conduct. I also declare that, as required by these rules and conduct, I have fully cited and referenced all material and results that are not original to this work.

Name, Last name: Süleyman Serkan Altıntaş

Signature :

ABSTRACT

ATTENUATION RELATIONSHIP FOR PEAK GROUND VELOCITY BASED ON STRONG GROUND MOTION DATA RECORDED IN TURKEY

ALTINTAŞ, Süleyman Serkan
M.S., Department of Civil Engineering
Supervisor: Prof. Dr. Polat GÜLKAN

December 2006, 104 pages

Estimation of the ground motion parameters is extremely important for engineers to make the structures safer and more economical, so it is one of the main issues of Earthquake Engineering. Peak values of the ground motions obtained either from existing records or with the help of attenuation relationships, have been used as a useful parameter to estimate the effect of an earthquake on a specific location.

Peak Ground Velocities (PGV) of a ground motion is used extensively in the recent years as a measure of intensity and as the primary source of energy-related analysis of structures. Consequently, PGV values are used to construct emergency response systems like Shake Maps or to determine the deformation demands of structures.

Despite the importance of the earthquakes for Turkey, there is a lack of suitable attenuation relationships for velocity developed specifically for the country. The aim of this study is to address this deficiency by developing an attenuation relationship for the Peak Ground Velocities of the chosen database based on the strong ground motion records of Turkey. A database is processed with the established techniques and corrected database for the chosen ground motions is formed. Five different forms of equations that were used in the previous studies are

selected to be used as models and by using nonlinear regression analysis, best fitted mathematical relation for attenuation is obtained.

The result of this study can be used as an effective tool for seismic hazard assessment studies for Turkey. Besides, being a by-product of this study, a corrected database of strong ground motion recordings of Turkey may prove to be a valuable source for the future researchers.

Keywords: Attenuation Relationship, Peak Ground Velocity, Data Processing, Nonlinear Regression Analysis, Seismic Hazard

ÖZ

AZAMI ZEMİN HIZLARI İÇİN TÜRKİYE KUVVETLİ YER HAREKETLERİ KAYITLARINDAN AZALIM İLİŞKİSİ BULUNMASI

ALTINTAŞ, Süleyman Serkan
Yüksek Lisans, İnşaat Mühendisliği Bölümü
Tez Yöneticisi : Prof. Dr. Polat GÜLKAN

Aralık 2006, 104 sayfa

Deprem Mühendisliği'nin temel unsurlarından biri olarak yer hareketi parametrelerinin tayini daha güvenli ve ekonomik yapıların yapılabilmesi açısından son derece önemlidir. Mevcut kayıtlardan yahut azalım ilişkilerinden elde edilen yer hareketlerinin azami değerleri, bir depremin belirli bir noktadaki etkisini tahmin etmek amacı için faydalı bir değişken olarak kullanılagelmiştir.

Yer hareketlerinin Azami Zemin Hızları (AZH), şiddet ölçümlerinde ve yapıların enerji yöntemleri ile analizlerinde yoğun olarak kullanılmaya başlanmıştır. Dolayısıyla, AZH değerleri, Sarsıntı Haritaları gibi acil durum sistemlerinin oluşturulmasında yahut yapıların deformasyon gerekliliklerinin tespitinde kullanılmaktadır.

Türkiye için depremlerin önemine rağmen, özellikle ülke için geliştirilmiş uygun hız azalım ilişkileri eksikliği mevcuttur. Bu çalışmanın amacı, Azami Zemin Hızları için Türkiye kuvvetli yer hareketi kayıtlarından seçilmiş bir veritabanı ile azalım ilişkisi geliştirerek bu noksanlığı azaltmaktır. Bunu yapabilmek için, veritabanı tespit edilen yöntemler ile işlenmiş ve seçilmiş yer hareketleri için düzeltilmiş veritabanı oluşturulmuştur. Daha önce yapılmış olan çalışmalarda

kullanılan beş farklı denklem model olarak kullanılarak doğrusal olmayan regresyon analizi ile azalımı tanımlayan en uygun matematiksel bağıntı oluşturulmuştur.

Bu çalışmanın sonuçları Türkiye’de deprem tehlikesinin tespiti çalışmalarında etkili bir araç olarak kullanılabilir. Bunun yanında, bu çalışmanın bir yan ürünü olarak Türkiye yer hareketi kayıtları için işlenmiş veritabanının sonraki araştırmacılara değerli bir kaynak olabileceği düşünülmektedir.

Anahtar Kelimeler: Azalım İlişkisi, Azami Zemin Hızları, Veri İşleme, Doğrusal Olmayan Regresyon Analizi, Deprem Tehlikesi

To My Parents and Nur

ACKNOWLEDGMENTS

The author wishes to express his deepest gratitude to his supervisor Prof. Dr. Polat Gülkan for his guidance, careful supervision, criticisms, patience and insight throughout the research.

The author would also like to thank Professor Sinan Akkar for allowing the use of his software and for his congenial assistance.

The author would like to express his sincere appreciations to Prokon Eng. and especially to Mr. Serdar Sarman for their tolerance and permissions throughout the study.

The author finally thanks to Ms. Nur Alkış, his family and friends for their support and encouragements.

TABLE OF CONTENTS

PLAGIARISM	iii
ABSTRACT	iv
ÖZ	vi
ACKNOWLEDGEMENTS	ix
TABLE OF CONTENTS	x

CHAPTER

1. INTRODUCTION	1
1.1. GENERAL.....	1
1.2. USE OF PEAK GROUND VELOCITY IN EQ ENGINEERING.....	2
1.3. STRONG GROUND MOTION NETWORK IN TURKEY.....	3
1.4. PREVIOUS STUDIES ON PGV.....	7
1.5. OBJECT AND SCOPE.....	11
1.6. ORGANIZATION AND CONTENTS.....	11
2. THE STRONG MOTION DATABASE AND ITS FEATURES	12
2.1. GENERAL.....	12
2.2. MOMENT MAGNITUDE	17
2.3. SOURCE-TO-SITE DISTANCE.....	18

2.4. LOCAL SITE CONDITIONS.....	23
2.5. FAULT MECHANISM.....	25
3. DATA PROCESSING.....	29
3.1. GENERAL.....	29
3.2. ANALOG INSTRUMENTS.....	30
3.3. DIGITAL INSTRUMENTS.....	34
3.4. NOISE CHARACTERISTICS AND ADJUSTMENT PROCEDURES.....	36
3.4.1. BASELINE PROBLEMS	37
3.4.2. LOW-FREQUENCY NOISE	40
3.4.3. HIGH-FREQUENCY NOISE AND TRANSDUCER ERRORS.....	46
3.5. DATA PROCESSING METHODOLOGY.....	48
3.6. PEAK GROUND VELOCITY.....	56
4. DERIVATION OF GROUND MOTION PREDICTION EXPRESSION.....	59
4.1. GENERAL.....	59
4.2. MODEL ADEQUACY CHECK	60
4.3. ESTIMATION OF VARIANCE.....	61
4.4. DEVELOPING ATTENUATION RELATIONSHIP.....	62
4.4.1. CONSTITUTION OF THE METHODOLOGY.....	62
4.4.2. MODIFYING PROPOSED RELATIONSHIPS	66
4.4.3. FINALIZING THE ATTENUATION RELATIONSHIP.....	70

4.5. COMPARISON WITH OTHER GROUND MOTION PREDICTION EXPRESSIONS.....	75
4.7. A-POSTERIORI CHECK OF THE PROPOSED EQUATION.....	81
5. CONCLUSIONS AND RECOMMENDATIONS.....	82
REFERENCES.....	84
APPENDIX A – DATABASE OF STRONG GROUND MOTION RECORDS IN TURKEY.....	95
APPENDIX B – FILTER CHOICES AND PGV PROPERTIES OF THE CHOSEN DATABASE.....	99
APPENDIX C – COEFFICIENTS FOR THE STUDIED PREDICTION EQUATIONS AND COMPARISON OF MODEL ADEQUACY AND UNBIASED ESTIMATOR.....	103
APPENDIX D – EARTHQUAKE AND STATION INFORMATIONS, FILTER CHOICES AND PGV PROPERTIES OF 24/10/2006 GEMLİK EARTHQUAKE.....	104

LIST OF TABLES

Table 1.1 Characteristics of prediction equation for peak ground velocity	9
Table 2.1 Earthquakes used in the analysis.....	15
Table 2.2 Defined r_{cl} values for different databases and selected r_{cl} values in km for 1999 Kocaeli and Düzce Earthquakes.....	22
Table 4.1 Functional forms of relationships considered.....	63
Table 4.2 Regression coefficients and standard deviation for the prediction equation derived in this study	75
Table A.1 Database of strong motion records in Turkey (August 1976 – July 2003)	95
Table B.1 Filter choices and PGV properties of chosen database.....	99
Table C.1 Coefficient for the studied prediction equations and comparison of model adequacy and unbiased estimator.....	103
Table D.1 Earthquake information for the Gemlik earthquake.....	104
Table D.2 Station information for the Gemlik earthquake.....	104
Table D.3 Filter choices and PGV properties of the Gemlik earthquake.....	104

LIST OF FIGURES

Figure 1.1	ERD array of strong motion accelerographs.....	4
Figure 1.2	KOERI array of strong motion accelerographs.....	5
Figure 1.3	Dynamic range comparison of selected strong motion accelerographs.....	6
Figure 1.4	Natural frequency, f_n , and useable bandwidth of commonly used strong motion accelerographs between 1930 and 2000.....	7
Figure 2.1	Major earthquakes that occurred in Turkey from 1976 to 2003...	14
Figure 2.2	Relationship between various magnitude scales.....	19
Figure 2.3	Relationship between distance measures used in the development of the ground motion relations.....	20
Figure 2.4	Distribution of recordings in terms of magnitude and distance...	21
Figure 2.5	Pie-chart distribution of local site geology for selected database.	25
Figure 2.6	Records in terms of magnitude, distance and local site geology.	27
Figure 2.7	Distribution of records in the database in terms of magnitude, distance and faulting mechanism.....	28
Figure 3.1	Schematic diagrams of analog instruments and photograph of SMA-1 accelerograph.....	31
Figure 3.2	Measured and true acceleration values for an analog accelerograph.	32
Figure 3.3	Uncorrected acceleration time series of İzmit Meteoroloji İstasyonu N-S component record of the 12.11.1999 Düzce earthquake.....	33
Figure 3.4	Uncorrected acceleration, velocity and displacement time series of Göynük Devlet Hastanesi E-W component record of the 17.08.1999 Kocaeli earthquake.....	34

Figure 3.5	Uncorrected acceleration, velocity and displacement time series of Yarımca Petkim Tesisleri E-W component record of the 12.11.1999 Düzce earthquake.....	35
Figure 3.6	Uncorrected acceleration time series of Sakarya Bayındırlık ve İskan Müdürlüğü N-S component record of the 11.11.1999 Sapanca-Adapazarı earthquake.....	36
Figure 3.7	Uncorrected acceleration, velocity and displacement time series of Yarımca Petkim Tesisleri N-S component record of the 17.08.1999 Kocaeli earthquake.....	38
Figure 3.8	Acceleration, velocity and displacement time series of Yarımca Petkim Tesisleri N-S component record of the 17.08.1999 Kocaeli earthquake after velocity fit from 30 to 135 s.....	38
Figure 3.9	Acceleration Fourier spectrum of the Yarımca Petkim Tesisleri N-S component record of the 17.08.1999 Kocaeli earthquake before (left) and after (right) baseline correction.....	39
Figure 3.10	Schematic representations of baseline adjustment schemes.....	39
Figure 3.11	Differences in the result obtained for accelerations, velocity and displacements time series for acausal and causal filtering for different filtering periods.....	42
Figure 3.12	Fall offs for Butterworth type filter for both frequency (left) and time (right) domains.....	42
Figure 3.13	Acceleration FAS of the Malazgirt Meteoroloji İst. N-S (left) and E-W (right) components records of the 03.11.1997 Malazgirt earthquake.....	44
Figure 3.14	Use of f^2 decay model for analog (left) and digital instruments (right).....	45
Figure 3.15	High frequency noise in Fourier acceleration spectra in analog and digital accelerograms.....	47
Figure 3.16	Data processing procedure applied for this study.....	50

Figure 3.17	Velocity and displacement time-series of Heybeliada Sanatoryumu N-S component record of the 17.08.1999 Kocaeli earthquake after filtering for both baseline corrected and non-corrected data.....	52
Figure 3.18	Corrected acceleration, velocity and displacement time series of Göynük Devlet Hastanesi E-W component record of the 17.08.1999 Kocaeli earthquake.....	53
Figure 3.19	Corrected and uncorrected FAS of Göynük Devlet Hastanesi E-W component record of the 17.08.1999 Kocaeli earthquake.....	53
Figure 3.20	Corrected acceleration, velocity and displacement time series of Yarımca Petkim Tesisleri E-W component record of the 12.11.1999 Düzce earthquake.....	54
Figure 3.21	Corrected and uncorrected FAS of Yarımca Petkim Tesisleri E-W component record of the 12.11.1999 Düzce earthquake.....	54
Figure 3.22	Theoretical and selected low-cut filter frequencies.....	55
Figure 3.23	Low-cut filter frequency choices for stations for 1999 Kocaeli EQ among different researchers.....	57
Figure 3.24	Velocity and displacement time series of Göynük Devlet Hastanesi E-W component record of the 17.08.1999 Kocaeli earthquake for different low-cut filter frequencies.....	58
Figure 4.1	Predictive curves for 5 candidate equations for rock site conditions for $M_w= 7.5, 6.5$ and 5.5	65
Figure 4.2	Residuals for the used database with respect to the mean of proposed relationships.....	67
Figure 4.3	Predictive curves for five different forms of attenuation relationship for rock site conditions for $M_w= 7.5, 6.5$ and 5.5	69
Figure 4.4	Ground motion prediction curves for five different expression forms obtained from the reduced database for rock site conditions for $M_w= 7.5, 6.5$ and 5.5	72
Figure 4.5	Ground motion prediction curves for five different expression forms obtained from the reduced database for stiff soil site conditions for $M_w= 7.5, 6.5$ and 5.5	73

Figure 4.6	Ground motion prediction curves for five different expression forms obtained from the reduced database for soil site conditions for $M_w = 7.5, 6.5$ and 5.5	74
Figure 4.7	Residuals of logarithm of PGV as a function of closest distance and moment magnitude.....	76
Figure 4.8	Comparison of PGV_{max} predictions of the new equation with other expressions for rock site conditions for $M_w = 7.5, 6.5$ and 5.5	78
Figure 4.9	Comparison of PGV_{max} predictions from the new equation with other expressions for stiff soil site conditions for $M_w = 7.5, 6.5$ and 5.5	79
Figure 4.10	Comparison of PGV_{max} predictions from the new equation with other expressions for soil site conditions for $M_w = 7.5, 6.5$ and 5.5	80
Figure 4.11	Comparison of PGV_{max} predictions of the proposed attenuation relationship with observed PGV values of the 24/10/2006 Gemlik earthquake.....	81

LIST OF SYMBOLS

PGA	:Peak ground acceleration
PGV	:Peak ground velocity
PGD	:Peak ground displacement
A	:Area of rupture surface
A_{\max}	:Largest amplitude that can be recorded by the accelerograph
A_{\min}	:Smallest amplitude that can be recorded by the accelerograph
CSS	:Corrected sum of squares
D	:Average displacement across the fault zone
d_i	:Depth of i^{th} soil layer
f_c	:Low-cut filter frequency
f_o	:Estimated filter frequency according to single-corner frequency spectrum of acceleration model
f_a, f_b	:Estimated filter frequency according to double-corner frequency spectrum of acceleration model
h_{hypo}	:Focal depth of earthquake
M_w	:Moment magnitude
M_s	:Surface wave magnitude
M_L	:Local magnitude
M_{JMA}	:Japanese Meteorological Society magnitude scale
M_o	:Seismic moment
m_B	:Body wave magnitude
$N(f)$:Fourier transform of the noise
n	:Filter order
R^2	:Coefficient of determination
$R_{\text{sn}}(f)$:Normalized signal to noise ratio

RSS	:Residual sum of squares
r_{cl}	:Closest distance
r_{jb}	:Closest distance or Joyner-Boore distance
r_{epi}	:Epicentral distance
r_{hypo}	:Hypocentral distance
r_{rup}	:Closest distance to the fault rupture plane
r_{seis}	:Closest distance to the seismogenic part of the fault rupture plane
$S(f)$:Fourier transform of the signal
SF	:Scale factor for the noise Fourier spectrum
T_{zpad}	:Total length of the zero pads added
t_s	:Time length of the record
t_n	:Time length of the pre-event portion of the record
V_{s30}	:Average shear wave velocity of the top 30 m of the deposit
V_{si}	:Shear-wave velocity of the i^{th} soil layer
μ	:Shear modulus
σ^2	:Unbiased Estimator for Error
Δt	:Sampling interval

CHAPTER 1

INTRODUCTION

1.1. GENERAL

Earthquakes are among great phenomena of the nature. Today, we know that the source of the earthquakes is not based on mythological explanations, but there are still many questions to answer. Apart from the arguments on whether the destructiveness of earthquakes originate from quality of human made structures, scientists and engineers should be able to interpret rationally the effects of earthquakes for safer facilities in the future.

As an empirical approach to quantify interior mechanisms of the earth's crust during an earthquake, attenuation relationships are developed by the engineers. Attenuation relationships, that are now more correctly called the ground motion prediction expressions, have been used excessively to model earthquake effects for many years as a practical way of estimating seismic motion on a specific location. Generally used with peak values of ground motion, attenuation relationships have served as the primary damage predictor of earthquakes in engineering practice.

Turkey is an earthquake prone country. Nevertheless, there is a lack of suitable attenuation relationships developed uniquely for the country because of the grossly inadequate number of strong ground motion recording instruments deployed. Specifically, attenuation relationship for Peak Ground Velocity (PGV) derived from earthquake records of Turkey is a missing item that should be studied. The aim of this study is to address this deficiency.

1.2. USE OF PEAK GROUND VELOCITY IN EARTHQUAKE ENGINEERING

Traditionally, the most commonly used parameter of ground motion in earthquake engineering is the peak ground acceleration (PGA). Ease of defining inertial forces in terms of ground acceleration is the main reason behind this fact. Use of response spectrum methodology in earthquake engineering makes PGA the primary objective to determine for analysis and design of structures against earthquake effects.

Although there are various possible uses of peak ground velocity in earthquake engineering, prediction of PGV is a relatively new item to be studied. Listed below are some applications that use PGV in earthquake engineering (Bommer and Alarcon, 2006):

i. PGV can be used to predict the damage potential of an earthquake. There are various research results that correlate PGV with intensity of the earthquake (Trifunac and Brady, 1975; Wald *et al.*, 2003; Wu *et al.*, 1999). Rapid response system tools, e.g. Shake Maps, are based on PGV values obtained from accelerograms. Influence of PGV on inelastic demand of SDOF systems and effects of PGV on vulnerability of structures to damage are also studied (Akkar and Özen, 2005; Zhu *et al.*, 1987, 1988; Sucuoğlu, *et al.*, 1998).

ii. Damage in buried pipelines correlated well with PGV in many empirical studies. Peak horizontal strain in the soil due to the passage of seismic waves is proportional to the PGV (Bommer and Alarcon, 2006); therefore, a relationship can be defined between the damage and PGV.

iii. Liquefaction potential is also correlated with PGV in some researches. It has been found that capacity of ground shaking triggering liquefaction can be defined in terms of PGV for saturated cohesionless soils (Trifunac, 1995; Kostadinov and Towhata, 2002; Orense, 2005).

iv. Although the periods of most structures are within the limits of acceleration-sensitive part of the response spectrum, structures with relatively long natural periods should be defined in velocity-sensitive part of the spectrum. Therefore, scaling of response spectra in terms of PGV for velocity-sensitive branches should be evaluated. Colombian and Canadian Seismic Codes use PGV as a scaling factor for intermediate period sections of the response spectrum (IAEE, 1996; Basham *et al.*, 1985).

v. An increasing number of studies demonstrate the important role that PGV plays in building fragility estimates where seismic intensity is measured in terms of PGV since maximum inelastic displacements are better correlated with PGV than peak ground acceleration PGA (Akkar *et al.*, 2005).

1.3. STRONG GROUND MOTION NETWORK IN TURKEY

The main source of information for this study is the raw acceleration records database of Turkey for selected earthquakes. These records are obtained from special instruments operated uniquely for the purpose of recording strong ground motions and they are called accelerographs. During an earthquake, accelerographs record ground acceleration for two horizontal orthogonal directions according to their emplacement, N-S and E-W traditionally, and in the vertical direction.

The greater part of the strong ground motion network of Turkey is operated by Earthquake Research Department of General Directorate of Disaster Affairs (ERD) and Kandilli Observatory and Earthquake Research Institute (KOERI). Instruments deployed by ERD cover the entire seismic geography of the country whereas those that have been procured by KOERI are supposed to serve as sensors for an early warning system in Istanbul. There are also other institutions that have local instrument arrays located for special purposes (Akkar and Gülkan, 2002). İstanbul Technical University (ITU) has an array with limited number of instruments set up in İstanbul, whose records are also used within this study. For more specific purposes, monumental structures like Hagia Sophia Museum or Süleymaniye Mosque are equipped with strong motion accelerographs in order to observe their

structural behavior and to determine their possible weaknesses against earthquakes. General Directorate of State Highways (KGM) established accelerographs on the suspension bridges crossing Bosphorus for the purpose of health monitoring. The Scientific and Technical Research Establishment of Turkey (TÜBİTAK) supports research programs that have enabled the setting up of small local networks. Despite these efforts, number of instruments is far being sufficient for Turkey. Altogether, there are around 300 strong ground motion stations in the country. Among 300 strong ground motion stations all over the country, 156 of them belong to ERD and 117 to KOERI. These instruments are mostly located near active earthquake zones of Turkey like North Anatolian Fault. Although digital instruments are taking place of analog ones, there are still a number of analog instruments mostly belonging to ERD. SMA-1 is the only type of analog instrument still operated. SM2, GSR16, GSR18, ETNA and GURALP are some of the digital based instrument types. Strong motion instrument array of ERD and KOERI are shown in Figure 1.1 and Figure 1.2 respectively.



Figure 1.1 ERD array of strong motion accelerographs (○ Analog Ins., △ Digital Ins.) (from internet site of Turkey National Strong Motion Program).

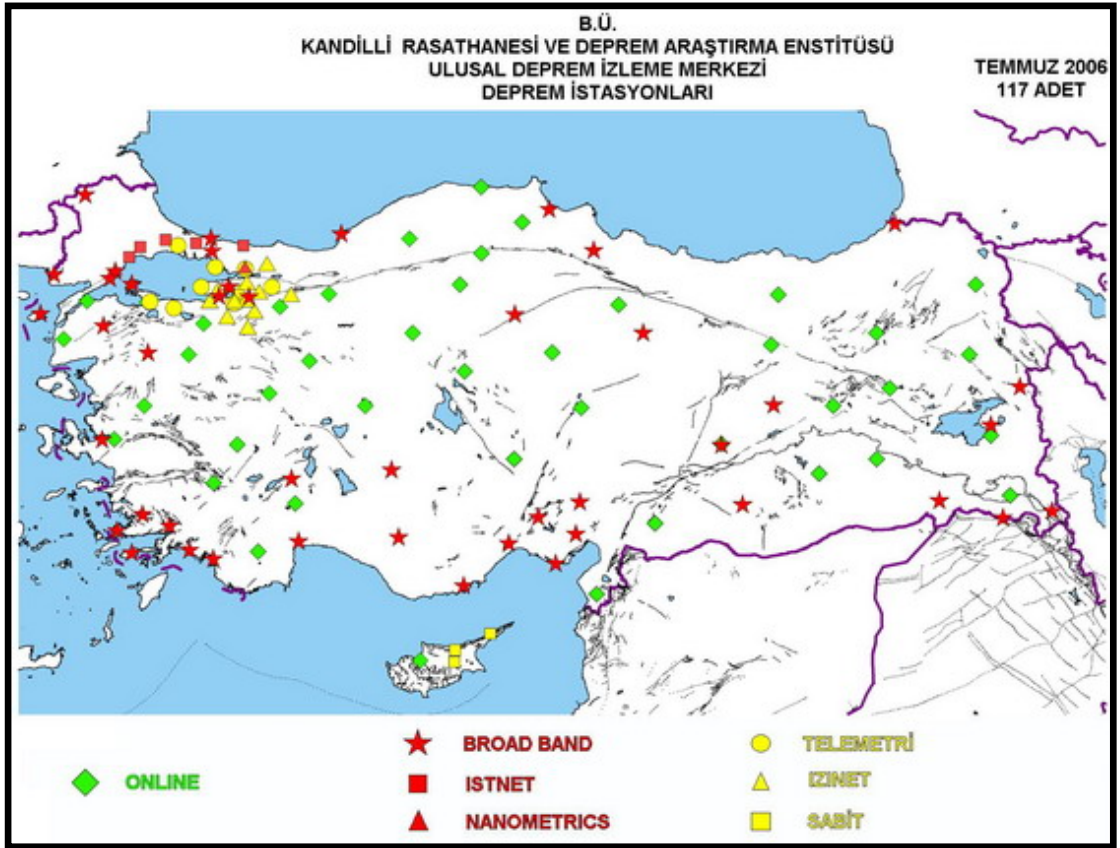


Figure 1.2 KOERI array of strong motion accelerographs (from internet site of KOERI).

To make a comparison, at the end of 1980, there were about 1700 accelerographs in the United States and by January of 1982 there were over 1400 instruments in Japan (Trifunac and Todorovska, 2001). In 2005 Greece, a country with 1/7 the area of Turkey, the number of sensors deployed was 500.

There are various types of accelerographs that have been used for recording purposes. The main differentiation among them is their recording medium. Analog instruments, developed in United States in 1930's, were optical-mechanical devices. These instruments produced traces of the ground acceleration against time on film or paper (Trifunac and Todorovska, 2001). Digital instruments, which record on reusable media were started to be used approximately 50 years after the analog ones.

Main advantages of digital instruments over analog ones can be summarized as follows:

i. Digital instruments record continuously, so they have adjustable-duration pre-event memory which is an important aspect of data processing. In contrast, analog instruments are triggered by a specific threshold of acceleration so that they do not have pre-event recordings.

ii. The second important difference is about their dynamic characteristics. Dynamic range, which is related to the amplitude range that can be recorded is about 40-55 dB for analog instruments, whereas modern digital recorders have a range of 135 dB (Trifunac and Todorovska, 2001). Also natural frequencies of transducers that limit the useable frequency range of recorded motion are much higher for digital accelerographs than their analog counterparts. (See Figures 1.3 and 1.4 for a comparison between dynamic characteristics of instrument types).

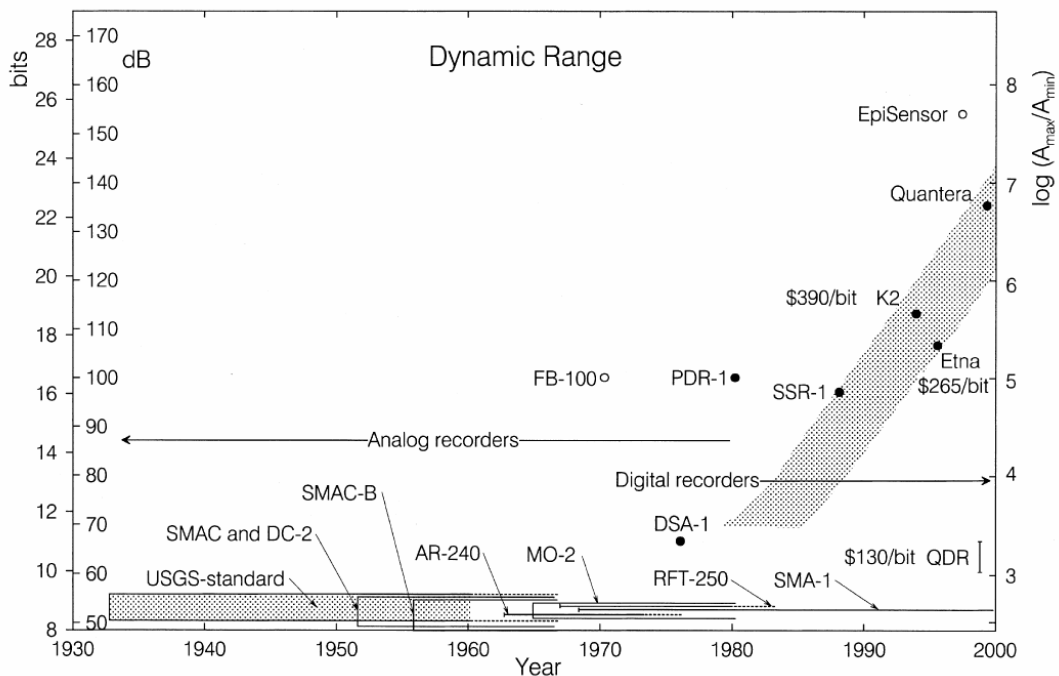


Figure 1.3 Dynamic range comparison of selected strong motion accelerographs (Trifunac and Todorovska, 2001).

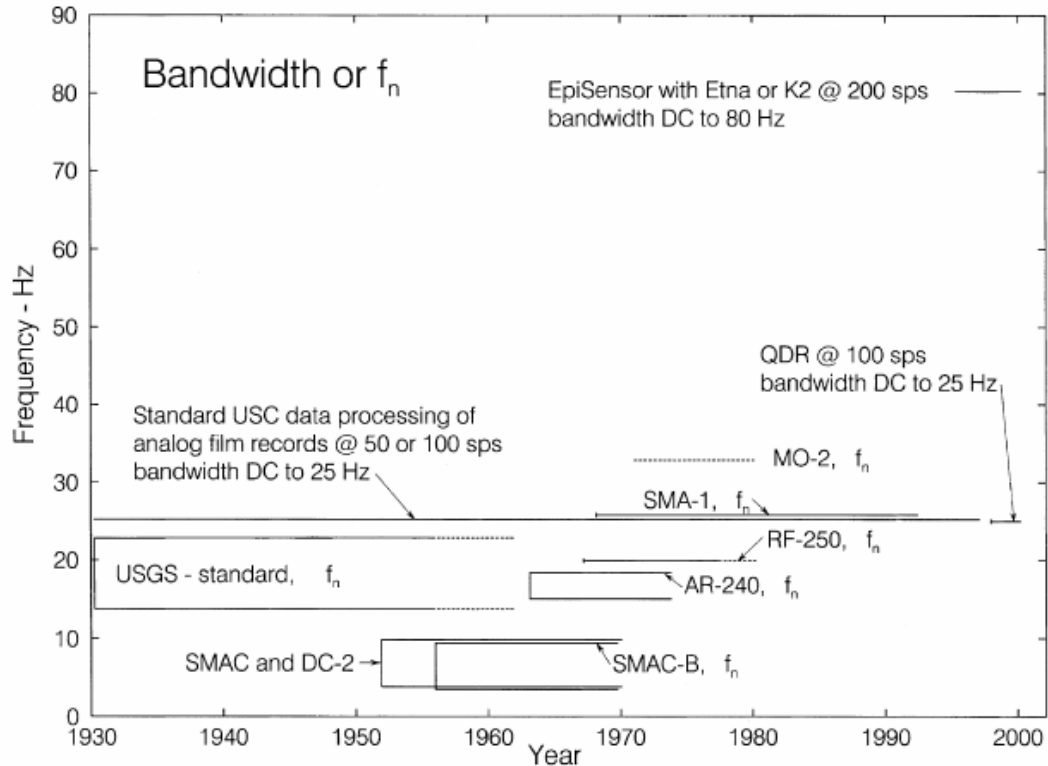


Figure 1.4 Natural frequency, f_n , and useable bandwidth of commonly used strong motion accelerographs between 1930 and 2000 (Trifunac and Todorovska, 2001).

iii. Digital instruments perform analog-to-digital conversion within the instrument. Since analog recordings must be digitized by an operator, human originated error is stored within the record which is the primary source of noise that must be eliminated during data processing (Boore and Bommer, 2005). This introduces an error into the derived velocity values that is difficult to quantify.

1.4. PREVIOUS STUDIES ON PGV

There are about 30 prediction relationships developed for PGV. They have been developed from worldwide records, from records of specific regions like Europe or from country wide records. In Table 1.1, a list of these attenuation relationships categorized according to the geographical region, number of records and earthquakes used in the analysis, use of horizontal component of each record, magnitude range and type, distance range and type and site classes used is given. The

first conspicuous property of the tabulated equations is the differences in defining magnitude, use of component and distance terms. Although the range differences in magnitude or distance or even number of site class differences do not violate comparison purposes to some extent, it is not easy to state an opinion to the results obtained for different investigations if distance, magnitude or choice of horizontal components are different. It is possible to use empirical equations to adjust different magnitude scales, different definitions of the horizontal component or even the different terminologies used for distance definition; but their standard deviations are so high that unreliable results may be obtained.

In the regional base, a number of investigations can be made for the equations given. For western North America, there are a few new equations for PGV although there are many more for PGA and for response spectral ordinates (Bommer and Alarcon, 2006). Despite the fact that the western part of North America is tectonically more active than Eastern region, Eastern region seems to be equally studied. Among the dated studies, Joyner and Boore (1981) and Campbell (1997) are noticeable ones within the given set. Joyner and Boore (1981) used r_{jb} and M_w in defining their equations. Campbell (1997) has a complex form including distance definition, r_{seis} , which is not easy to identify for most of the recordings of Turkish database. Besides, distance range for Campbell (1997) is limited to 50 km. Note that, neither Sadigh and Egan (1998) nor Gregor et al. (2002) are published in the scientific journals (Bommer and Alarcon, 2006).

For the worldwide records, Bray and Rodriguez-Marek (2004) studied near-fault effects by limiting their equation to within 20 km. Pankow and Pechmann (2004) used the database of Spudich *et al.* (1999) for extensional tectonic regions. Japanese researchers have derived a number of equations for both crustal earthquakes and subduction zone earthquakes with focal depth down to about 120 km (Bommer and Alarcon, 2006). Although older expressions have used magnitude term as Japanese Agency Magnitude, M_{JMA} , moment magnitude seems to be used commonly for the newer expressions. Note that all Japanese researchers use r_{rup} , except Kawashima et al. (1986).

Table 1.1 Characteristics of prediction equation for peak ground velocity (Bommer and Alarcon, 2006; Akkar and Bommer, 2006b)

Study	Region	N_R , N_E	C	M_{min} , M_{max}	M	R_{min} , R_{max}	R	SC
Trifunac & Brady (1976)	Western USA	187, 57	B	3.0, 7.7	M_L	20, 200	R_{epi}	3
McGuire (1978)	Western USA	70, >30	B	5.0, 7.7	M_L	11, 210	R_{hyp}	2
Joyner & Boore (1981)	Western North America	62, 10	L	5.0, 7.7	M_W	1, 109	R_{jb}	2
Kawashima et al. (1986)	Japan	197, 90	M	5.0, 7.9	M_{JMA}	< 500	R_{epi}	3
Gaul (1988)	S.W. of western Australia	>21, 16	U	2.0, 6.3	M_L	< 200	R_{epi}	2
Kamiyama et al. (1992)	Japan	197, 90	B	4.1, 7.9	M_{JMA}	3, 413	R_{hyp}	S
Theodulidis & Papazachos (1992)	Primarily Greece	61, 40	U	4.5, 7.5	M_S	< 35	R_{epi}	2
Atkinson & Boore (1995) *	Eastern North America	U, 22	R	4.0, 7.0	M_W	10, 400	R_{hyp}	2
Molas & Yamazaki (1995)	Japan	2166, 387	L	4.1, 7.8	M_{JMA}	< 1000	R_{hyp}	S
Sabetta & Pugliese (1996)	Italy	95, 17	L	4.6, 6.8	M_S , M_L	< 100	R_{epi} , R_{jb}	3
Atkinson & Boore (1997) *	Primarily West Canada	>1000, >68	R	3.7, 6.7	M_W	10, 400	R_{hyp}	2
Campbell (1997)	Worldwide Primarily California	226, 30	G	4.7, 8.1	M_W	3, 50	R_{seis}	3
Rinaldis et al. (1998)	Italy and Greece	310, U	U	4.5, 7.0	M_S , M_W	7, 138	R_{epi}	2
Sadigh & Egan (1998)	Primarily California	960, 51	G	3.8, 7.4	M_W	0, 100	R_{hyp}	2
Si & Midorikawa (2000)	Japan	394, 21	L	5.8, 8.3	M_W	< 300	R_{hyp} , R_{hyp}	1
Gregor et al. (2002)	Worldwide Primarily California	993, 143	U	4.4, 7.6	M_W	0.1, 267	R_{hyp}	2
Margaris et al. (2002)	Greece	474, 142	B	4.5, 7.0	M_W	1, 150	R_{epi}	3
Shabestari & Yamazaki (2002)	Taiwan	95, 1	A	7.6	M_W	U	R_{seis}	2
Tromans & Bommer (2002)	Europe	249, 51	L	5.5, 7.9	M_S	1, 359	R_{jb}	3
Sigh et al. (2003) *	India	U, 5	U	5.7, 7.6	M_W	23, 2437	U	1
Skarlatoudis et al. (2003)	Aegean Area Primarily Greece	619, 225	B	4.5, 7.0	M_W	1, 160	R_{epi}	3
Bray & Rodriguez-Marek (2004)	Worldwide	54, 13	F	6.1, 7.6	M_W	< 20	R_{hyp}	2
Hao & Gaul (2004) *	S.W. of western Australia	10, 5	U	4.1, 6.2	M_L	6, 96	R_{hyp}	1
Midorikawa & Ohtake (2004)	Japan	1980, 33	L	5.5, 8.3	M_W	< 300	R_{hyp}	2
Pankow & Pechmann (2004)	Worldwide	124, 39	G	5.0, 7.7	M_W	0, 100	R_{jb}	2
Dost et al. (2004)	The Netherlands	66, U	G	U, 3.9	M_L	2.3, 20	R_{epi}	1
Frisenda et al. (2005)	Northwestern Italy	>14000, U	U	0.03, 5.1	M_L	0, 200	R_{hyp}	2
Bragato & Slejko (2005)	Eastern Alps	1402, 240	V	2.5, 6.3	M_L	0, 130	R_{epi} , R_{jb}	1
Atkinson & Boore (2006) *	Eastern North America	38400, U	G	3.5, 8.0	M_W	1, 1000	R_{hyp}	S
Boore & Atkinson (2006)	Western North America	N/A	G	N/A	M_W	N/A	R_{jb}	S
Akkar & Bommer (2006)	Europe and Middle East	532, 133	L, G	5.0, 7.6	M_W	< 100	R_{jb}	3

Notes: Stochastic model, N_R : Number of records; N_E : Number of earthquakes U- unknown. C: Use of horizontal component of ecan record: A- arunnetic mean; B - don components; F- fault-normal component; G- geometric mean; L - largest component; M - maximum vector value; R - random component. M: Magnitude scale used: M_{JMA} - Japanese Meteorological Agency Magnitude; M_L - local magnitude; M_S - surface wave magnitude; M_W - moment magnitude. R: Source-to-site distance definition: R_{epi} - epicentral distance; R_{hyp} - hypocentral distance; R_{jb} - closest horizontal distance to the fault rupture projection on the surface; R_{seis} - closest distance to the presumed zone of seismic rupture on the fault; R_{rup} - closest distance to rupture surface. SC: Number of site classification used: S - individual classification for each recording station based on V_{s30} values.

PGV is extensively studied also in Europe. Ten of the 30 equations presented are from European database. They are primarily developed from the records of Italy, Greece and Turkey, which are tectonically active regions of Europe and Middle East. Excluding equations of Dost *et al.* (2004), Frisenda *et al.* (2005) and Bragato and Slejko (2005) which have small magnitude ranges limiting their usage in terms of earthquake-engineering (Akkar and Bommer, 2006b) and Theodulidis and Papazachos (1992) and Rinaldis *et al.* (1998) because their usage of horizontal component are not defined; Sabetta and Pugliese (1996), Margaris *et al.* (2002), Tromans and Bommer (2002), Skarlatoudis *et al.* (2003) and Akkar and Bommer (2006a) are prediction equations that should be evaluated. Sabetta and Pugliese (1996) does not include style of faulting as a predictive parameter although earthquakes in central and southern Italy are predominantly reverse events (Akkar and Bommer, 2006a). Tromans and Bommer (2002) have been updated by Akkar and Bommer (2006a) because of its limitations such as severe filters used in the analysis and availability of new records coming from both new recordings and change in lower limit of earthquake magnitude (Akkar and Bommer, 2006a). Note that, both Margaris *et al.* (2002) and Skarlatoudis *et al.* (2003) used epicentral distance terms which are poor measures of distance for earthquakes with large rupture areas (Bozorgnia and Campbell, 2004), which is also mentioned in Chapter 2 describing source-to-site distance terms.

There are also relationships serving special purposes. Shabestari and Yamazaki (2002) only include records from 1999 Chi-Chi earthquake and separated hanging wall and footwall region recordings (Bommer and Alarcon, 2006). Singh *et al.* (2003), Gaull (1988) and its subsequent study Hao and Gaull (2004) used records from stable continental regions such as India and Australia.

Another common approach to estimate PGV is dividing the pseudo spectral velocity (PSV) at 1.0 s by 1.65 (Bommer and Alarcon, 2006). Pankow and Pechmann (2002) pointed out that approach was gaining popularity due to lack of recent PGV predictive relations. In a recent study by Bommer and Alarcon (2006), this approach is defined as a part of earthquake engineering ‘folklore’ with no scientific basis.

1.4. OBJECT AND SCOPE

The object of this study is to provide a comprehensive methodology and supporting commentary for the derivation of attenuation relationship for peak ground velocity for Turkey based on strong ground motion records of Turkey. The same database is used for the scope as had been used in deriving prediction equations for peak ground acceleration and spectral acceleration ordinates (Kalkan and Gülkan, 2004). The aim of this study is to construct site geology, magnitude and distance dependent attenuation relationship for possible use in design and research objectives in Turkey. This study is intended to serve as a reference for the design of structures and seismic hazard studies.

1.5. ORGANIZATION AND CONTENTS

There are five chapters in this thesis. Chapter 1 is the introductory part where the basics of the study are introduced. Chapter 2 provides detailed information on the strong motion database and its contents. Chapter 3 defines data processing techniques and their applications to the database used in this study. Chapter 4 presents derivation of attenuation relationship for the processed database and discusses the results obtained. Finally, Chapter 5 contains conclusions and a discussion of the findings.

CHAPTER 2

THE STRONG MOTION DATABASE AND ITS FEATURES

2.1. GENERAL

Being a characteristics of all statistical studies, selected database defines the output, so the outcome of the work. Since aim of this study is to construct attenuation relationship for Peak Ground Velocity for Turkey, selected strong ground motion records are chosen from earthquakes that have occurred in Turkey. Another goal of this study is to be a continuation and complementation of the studies done by Kalkan and Gülkan for attenuation of PGA and Site-Dependent Spectra for earthquake records of Turkey (Kalkan, 2001; Gülkan and Kalkan, 2002; Kalkan and Gülkan, 2004). Therefore, selected strong ground motion records within the Turkey database by Kalkan and Gülkan (2004) are used for this work also.

Selected database consists of 223 horizontal components from 112 strong motion records from 57 earthquakes that occurred between 1976 and 2003 in Turkey. First and last entries of the database are 19.08.1976 Denizli and 26.07.2003 Buldan-Denizli earthquakes. Seismic activity of Turkey within this period for $M_w > 5.0$ is shown in Figure 2.1. Epicenter distance range for the records varies from 1 km to 300 km with the moment magnitude range of 4.0 to 7.4. All of the earthquakes occurred in the shallow crustal tectonic zones of Turkey. List of the events, corresponding faulting type, seismic moment and moment magnitudes of earthquakes with epicentral coordinates together with the number of recordings for each event classified according to the site conditions are given in Table 2.1.

For the purpose of studying attenuation relationship of PGV, several properties of recording stations and related earthquakes must be known. That the more complex the final prediction relationship is, more information should be identified for the stations, is a general rule for these studies. With the knowledge

gained over time, it generally becomes possible to enhance the information for each recording station. As mentioned earlier, the same database used by Kalkan and Gülkan (2004) is used as a starting point for database knowledge but information sources are broadened with time, so a more comprehensive dataset became possible.

Three information sources deserve to be mentioned here. First among them is the dissemination of European strong motion data (Ambraseys *et al.*, 2002). Supported by the European Commissions, this catalog provides an interactive, fully relational database and databank with more than 3,000 uniformly processed and formatted European strong-motion records and associated earthquake, station and waveform parameters. It is possible to search the database and databank interactively and download selected strong motion records and associated parameters. Originally published in CD-ROM format, it is possible to update the database by use of Internet (Imperial College of London Department of Civil and Environmental Engineering Internet Site for European Strong Motion Database). Turkish data covers much of the database especially for strong earthquakes. As will be discussed in the following chapters, raw data processing is also achieved in the database which makes the catalog more valuable and a better tool for comparison purposes. The second important source is the PEER Strong Motion Database (Pacific Earthquake Engineering Research Center Internet Database). A new database, called the Next Generation Attenuation expression or NGA, is available on the Internet. This has also very valuable information for Turkey ground motion records and stations. The third source is the catalog derived by National Strong Motion Project (NSMP) team¹. NSMP is comprehensive project aims to arrange and improve the seismic network and strong motion database of Turkey. Financed by TÜBİTAK, the project is being carried out under the supervision of researchers from METU.

By using above mentioned sources, earthquake and station information are updated. Moment magnitudes of 36 earthquakes out of 57 are changed in the process. Number of recordings with known V_{s30} value is increased from 22 to 48. Local site conditions of 21 recordings have been renewed. With the new information set

¹ Remark: There may be further revisions in the data because the project is still ongoing.

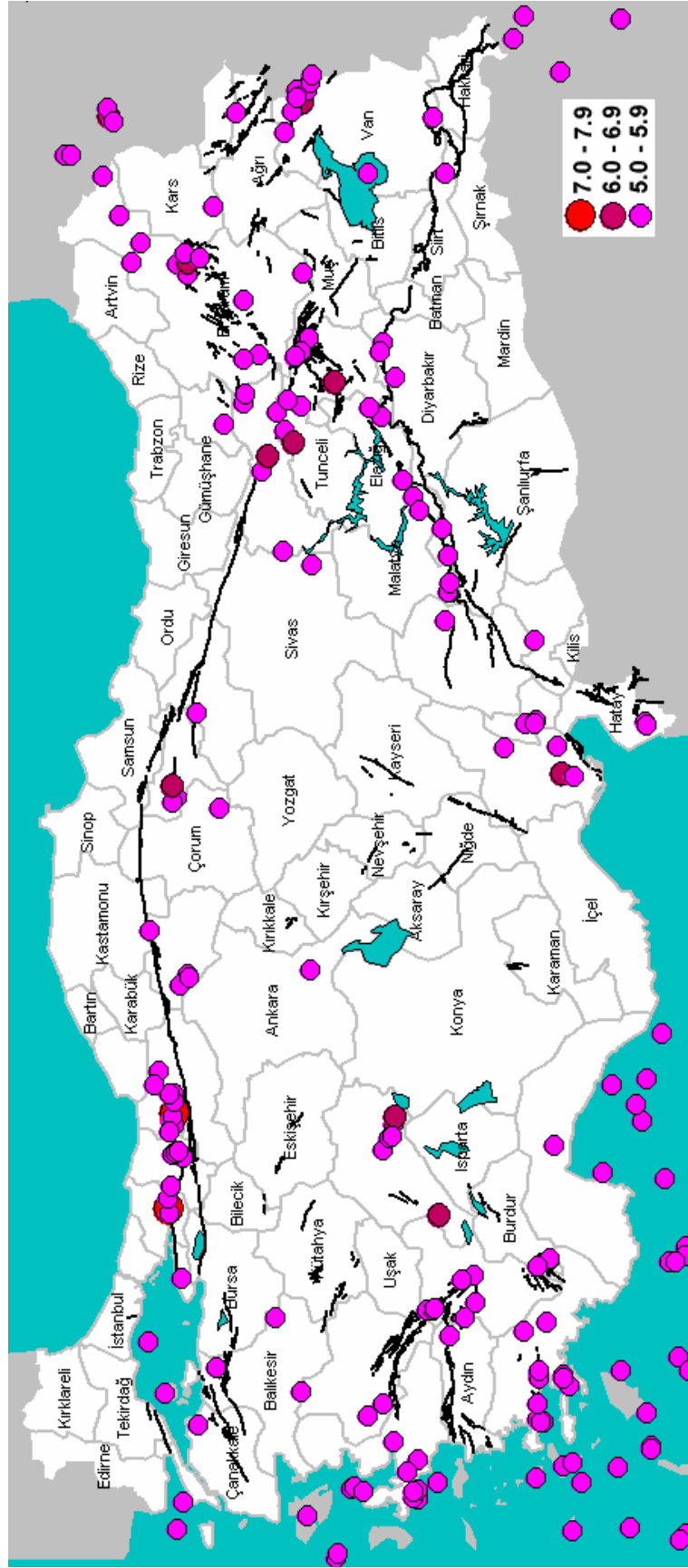


Figure 2.1 Major earthquakes that occurred in Turkey from 1976 to 2003 (<http://sayisalgrafik.com.tr/deprem/>).

Table 2.1 Earthquakes used in the analysis.

Event No	Date (dd.mm.yy)	Event	Earthquake Location*	Faulting Type	Seismic M ₀ (dyne.cm)	M _w **	Depth** (km)	Epicenter Coordinates		Number of Recordings	
								Rock	Stiff Soil	Soil	
1	19.08.1976	DENİZLİ	Merkez - DENİZLİ	Normal	1.48E+25 ^{*13}	6.1	3.0	37.7100 N - 29.0000 E			1
2	05.10.1977	ÇERKEŞ	Bornova - İZMİR	Strike-Slip	6.09E+24 ^{*2}	5.8	16.1	41.0200 N - 33.5700 E			1
3	16.12.1977	İZMİR	İlgaz - CANKIRI	Normal	6E+24 ^{*13}	5.6	34.0	38.4100 N - 27.1900 E			1
4	11.04.1979	MURADIYE	Caldiran - VAN	Strike-Slip	N/A	4.9	34.0	39.1200 N - 43.9100 E			1
5	28.05.1979	BUCAK	ANTALYA GULF	Normal	9.48E+24 ^{*2}	5.9	98.0	36.4600 N - 31.7200 E			1
6	18.07.1979	DURSUNBEY	Dursunbey - BALIKESİR	Strike-Slip	1.15E+24 ^{*2}	5.3	5.0	39.6600 N - 28.6500 E			1
7	30.06.1981	HATAY	Samandagi - HATAY	Strike-Slip	N/A	4.7	33.0	36.1700 N - 35.8900 E			1
8	05.07.1983	BIĞA	Biga - CANAKKALE	Reverse	1.64E+25 ^{*2}	6.1	7.0	40.3300 N - 27.2100 E			2
9	30.10.1983	HORASAN	Senkaya - ERZURUM	Strike-Slip	8.70E+25 ^{*2}	6.6	12.0	40.3500 N - 42.1800 E			2
10	29.03.1984	BALIKESİR	Merkez - BALIKESİR	Strike-Slip	N/A	4.5	12.0	39.6400 N - 27.8700 E			1
11	17.06.1984	FOÇA	AEGEAN SEA	Normal	6.24E+23 ^{*2}	5.1	15.0	38.8700 N - 25.6800 E			1
12	12.08.1985	KIĞI	Kelkit - GUMUSHANE	Strike-Slip	N/A	4.9	20.0	39.9500 N - 39.7700 E			1
13	06.12.1985	KÖYCEĞİZ	Koycegiz - MUĞLA	Strike-Slip	N/A	4.6	8.0	36.9700 N - 28.8500 E			1
14	05.05.1986	MALATYA	Dogansehir - MALATYA	Strike-Slip	1.42E+25 ^{*2}	6.0	15.0	38.0200 N - 37.7900 E			1
15	06.06.1986	SÜRGÜ	Dogansehir - MALATYA	Strike-Slip	6.39E+24 ^{*2}	5.8	11.0	38.0100 N - 37.9100 E			1
16	20.04.1988	MURADIYE	Caldiran - VAN	Strike-Slip	2.12E+24 ^{*2}	5.5	15.0	39.1100 N - 44.1200 E			1
17	12.02.1991	İSTANBUL	MARMARA SEA	Strike-Slip	N/A	4.8	10.0	40.8000 N - 28.8200 E			1
18	13.03.1992	ERZİNCAN	Uzumlu - ERZİNCAN	Strike-Slip	1.16E+26 ^{*2}	6.6	10.0	39.7200 N - 39.6300 E			1
19	06.11.1992	SİVRİHİSAR	Menderes - İZMİR	Normal	1.41E+25 ^{*2}	6.0	17.0	38.1600 N - 26.9900 E			1
20	03.01.1994	İSLAHIYE	Ceyhan - ADANA	Strike-Slip	N/A	5.0	26.0	37.0000 N - 35.8400 E			1
21	24.05.1994	GİRİT	AEGEAN SEA	Normal	2.33E+24 ^{*1}	5.5	17.0	38.6600 N - 26.5400 E			1
22	13.11.1994	KÖYCEĞİZ	Koycegiz - MUĞLA	Strike-Slip	1.33E24 ^{*2}	5.4	15.0	36.9700 N - 28.8090 E			1
23	29.01.1995	TERCAN	Ilica - ERZURUM	Strike-Slip	7.65E22 ^{*2}	5.2	31.0	39.9008 N - 40.9900 E			1
24	26.02.1995	VAN	Merkez - VAN	Strike-Slip	N/A	4.7	33.0	38.6000 N - 43.3300 E			1
25	01.10.1995	DİNAR	Dinar - AFYON	Normal	4.72E+25 ^{*2}	6.4	15.0	38.1100 N - 30.0500 E			1
26	02.04.1996	KUŞADASI	AEGEAN SEA	Normal	1.57E+24 ^{*2}	5.4	15.0	37.7800 N - 26.6400 E			1
27	14.08.1996	MERZİFON	Gumus.koy - AMASYA	Strike-Slip	3.54E+24 ^{*2}	5.6	15.0	40.7900 N - 35.2300 E			1
28	21.01.1997	BULDAN	Esme - DENİZLİ	Normal	7.83E+23 ^{*2}	5.2	18.0	38.1200 N - 28.9200 E			1
29	22.01.1997	HATAY	Merkez - HATAY	Strike-Slip	4.32E+24 ^{*2}	5.7	15.0	36.1400 N - 36.1200 E			2
30	28.02.1997	MERZİFON	Merkez - CORUM	Strike-Slip	8.50E23 ^{*8}	5.2	10.0	40.6800 N - 35.3000 E			1

Table 2.1 Continued

Event No	Event Date (dd.mm.yy)	Event	Earthquake Location*	Faulting Type	Seismic M.* M ₀ (dyne.cm)	M _w **	Depth** (km)	Epicenter Coordinates	Number of Recordings		
									Rock	Stiff Soil	Soil
31	03.11.1997	MALAZGIRT	Ahlat - BITLIS	Strike-Slip	N/A	4.9	33.0	38.7600 N - 42.4000 E			1
32	04.04.1998	DINAR	Dinar - AFYON	Normal	8.58E23*2	5.2	15.0	38.1400 N - 30.0400 E		1	1
33	27.06.1998	CEYHAN	Yuregir - ADANA	Strike-Slip	2.96E+25*2	6.2	29.5	36.8500 N - 35.5500 E	1	3	2
34	09.07.1998	BORNOVA	AEGEAN SEA	Normal	N/A	4.6	20.0	38.0800 N - 26.6800 E			1
35	17.08.1999	KOCAELI	Merkez - KOCAELI	Strike-Slip	2.88E+27*2	7.4	18.0	40.7000 N - 29.9100 E	8	9	9
36	11.11.1999	SAPANCA	Merkez - KOCAELI	Strike-Slip	3.56E+24*2	5.6	8.9	40.8100 N - 30.2000 E		1	
37	12.11.1999	DÜZCE	Merkez - DÜZCE	Strike-Slip	6.65E+26*2	7.2	25.0	40.7400 N - 31.2100 E	4	3	5
38	06.06.2000	ORTA	Cerkes - CANKIRI	Strike-Slip	1.11E25*2	6.0	10.0	40.7200 N - 32.8700 E			1
39	23.08.2000	AKYAZI	Akyazi - SAKARYA	Strike-Slip	8.6E23*8	5.2	15.3	40.6800 N - 30.7100 E		1	3
40	04.10.2000	DENIZLI	Merkez - DENIZLI	Normal	3.5E23*8	5.0	8.4	37.9100 N - 29.0400 E		1	
41	15.11.2000	TATVAN	Tatvan-VAN	Strike-Slip	2.3E24*8	5.5	10.0	36.9300 N - 44.5100 E			1
42	10.07.2001	PASINLER	Pasinler - ERZURUM	Strike-Slip	1.52E+24*2	5.4	5.0	39.8273 N - 41.6200 E			1
43	26.08.2001	DÜZCE	Yigilca - DÜZCE	Strike-Slip	4.2E23*8	5.0	7.8	40.9455 N - 31.5728 E			1
44	02.12.2001	VAN	Merkez - VAN	Strike-Slip	1.63E23*8	4.8	5.0	38.6170 N - 43.2940 E			1
45	03.02.2002	SULTANDAĞI	Sultandagi - AFYON	Reverse	7.4E25*8	6.5	5.0	38.5733 N - 31.2715 E			2
46	03.04.2002	BURDUR	Basmakci - ISPARTA	Strike-Slip	N/A	4.2	5.0	37.8128 N - 30.2572 E		1	
47	14.12.2002	ANDIRIN	Sumbas - OSMANIYE	Strike-Slip	1.9E23*8	4.8	13.6	37.4720 N - 36.2210 E		1	
48	10.03.2003	AKYAZI	Akyazi - SAKARYA	N/A	N/A	4.0	14.7	40.7283 N - 30.5900 E			1
49	10.04.2003	URLA	Seferihisar - IZMIR	N/A	4.34E24*2	5.7	15.8	38.2568 N - 26.8345 E			1
50	01.05.2003	BİNGÖL	Merkez - BİNGÖL	Strike-Slip	3.85E25*2	6.3	6.0	38.9400 N - 40.5100 E			1
51	21.05.2003	DÜZCE	Cumayeri - DÜZCE	N/A	4.58E23*7	4.4	7.7	40.8700 N - 30.9800 E			1
52	09.06.2003	BANDIRMA	Bandirma - BALIKESİR	N/A	1.55E23*7	4.8	14.7	40.2000 N - 27.9700 E		1	
53	06.07.2003	SAROS	Bandirma - BALIKESİR	N/A	1.55E23*7	4.8	9.1	40.4200 N - 26.2100 E			1
54	23.07.2003	BUL.-DENİZLİ-1	Buldan - DENİZLİ	N/A	1.18E24*2	5.3	5.0	38.1718 N - 28.8533 E		1	
55	26.07.2003	BUL.-DENİZLİ-2	Buldan - DENİZLİ	N/A	2.23E23*7	4.9	5.0	38.1100 N - 28.8800 E			1
56	26.07.2003	BUL.-DENİZLİ-3	Buldan - DENİZLİ	N/A	1.63E24*2	5.4	4.3	38.1100 N - 28.8900 E		1	
57	26.07.2003	BUL.-DENİZLİ-4	Buldan - DENİZLİ	N/A	2.44E23*7	4.9	8.5	38.1200 N - 28.8400 E			1
Total									21	37	54

* Data are obtained from NSMP database

** Data are updated according to the NSMP database

provided, the database of strong motion records used in this study is given in Table A.1 in Appendix A.

Since definitions of expressions that are used for defining the earthquake and station parameters are of primary importance, the rest of Chapter 2 is devoted to the definitions and concepts that are used within the context of this thesis study.

2.2. MOMENT MAGNITUDE

Although there had been ways to identify the intensity of an earthquake objectively, instrumental measure of earthquake size became possible by the relationship defined by C. Richter in 1930's. Known by his name, Richter magnitude of a local earthquake, M_L , was the logarithm to the base ten of the maximum seismic wave amplitude in microns recorded on a Wood-Anderson seismograph located at a standard distance of 100 km from the earthquake epicenter.

Today, there are a number of magnitude scale definitions based on different formulas for epicenter distance and ways of choosing and measuring appropriate wave amplitude. According to the definitions adopted by Bolt (2004), Surface Wave Magnitude (M_s) is based on measuring the amplitude of surface waves with a period of 20 s. Distant earthquake (epicentral distances more than 1000 km) records are predominantly filled with surface waves with periods of 20 s. Body Wave Magnitude (m_b) measures the amplitude of the P-wave, which is not affected by the focal depth of the source, whereas deep focus earthquakes have no trains of surface waves. Moment Magnitude (M_w) scale was defined to be able to constitute a relationship between the magnitude of the earthquake with its seismic moment (M_o), which is a direct mechanical measure of size of the earthquake source:

$$M_w = \frac{\log M_o}{1.5} - 10.7 \quad (2.1)$$

where M_o is in dyn-cm. Keeping in mind the relationship to define the seismic moment:

$$M_o = \mu AD \quad (2.2)$$

where μ is the shear modulus, D is the average displacement across the fault zone and A is the area of the surface that ruptured, M_w is directly related to the energy that is spread from the fault rupture to produce the earthquake.

Moment magnitude scale is used in this study since others are empirical quantities based on various instrumental measurement of ground shaking characteristics, which results in a phenomenon called *saturation* for these scales. Saturation is the insensitivity of the scale for relatively strong earthquakes. Saturation of various magnitude scales with respect to the moment magnitude scale is shown in Figure 2.2. Local magnitude (M_L) and body wave magnitude (m_b) saturate about $M_L=7$, whereas surface wave magnitude saturates at about $M_S=8.0$. The m_B scale is similar to m_b but calculated at slightly longer periods. M_{JMA} is the magnitude scale of the Japanese Meteorological Society, which is calculated from the ground-motion amplitudes measured from medium period seismographs. The M_w is the only extant magnitude scale that does not suffer from saturation for strong earthquakes.

As mentioned earlier, moment magnitude data given by Kalkan and Gülkan (2004) is updated according to the NSMP database. Magnitudes are restricted to about $M_w > 4.0$ to emphasize those ground motions having greatest engineering interest and to limit the analysis to the more reliable recorded events.

2.3. SOURCE-TO-SITE DISTANCE

Source-to-site distance is used to characterize the diminution of ground motion in terms of both geometric and anelastic attenuation, as it propagates away from the earthquake source (Bozorgnia and Campbell, 2004).

Depending on the treatment of the source of an earthquake, distance measures can be grouped into two broad classes. If source of an earthquake is treated as a point, epicentral, r_{epi} , and hypocentral distance, r_{hypo} , definitions are used. Hypocenter

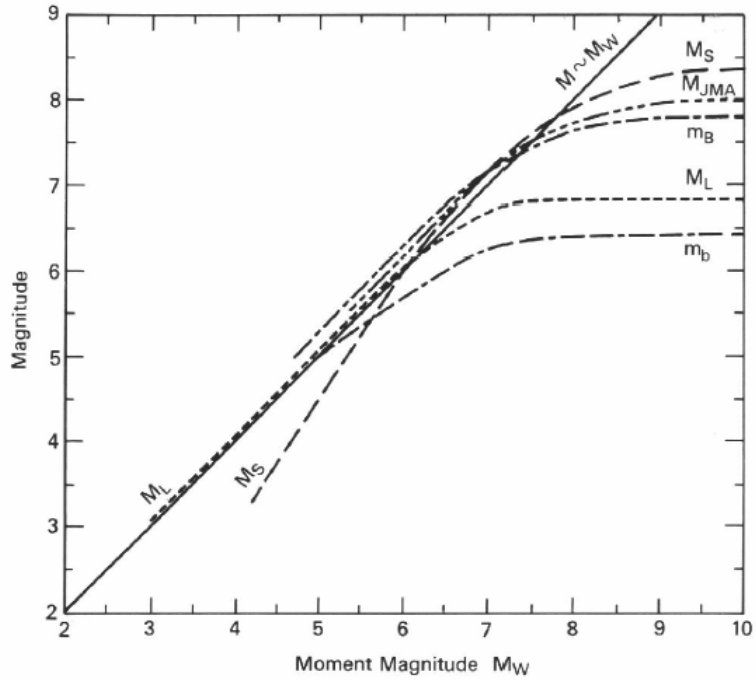


Figure 2.2 Relationship between various magnitude scales (Kramer, 1996).

is the point in the earth crust where the rupture begins and epicenter is the surface projection of that point. Relation between them can be defined as (Bozorgnia and Campbell, 2004):

$$r_{hypo} = \sqrt{r_{epi}^2 + h_{hypo}^2} \quad (2.3)$$

where h_{hypo} is the focal (hypocentral) depth of the earthquake. Generally speaking, r_{epi} and r_{hypo} , are poor measures of distance for earthquakes with large rupture areas (i.e., large magnitudes). Therefore, they are used to define distance terms for small earthquakes where it is more likely to define the earthquake source as a point source. It has been shown that ground motion relations that use point-source measures should not be used to estimate ground motions close to large earthquakes unless some approximate adjustment is made to account for finite-faulting effects (Bozorgnia and Campbell, 2004).

The three finite-source distance measures used in the ground motion relations must be defined. The first one is the Joyner-Boore distance or closest distance, r_{jb} or r_{cl} . Defined by Joyner and Boore (1981), r_{jb} is the closest horizontal distance to the vertical projection of the fault rupture plane. The second is the closest distance to the fault rupture plane, r_{rup} . The third one is defined by Campbell (1997) as the shortest distance between the recording station and the presumed zone of seismogenic rupture on the fault, r_{seis} . With the assumption that the fault rupture within the softer sediments and within the upper 2 to 4 km of the fault zone is primarily non-seismogenic, this shallow part will not contribute to the recordings within the periods of engineering interest. The descriptive figure of these definitions can be shown in Figure 2.3. Although r_{cl} is reasonably easy to estimate for a future (e.g., design) earthquake, r_{rup} and r_{seis} are not so easily determined, particularly when the earthquake is not expected to rupture the entire seismogenic width of the crust (Bozorgnia and Campbell, 2004).

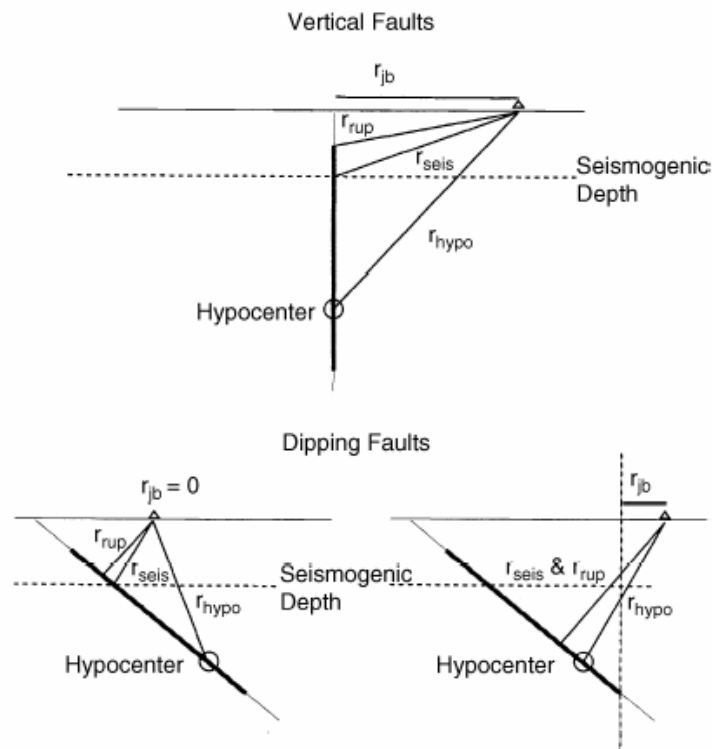


Figure 2.3 Relationship between distance measures used in the development of the ground motion relations (Bozorgnia and Campbell, 2004).

In this study, the distance term is defined as the closest distance between the recording station and a point on the horizontal projection of the rupture zone on earth's surface. Since abbreviation r_{cl} , and term "closest distance" is used instead of abbreviation r_{jb} and term "Joyner-Boore distance" for the studies made by Kalkan and Gülkan, the same definitions are used in this study also. There are two basic interdependent reasons for selecting closest distance term for the analysis made. The first reason is the choice of form of relationship selected. Most of the attenuation relationships selected to be used as the basis of study and comparison purposes use the r_{cl} definition. Secondly, r_{cl} values can be obtained easily when compared to r_{seis} or r_{rup} . However, for some of the smaller events, rupture surfaces have not been defined clearly therefore epicentral distances are used instead. Since smaller events may be interpreted as point source, it is believed that there would not be significant error (Kalkan, 2001). Closest distance values for each recording station are given in Table A.1 and closest distance vs. moment magnitude graph for the used database is shown in Figure 2.4.

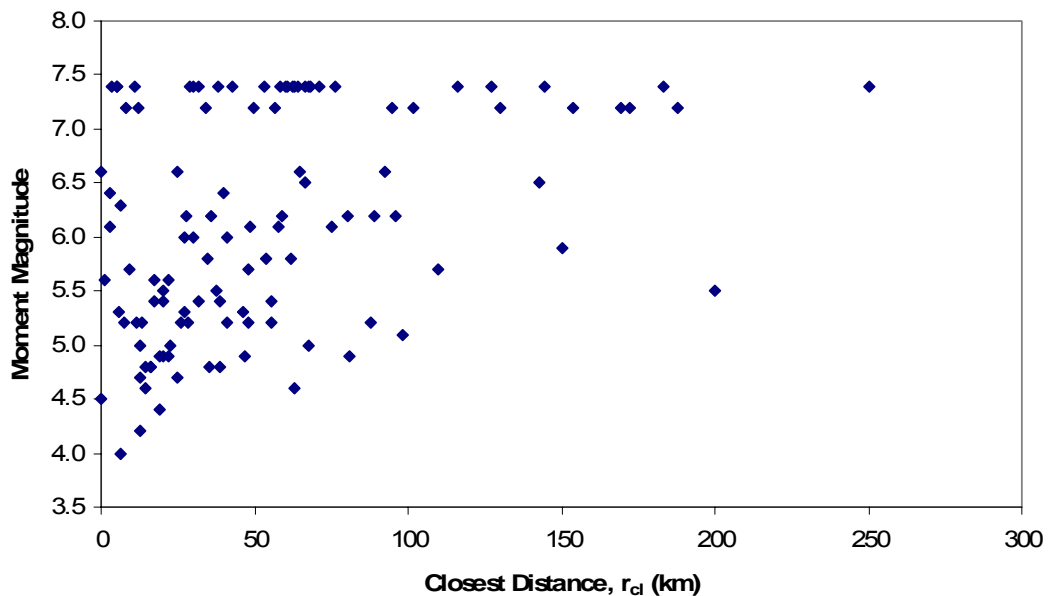


Figure 2.4 Distribution of recordings in terms of magnitude and distance.

As mentioned in Chapter 2.1, distance values are updated by searching new databases. Unavoidably, there are some differences between the databases mentioned for r_{cl} values which results in significant differences in the outcome. With the new information obtained, closest distance values of 18 recordings that seems to be defective are renewed, most of which belong to the 1999 Kocaeli and Düzce earthquakes. The differences between mentioned databases and selected r_{cl} values are shown for the 1999 Kocaeli and Düzce earthquakes in Table 2.2.

Table 2.2 Defined r_{cl} values for different databases and selected r_{cl} values in km for the 1999 Kocaeli and Düzce earthquakes.

	Station	Station Code	from Kalkan & Gülkan (2004)	from PEER Database	from ESMD Catalog	Values used in this study
17.08.1999 KOCAELI EVENT	BURSA	BRS	66.6	65.5	79.0	66.6
	CEKMECE	CEK	76.1	65.0	94.0	76.1
	DUZCE	DZC	11.0	13.6	12.0	11.0
	EREGLI	ERG	116.0	141.4	171.0	116.0
	GEBZE	GBZ	15.0	7.6	30.0	30.0
	GOYNUK	GYN	32.0	31.7	31.0	32.0
	ISTANBUL	IST	49.0	49.7	71.0	71.0
	IZNIK	IZN	30.0	30.7	29.0	29.0
	IZMIT	IZT	4.3	3.6	5.0	5.0
	SAKARYA	SKR	3.2	0.0	N/A	3.2
	BALIKESIR	BLK	183.4	180.2	199.0	183.4
	CANAKKALE	CNK	250.0	266.2	294.0	250.0
	KUTAHYA	KUT	144.6	145.1	140.0	144.6
	GEBZE	ARC	17.0	10.6	38.0	38.0
	AMBARLI	ATS	78.9	68.1	97.0	68.1
	BOTAŞ	BTS	136.3	127.1	156.0	127.1
	YEŞİLKÖY	DHM	69.3	58.3	87.0	58.3
	BURSA	BUR	62.7	60.4	77.0	60.4
	FATİH	FAT	63.0	53.3	79.0	53.3
	HEYBELİADA	HAS	43.0	N/A	62.0	43.0
	YARIMCA	YPT	3.3	1.4	5.0	5.0
	LEVENT	YKP	60.7	N/A	77.0	60.7
	MECİDİYEKÖY	MCD	62.3	51.2	77.0	62.3
	MASLAK	MSK	63.9	53.0	78.0	63.9
ZEYTİNBURNU	ZYT	63.1	52.0	80.0	63.1	
ATAKÖY	ATK	67.5	56.5	85.0	67.5	
21.11 1999 DÜZCE EVENT	BOLU	BOL	20.4	12.0	18.0	12.0
	DUZCE	DZC	8.2	0.0	0.0	8.2
	GOYNUK	GYN	56.4	N/A	47.0	56.4
	IZNIK	IZN	129.8	N/A	113.0	129.8
	IZMIT	IZT	95.0	N/A	86.0	95.0
	KUTAHYA	KUT	169.5	168.3	171.0	169.5
	MUDURNU	MDR	30.9	34.3	34.0	34.3
	SAKARYA	SKR	49.9	45.2	47.0	49.9
	AMBARLI	ATS	188.0	188.0	188.0	188.0
	FATİH	FAT	172.5	167.3	167.0	172.5
	HEYBELİADA	HAS	179.0	N/A	154.0	154.0
	YARIMCA	YPT	101.7	97.5	98.0	101.7

2.4. LOCAL SITE CONDITIONS

Local site conditions are the definition of type of deposits that lie beneath the corresponding site; in our case, beneath the station where the ground motion is recorded. Both the visual or instrumental studies can be used as the basis of the classification of the site conditions. For the purpose of making a subjective study, physical quantities that describe the soil conditions are preferred in determining the soil conditions. Shear-wave velocity and sediment depth are the foremost ones of these quantities (Bozorgnia and Campbell, 2004).

Most researchers use shear-wave velocity as the average value of shear wave velocities of the top 30 m of the deposit underlying the surface, V_{s30} . The 30-m velocity is calculated from the formula:

$$V_{s30} = \frac{\sum_{i=1}^n d_i}{\sum_{i=1}^n \frac{d_i}{V_{si}}} \quad (2.4)$$

where d_i is the thickness and V_{si} is the shear-wave velocity of the i^{th} soil layer within the upper 30m. Use of V_{s30} values as the basic indicator of the site classes is so wide that besides researchers, most seismic building codes including the Turkish Seismic Code in both 1998 and 2006 versions, 1997 edition of Uniform Building Code (UBC), 2000 edition of International Building Code (IBC) and European Seismic Code (EUROCODE8) defines the site classes on the basis of V_{s30} values. The second shear-wave velocity indicator is defined by Joyner *et al.* (1981) as the average velocity of shear waves over a depth equal to a quarter-wavelength of a ground-motion parameter of specified period or frequency, effective velocity. Effective velocity is used to calculate site amplification factors using stochastic methods (Boore, 2003).

Influence of local site characters on the ground motion amplification is an empirical fact. Although ground motion recordings for rock sites are “sharp” and

short period accelerations are dominant, soil sites amplify the peak values of ground motion for medium or long periods of ground motion. Analogous to the amplification of ground motion within the structure according to the natural vibration period of the structure, soil stratum above the bedrock has an amplification effect on the ground motion proportional to the vibration period of the stratum, which is related to the average shear-wave velocity of that stratum.

Studies of 17 August 1999 and the 12 November 1999 Düzce earthquakes indicated that the most damaging motions occur in zones of deeper, less consolidated soils, in contrast to bedrock sites (Marmara ve Düzce Depremleri Mühendislik Raporu, 2000). In several other earthquakes, many severe building damages have been identified in areas where deep alluvium soils were located over bedrock. Most interesting example of this effect was observed in 1985 Michoacan earthquake in Mexico where most of the damage zones were those located over an historical lake with silt and clay sediments that were 350 km away from the earthquake source, in the city of Mexico.

Actual shear wave velocity and detailed site descriptions are still not available for most stations in Turkey. For this reason, site classifications were estimated by analogy with information of similar geologic materials (Kalkan, 2001). Obeying the classification made by Kalkan and Gülkan (2004), three local site conditions are defined for the study as rock, soil and stiff soil sites. Sites with shear wave velocities below 300 m/s are designated as soil sites. Sites with shear wave velocities from 300m/s to 700m/s are classified as stiff soil sites. The rest are designated as rock sites. It has not been possible to use NEHRP ground stratification classification because the other relation utilized here as a yardstick with this work do not permit an unambiguous correspondence of metrics. For some of the recording stations, site condition information is revised by using new data for V_{s30} values. Updated shear wave velocities and local site classes for stations are mentioned in Table A.1. Pie-chart distribution of shear wave velocities for a total number of 112 events used in analysis is given in Figure 2.5. Also distribution of these events in terms of magnitude, closest distance to rupture and local geological conditions are given in Figure 2.6.

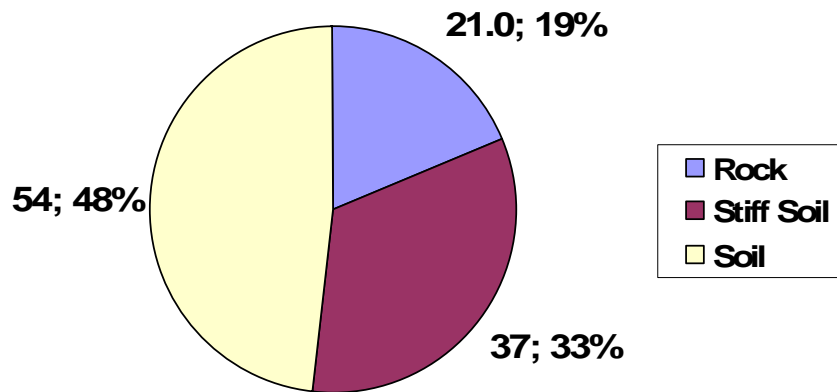


Figure 2.5 Pie-chart distribution of local site geology for selected database.

2.5. FAULT MECHANISM

There are basically three types of tectonic faults. When motion of the fault is horizontal, parallel to the strike of the fault, then it is named as a strike-slip fault. When the motions of the adjacent blocks are downward or upward with respect to each other, then the faulting is called as dip-slip fault. Dip slip faults are subdivided into two groups with respect to the sense of motion. If the block on the upper side of the fault drops down an inclined plane of constant inclination relative to the underlying block, that fault is called as normal. In reverse or thrust faulting, the block on the upper side of the fault moves up the fault-plane, overriding the underlying block.

Most active faults in Turkey are in strike-slip faults. Examination of the peak ground motion data from the small number of normal faulting earthquakes and reverse faulting earthquakes in the data set showed that they were not significantly different from ground motion characteristics of strike slip earthquakes (Kalkan, 2001). Since there is a limited number of data for reverse and normal faulting, it would probably be untrustworthy to construct a relationship considering fault

mechanism. Therefore, normal, reverse and strike slip earthquakes were combined into one single faulting category. The distributions of the used earthquakes in terms of magnitude, source to site distance and faulting mechanism are given in Figure 2.7. Earthquake information with unknown fault mechanism is eliminated from the data set of the Figure 2.7.

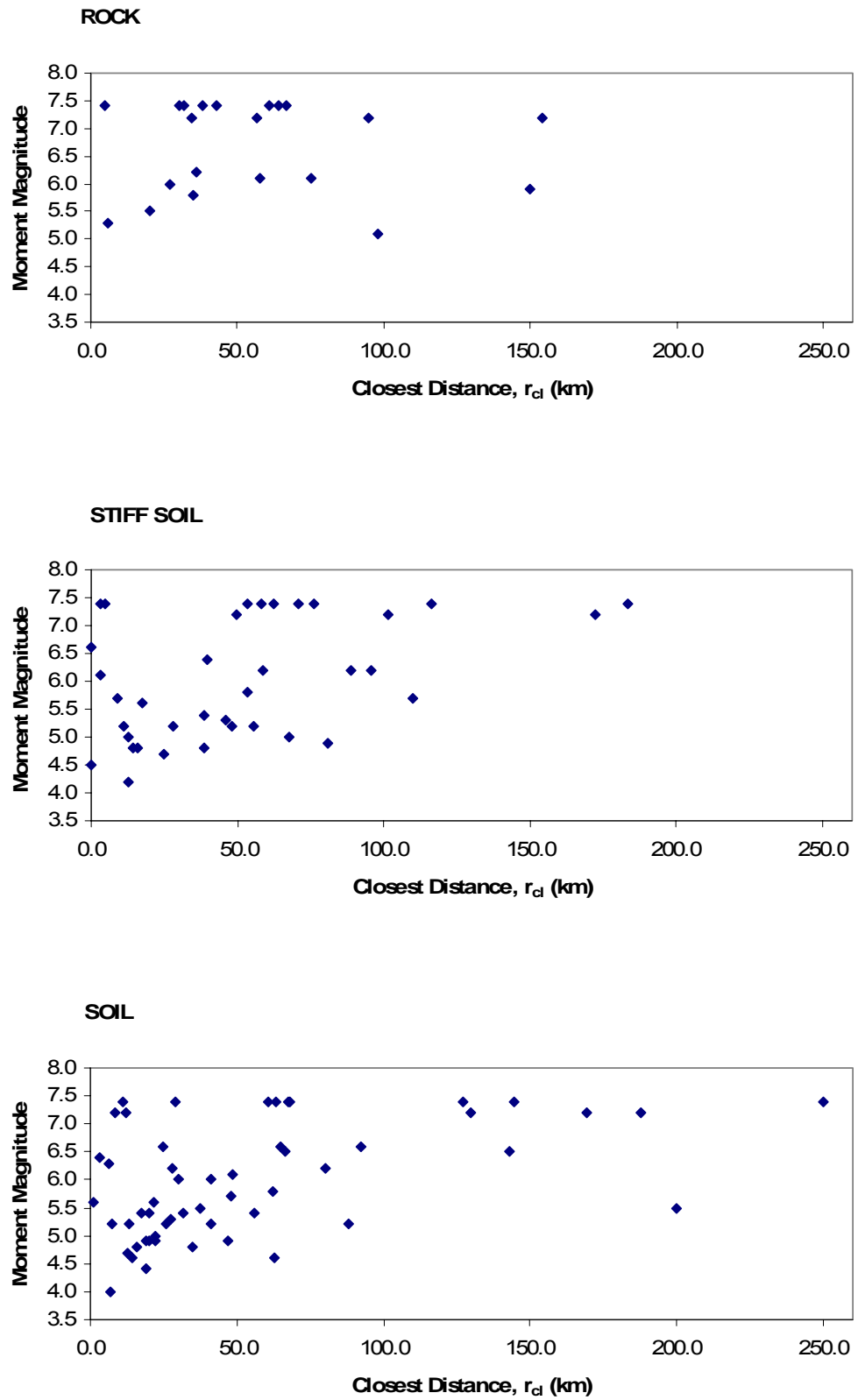
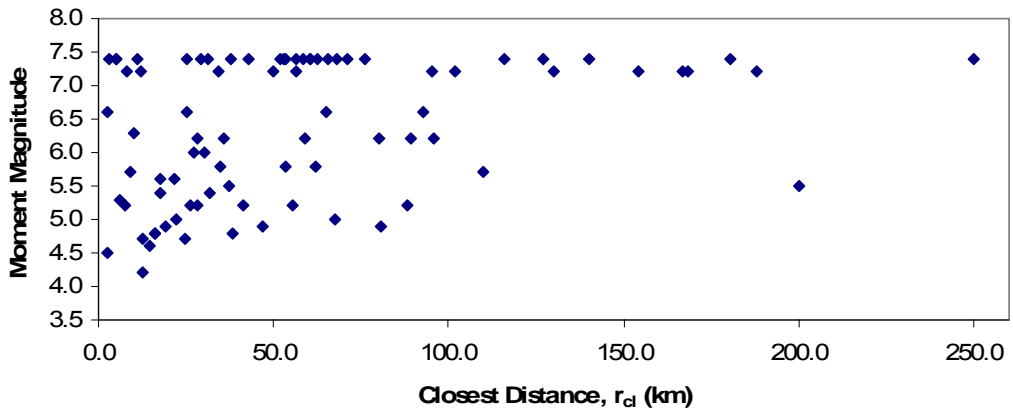
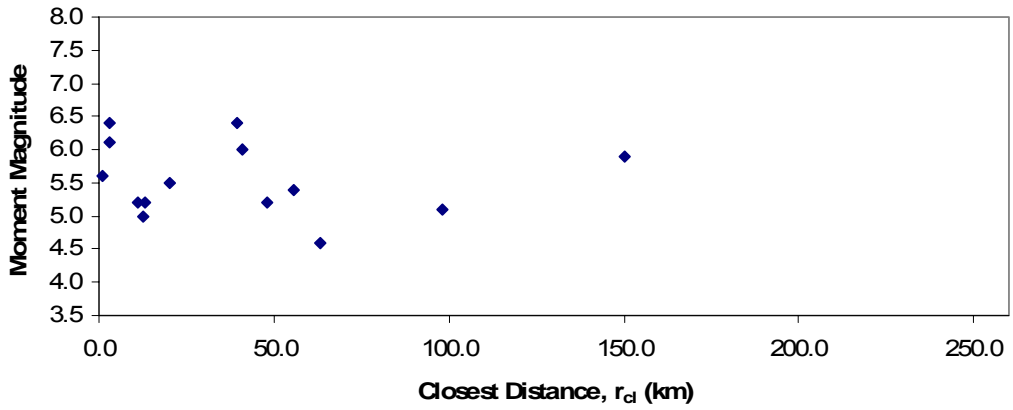


Figure 2.6 Records in terms of magnitude, distance and local site geology.

STRIKE-SLIP FAULTS



NORMAL FAULTS



REVERSE FAULTS

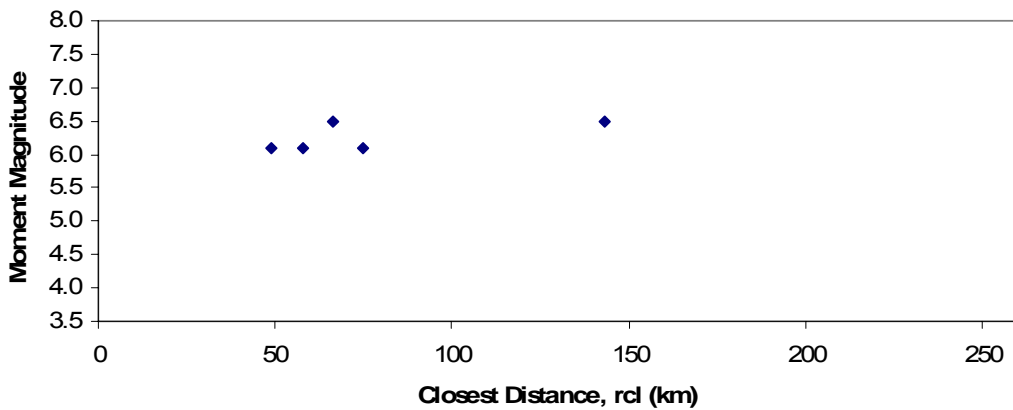


Figure 2.7 Distribution of records in the database in terms of magnitude, distance and faulting mechanism.

CHAPTER 3

DATA PROCESSING

3.1. GENERAL

Recorded either by analog or digital instruments, recordings from accelerographs are contaminated with data that has not originated from signals of the earthquake waves. This undesired stored energy in acceleration time series is called *noise* and there are various sources of it. Although noise has limited effect on acceleration time series in terms of peak values, velocity and displacement series can be seriously distorted and unrealistic PGV and PGD values can be obtained from such raw data, especially for analog recordings. Therefore, unlike the approach used for attenuation relationships for PGA, direct results for PGV obtained from raw accelerations files can not be used directly for analysis purposes. A number of processes should be done on raw material to obtain the reliable data for PGV.

There are various procedures to be applied to accelerograms to stabilize or lessen the error contained in the signal. What makes the correction or adjustment procedure complicated is that the true answer of the question is never known; i.e., pure velocity or displacement series are not available. Thus, considering the boundary conditions that are available and using some prescience, noise ratio of the actual recording is reduced to an acceptable level. As will be related later in the chapter, PGV values are highly sensitive to the choices of variables that are used during processing. For this reason, great care must be given to abide by the guidelines of the proposed methodology so as not to obtain unrealistic results.

In this chapter, analog and digital instrument properties, noise sources and its effects, ways of reducing noisy content and results obtained from data processing are discussed and presented in detail.

3.2. ANALOG INSTRUMENTS

As mentioned in the introductory chapter, analog instruments are optical-mechanical devices. Recordings may be in the form of: (1) a 35 or 70mm film negative, (2) a photographic enlargement or copy on film or paper, positive or negative, of a 35 or 75mm film, (3) a 12-inch wide photographic paper record or a copy of it (Hudson, 1979). The first earthquake record is obtained by an analog instrument was in 10 March 1933, Long Beach California Earthquake. In Turkey, after deployment of Strong Motion Network of Turkey in 1973, first accelerograms was obtained during the 19 August 1976 Denizli earthquake.

Most of the records of destructive earthquakes of 20th century were obtained by analog instruments and these recordings altered our understanding of earthquakes in a basic way. What is called earthquake engineering is developed by the information gained from strong motion accelerograms. 1940 El Centro, 1966 Parkfield, 1971 Pacoima Dam earthquake accelerograms are the milestones of this effort. Until 1995, in the Turkish database of accelerograms, almost all recordings were from analog instruments. For the database used here, all analog recordings are from SMA-1 type accelerographs, which is a type introduced by Kinematics Inc. in the late 1960s and sold more than 7200 units until its production was discontinued by the early 1990s (Trifunac and Todorovska, 2001). Figure 3.1 demonstrates the schematic diagram of analog instruments and photograph of SMA-1.

These instruments have proved themselves to be rugged and reliable but there are serious drawbacks of analog accelerographs. Since they record mechanically, a great deal of recording medium should be wasted. To limit this waste, they are operated on standby and triggered by a specific threshold of acceleration (generally triggered by shear wave), which means that some part of ground motion below the threshold value can not be recorded prior the strong motion, or captured subsequently. The importance of this prior recording will be discussed in the section on digital recordings. Also, ease of access to instruments is required since they do not use reusable medium.

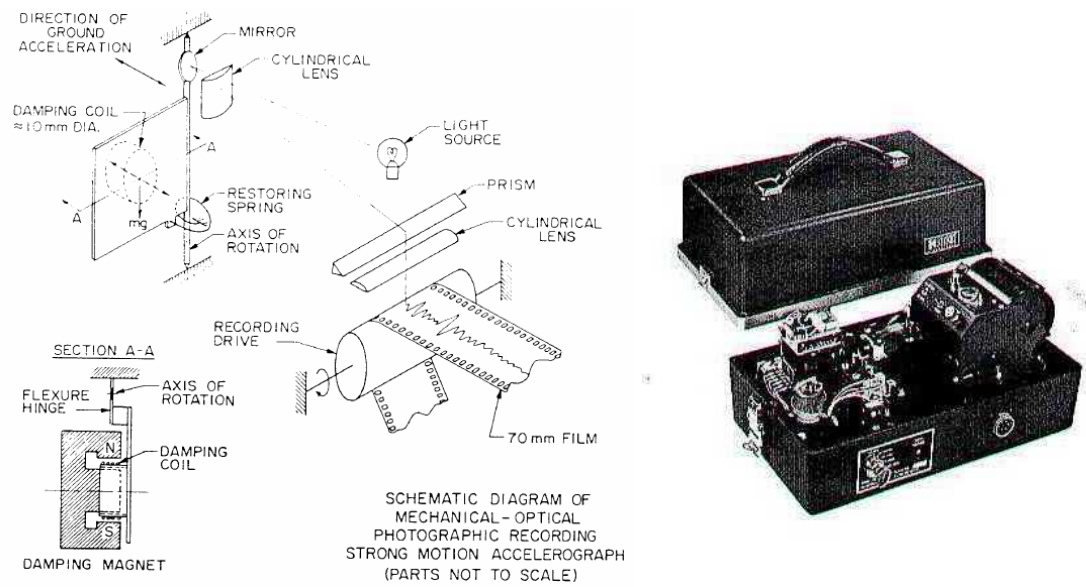


Figure 3.1 Schematic diagrams of analog instruments and photograph of SMA-1 accelerograph (Hudson, 1979).

The second drawback of analog instruments is related to their dynamic characteristics. Dynamic range of instruments is related to the largest and smallest amplitudes that can be recorded (A_{\max} , A_{\min}) with the following equation,

$$\text{DynamicRange} = 20 \log \left(\frac{A_{\max}}{A_{\min}} \right) \quad (3.1)$$

For analog instruments, dynamic range is limited by the width of the recording paper or film, thickness of the trace and resolution of the digitizing system and equals 40-55 dB (Trifunac and Todorovska, 2001) (Refer to Figure 1.1 for a comparison between dynamic ranges of instruments). Traditionally, seismometers are sensitive and accelerometers are less sensitive against ground motion in order to capture the strong motion. With a low dynamic range, it becomes impossible to capture the strongest parts of the ground motion and a phenomenon called *clipping* occurs. Clipping can be seen visually from acceleration time series. Another drawback of dynamic characteristics of analog instruments has to do with their

bandwidths. Since the theory behind accelerographs dictates that the displacement response of the instrument should be proportional to the base acceleration in order to evaluate the strong motion, the natural frequency of the accelerographs has to be much greater than the frequency of the recorded motion (Boore and Bommer, 2005). Because of physical limitations, it is not possible to have analog instruments with natural frequencies greater than 25 Hz (Refer to Figure 1.2 for a comparison between natural frequencies of instruments). Therefore, high frequency motions can not be evaluated in a correct manner beyond the natural frequency of the instrument itself. Figure 3.2 demonstrates this issue.

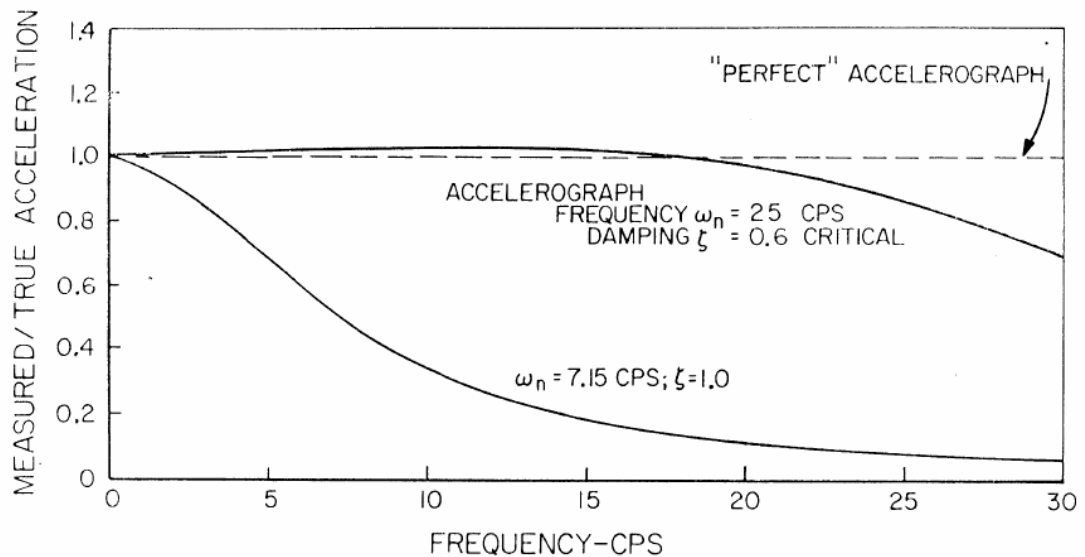


Figure 3.2 Measured and true acceleration values for an analog accelerograph (Hudson, 1979).

Computers are inevitably needed for any kind of data analysis considering strong motion records. To achieve this, analog instrument traces must be digitized. Besides being a very time consuming and laborious exercise, it is one of the main reasons of noise content stored in the traces. Digitization was made by hand till 1970s in US, then for approximately 10 years semi-automatic hand operated digitizers were used. From beginning of 1980s, automatic digitizers were introduced

(Trifunac and Todorovska, 2001). Each improvement decreased the amplitude of digitization noise and limited human-related errors. Another important drawback of digitization process is the effect of resolution on digitization. Figure 3.3 shows an example of digitized accelerogram with low resolution.

Although noise in the traces can be limited to some extent, it is generally not possible to remove the noise without processing the series after digitization. Most obvious indicator of the problematic recording is the unrealistic time series of velocity and displacement. Figure 3.4 displays an example of this phenomenon on an uncorrected time series. Although it is known that velocity at the end of the record should be zero as a terminal condition, this is not the case. Moreover, velocity and displacement traces must normally assumed to be zero as an initial condition to start plotting but this may not be the case since actual strong motion does not start as the acceleration trace shown in figure. As explained in the previous paragraphs, recording starts when acceleration exceeds a threshold limit. Also, displacement trace seems to be unrealistic with a 4m drift, increases in a parabolic sense (which is the integral of the linear shift in velocity trace).

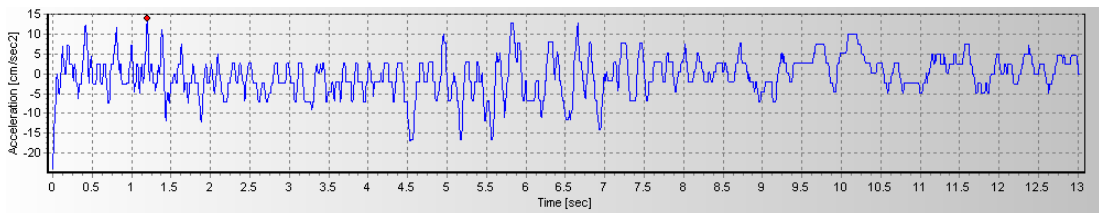


Figure 3.3 Uncorrected acceleration time series of İzmit Meteoroloji İstasyonu N-S component record of the 12.11.1999 Düzce earthquake.

All these evidences show that baseline of the acceleration trace is shifted and low-frequency noise content is involved in the traces (high frequency content has limited effect on traces). Long-period noise can also be introduced by lateral movements of the film during recording and warping of the analog record prior to digitization (Boore and Bommer, 2005).

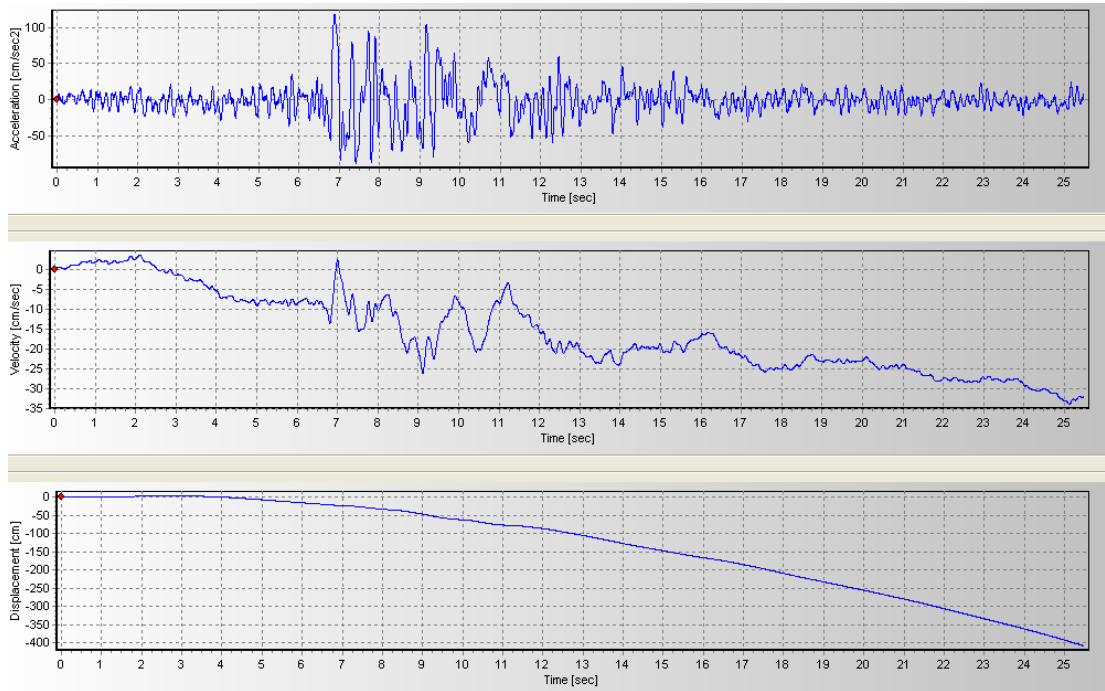


Figure 3.4 Uncorrected acceleration, velocity and displacement time series of Göynük Devlet Hastanesi E-W component record of the 17.08.1999 Kocaeli earthquake.

3.3. DIGITAL INSTRUMENTS

As stated earlier, digital accelerographs are superior compared to their analog counterparts in many aspects. First of all, they record on reusable media continuously so there is no waste of film or paper. They hold a pre-event memory for each recording so actual starting time of recording can be obtained contrary to unknown initial conditions of analog instruments. Besides, this pre-event memory serves as a basic source to identify the noise content of the recording.

The second important advantage of digital accelerographs is about their dynamic properties. As shown in Figure 1.1 and Figure 1.2, both dynamic range and bandwidth of the digital instruments are much better than analog ones. No high frequency limitations or dynamic range problems exist for digital instruments, at least in typical requirements of earthquake engineering.

Most important advantage of digital instruments is generated by its digital character. No external digitization is required for digital instruments because analog-to-digital conversion is made within the instrument. Therefore, noise originated from digitization process is not an issue for this kind of instruments. Nevertheless, noise and baseline problems can not be eliminated completely from the digital instruments. Data processing is still required for digital accelerographs. Figure 3.5 is the acceleration, velocity and displacement time series obtained from Yarımca Petkim Tesisleri during the 12.11.1999 Düzce earthquake. Although initial conditions are satisfied in time series for the time of event starts for velocity and displacement traces; i.e. excluding pre-event portion of time series, velocity and displacement are zero when ground motion is started, baseline shifts therefore noise intrusion can be realized when terminal condition of velocity trace and linear increase in the displacement time series are considered.

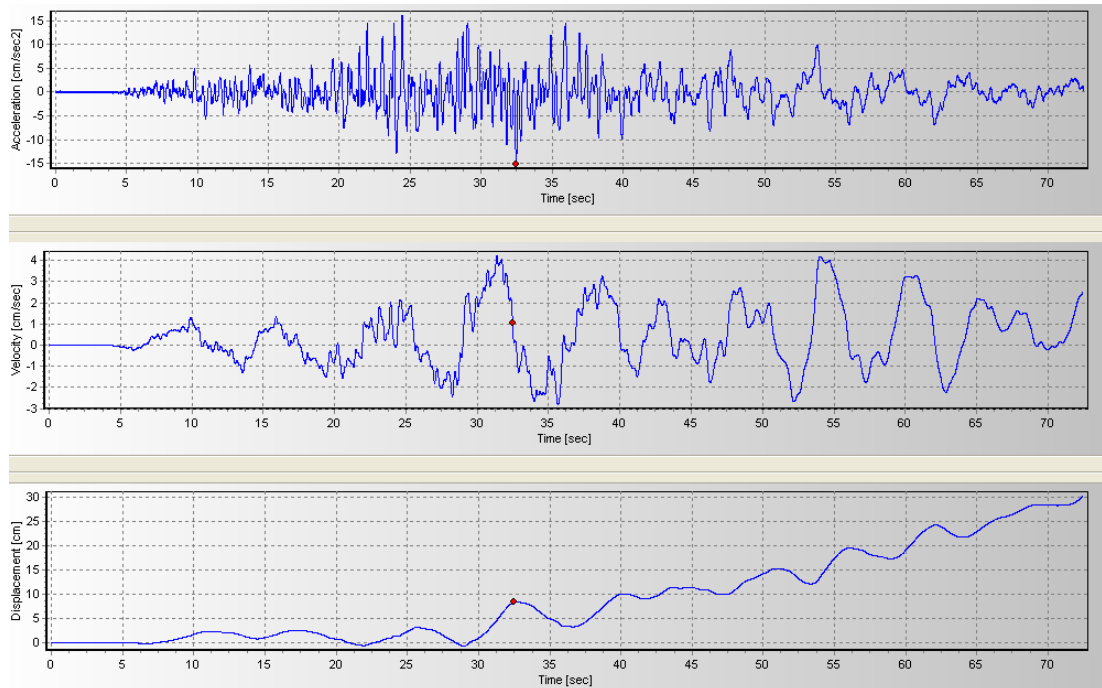


Figure 3.5 Uncorrected acceleration, velocity and displacement time series of Yarımca Petkim Tesisleri E-W component record of the 12.11.1999 Düzce earthquake.

3.4. NOISE CHARACTERISTICS AND ADJUSTMENT PROCEDURES

Noise characteristics encountered in the recordings can be grouped into two as standard and non-standard noise (Boore and Bommer, 2005). As explained briefly in the preceding parts, standard noise is originated from the signal itself for both kind of accelerographs or it stems from digitization process and the instrument itself for analog instruments. Nonstandard noise, on the other hand, can be seen in some of the records and they should be eliminated before routine process on the records is done.

Spikes are the unrealistic peaks shown in acceleration traces of digital accelerographs. An example of the spikes is shown in Figure 3.6. These kinds of spikes are eliminated from the records by interfering in the ground motion data. For this unique example, spikes are just deleted from end of the record since strong ground motion effect has already been diminished prior to that instant. As suggested by Boore and Bommer (2005), spikes can be eliminated by replacing the ordinate of spike with mean of acceleration data points on either side.

Another source of non-standard error is the baseline shifts (Boore and Bommer, 2005). For both analog and digital recordings, baseline shifts result in serious deviations on both velocity and displacement traces.

As “standard” errors, baseline problems, high frequency noise, transducer errors and low frequency noise can be listed. Each one of these will be discussed in detail in the succeeding parts.

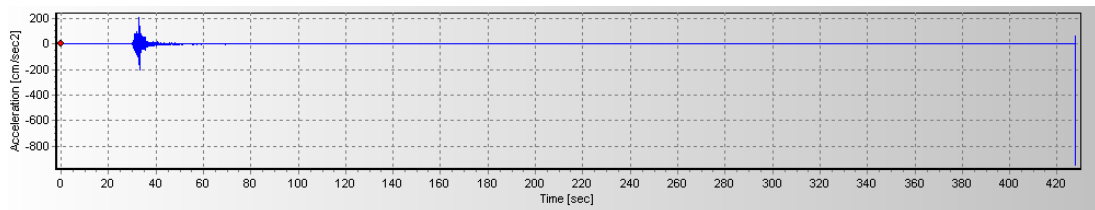


Figure 3.6 Uncorrected acceleration time series of Sakarya Bayındırlık ve İskan Müdürlüğü N-S component record of the 11.11.1999 Sapanca-Adapazarı earthquake.

3.4.1. BASELINE PROBLEMS

As can be seen from Figures 3.4 and 3.5, baselines for both analog and digital instruments can be shifted. Generally, it is not possible to identify these shifts or distortions from acceleration traces. With integration process for velocity and double integration process for displacement series, it becomes possible to identify baseline shifts.

There are several procedures to correct baselines. Sequential fitting of baselines to the velocity trace is one of these procedures. Figure 3.7 displays the uncorrected series of Yarımca Petkim Tesisleri N-S component record for the 1999 Kocaeli earthquake. The baseline shift in the velocity trace is obvious. Both velocity and displacement traces are unrealistic. To adjust the baseline, velocity fit from 30 to 135 s. is applied to the traces and the result obtained is shown in Figure 3.8. Not only the traces are more realistic after adjustment, but also it becomes possible to observe the permanent displacement after the earthquake ceases. Also shown in Figure 3.9 is the Fourier spectrum of the record before and after baseline correction. Only minor differences can be observed. Baseline corrections does not change Fourier spectrum of the record significantly. There is almost no difference before and after baseline correction. The spectrum in red in Figure 3.9 is the noise spectrum obtained from pre-event memory, green lines represents the theoretical f^2 decrease (explained in Part 3.4.2) of the spectrum amplitudes to identify low-cut filter frequency.

Baseline adjustments can also be used for removing low frequency noise. Application is generally fitting baselines to velocity traces. This can be in the form of fitting higher-order polynomials to the velocity trace such as Grazier (1979) has proposed, or shifting velocity trace between time limits where predefined threshold acceleration is exceeded as Iwan has suggested (Iwan *et al.*, 1985). Figure 3.10 shows the schematic representation of these approaches. In Figure 3.10 on the left side shaded line represents velocity from integration of the east–west component of acceleration recorded at TCU129, which is 1.9 km from the surface trace of the fault, from the 1999 Chi-Chi earthquake, after removal of the pre-event mean from the whole record. A least-squares line is fit to the velocity from 65 s to the end of the

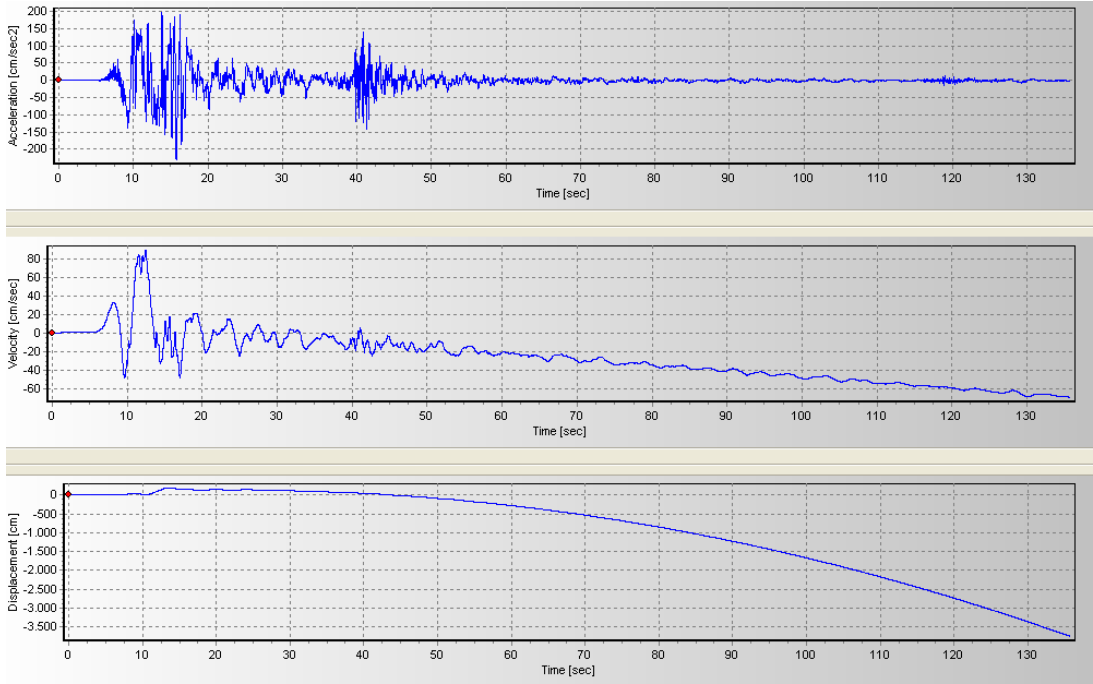


Figure 3.7 Uncorrected acceleration, velocity and displacement time series of Yarımca Petkim Tesisleri N-S component record of the 17.08.1999 Kocaeli earthquake.

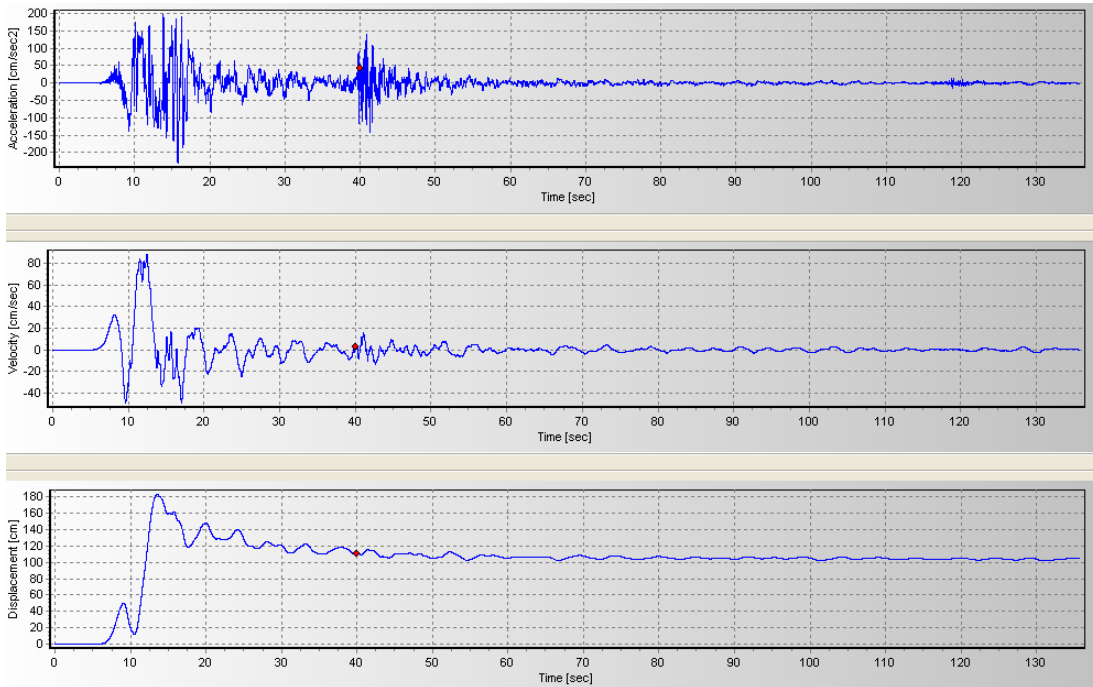


Figure 3.8 Acceleration, velocity and displacement time series of Yarımca Petkim Tesisleri N-S component record of the 17.08.1999 Kocaeli earthquake after velocity fit from 30 to 135 s.

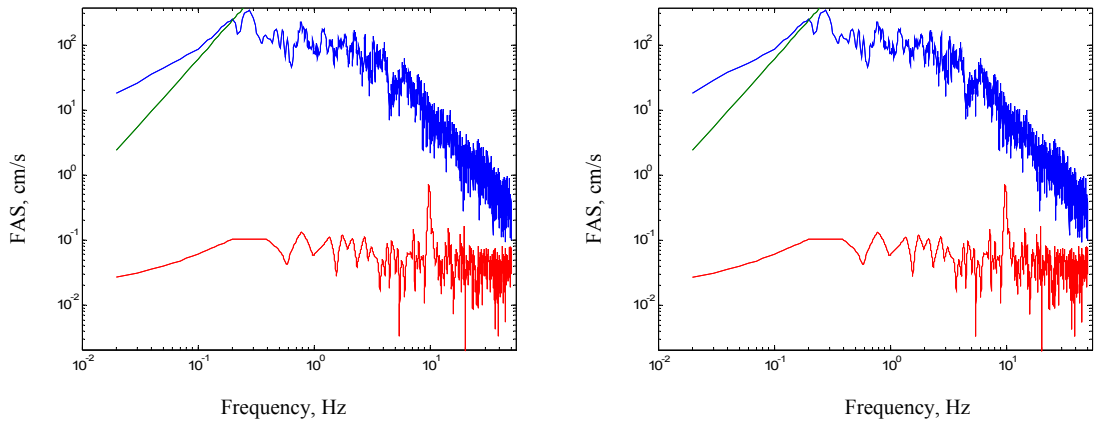


Figure 3.9 Acceleration Fourier spectrum of the Yarımca Petkim Tesisleri N-S component record of the 17.08.1999 Kocaeli earthquake before (left) and after (right) baseline correction.

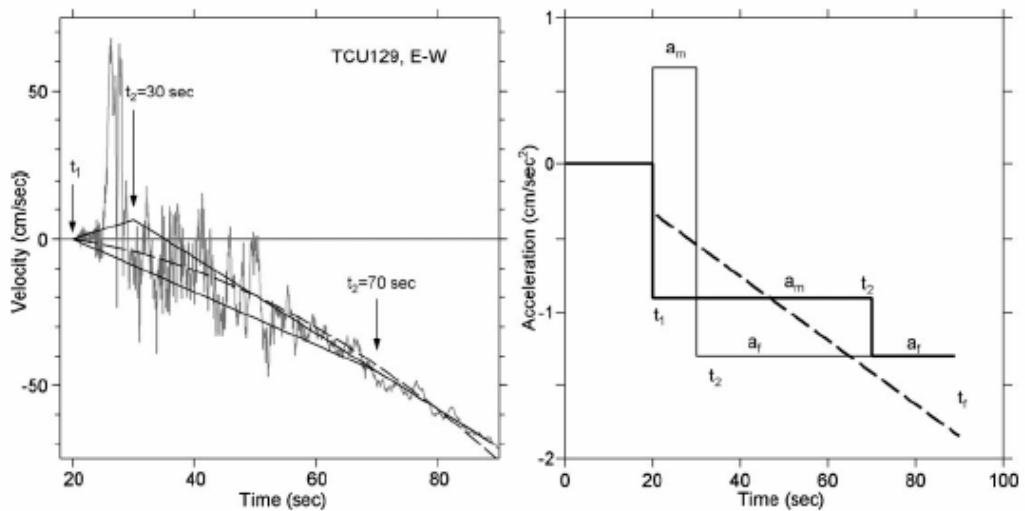


Figure 3.10 Schematic representations of baseline adjustment schemes (Boore and Bommer, 2005).

record. Various baseline corrections using the Iwan scheme are obtained by connecting the assumed time of zero velocity t_1 to the fitted velocity line at time t_2 . Two values of t_2 are shown: 30, and 70 s. The dashed line is the quadratic fit to the velocities, with the constraint that it is 0.0 at $t=20$ s. On the right hand side of the figure are the derivatives of the lines fit to the velocity are the baseline corrections applied to the acceleration trace (Boore and Bommer, 2005). Major drawback of the

Iwan approach is that significantly different results can be obtained especially for displacement time-series according to the selected shifting times, which are chosen subjectively.

3.4.2. LOW FREQUENCY NOISE

Low frequency noise in the signals can originate from digitization errors or from the noise within the signal. It can be effectively eliminated from the records by using low-cut filtering. Low-cut filters eliminate the noise content within the recording according to the subjectively selected low-cut filter frequency. Both velocity and displacement time series are very sensitive to the selected low-cut filter frequency. Therefore, despite the subjectivity of the selection, selection criteria are defined in order to limit the deviations from one to study to another. Besides selection of low-cut frequency, selected techniques of the filtering and true application are also very important to obtain results as much close as the actual ones.

A filter is a function that in the frequency domain has a value close to one in the range of frequencies that the analyst wishes to retain and close to zero in the range of frequencies that the analyst wishes to eliminate (Boore and Bommer, 2005). According to the function selected, filters are named as Butterworth, Ormsby, Chebychev, Bessel or elliptical. In practices, Butterworth filters are generally used but differences between results obtained from filter types are not to be considered here since the differences have limited effect to the results obtained.

If a Butterworth type of filtering is chosen to be applied, as will be done in this study, the items to be decided include type of filter and filter order. Type of filter can be causal or acausal. Acausal filters are actually causal filters that are applied to the time series twice (forward and backward), to achieve zero phase shift. Although they have very similar properties, acausal and causal filters can cause very different outcomes especially for displacement time series. In Figure 3.11 result obtained for accelerations, velocity and displacements time series from the 228⁰ component of the analog recording at Rinaldi during the 1994 Northridge earthquake for causal (top)

and acausal (bottom) filtering are plotted. Displacement time series deviate significantly according to the selected filter type (Boore and Bommer, 2005).

Data points with zero amplitude should be added to acceleration time series to be able to apply acausal filters. This procedure is known as adding pads. Total length of zero pads added is related to the filter order used in the analysis. Recommended total time length for zero pads needed is given by the equation:

$$T_{pad} = \frac{1.5n}{f_c} \quad (3.2)$$

where n is the filter order and f_c is the low-cut filter frequency for Butterworth acausal filter (Boore and Bommer, 2005).

Choice of filter order is decided by analyst according to the desired fall off rate of the filter. In Figure 3.12, fall offs of Butterworth type filter is shown for both time and frequency domains. It can be observed from the figure that, as the filter order increases, rapid fall off filter response is observed. According to the seismological theory, FAS of acceleration decays according to the square root of frequency (f^2), therefore it is desired to have a fall off for filter response that decays more rapidly than f^2 .

The most important part of the data processing scheme is selecting low-cut filter frequency. When signals are judged to be contaminated by the noise, it would be possible to identify the noise from acceleration FAS. Also most of the criteria adopted to decide the low-cut filter frequency are based on the studying on FAS. Based on the papers published by Boore and Bommer (2005) and Akkar and Bommer (2006b), four distinct ways of deciding low-cut filter frequency can be identified.

i. One way of deciding low-cut filter frequency is to study the noise spectrum and make a comparison between acceleration FAS of noise and record spectrum. Noise spectrum can be obtained from pre-event memory of the record for digital

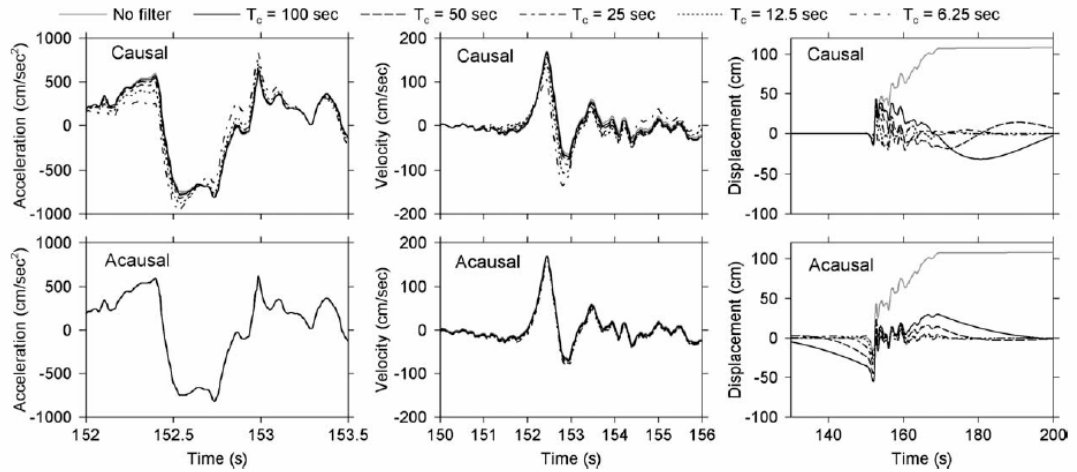


Figure 3.11 Differences in the result obtained for accelerations, velocity and displacements time series for acausal and causal filtering for different filtering periods (Boore and Bommer, 2005).

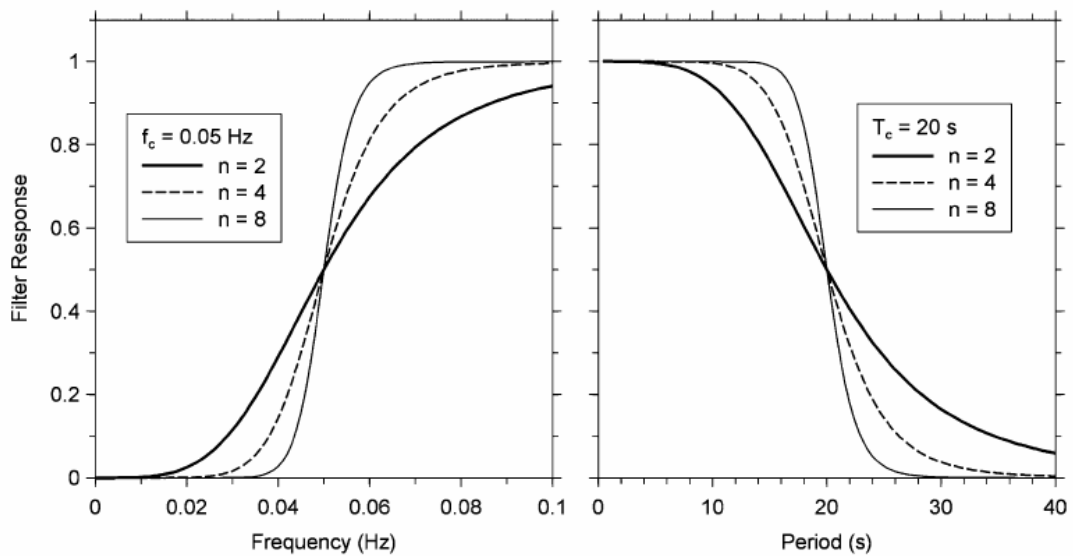


Figure 3.12 Fall offs for Butterworth type filter for both frequency (left) and time (right) domains (Boore and Bommer, 2005).

instruments and from fixed traces of analog instruments. Analog instruments produce two fixed traces on the film together with the three traces of motion (two horizontal, one vertical) and the time marks. Since these fixed traces only contain noise for the

record, noise spectrum can be obtained from them if digitization process is done also for these fixed traces. Nevertheless, in practice, no such effort is made. Even if they have been made, it is hardly possible to achieve these records. For the used database, no fixed trace information is available.

Another important issue about the pre-event memory noise spectrum is scaling the FAS to be able to use with record FAS. Acceleration FAS of the pre-event portion is scaled proportional to time length of the record and pre-event portion. As defined by Zare and Bard (2002), normalized signal to noise ratio is given in Equation 3.3,

$$R_{sn}(f) = \frac{S(f) / \sqrt{t_s}}{N(f) / \sqrt{t_n}} \quad (3.3)$$

where Fourier transform of the signal is computed ($S(f)$) over a length t_s and the Fourier transform of the noise $N(f)$ is computed over a length of t_n and (R_{sn}) is the normalized signal to noise ratio. With some mathematical arrangement scale factor for the noise spectrum can be defined as

$$SF = \frac{\sqrt{t_s}}{\sqrt{t_n}} \quad (3.4)$$

where SF is the Scale Factor, t_s is the time length of the record, t_n is the time length of the pre-event part of the record.

Finally, desired ratio of signal-to-noise should be decided. It is generally accepted by researchers that, noise ratio in the recording (by means of amplitude of FAS) should not exceed half of the signal. Considering noise is also contained in signal FAS, a signal-to-noise ratio of 3 is the limit for records to be evaluated. In Figure 3.13, acceleration FAS of noise and record for the Malazgirt Meteoroloji İst. 03.11.1997 earthquake is shown as an example of signal-to-noise ratio usage for filtering. In Figure 3.13, Blue spectrum is the signal spectrum whereas red one is the

noise spectrum obtained from pre-event memory. For a signal-to-noise ratio of 3, low-cut filter frequency is found as 0.56 Hz for N-S component and 0.55 Hz E-W component. 0.56 Hz is selected as the low-cut frequency for both components.

ii. According to the source theory, amplitudes of FAS of signal should decay in proportional to the square root of decay in frequencies. Known as f^2 model, deviation of FAS of record from decaying trend will be the frequency of low-cut filter to be activated. Figure 3.14 expresses two examples of how to use the model for both analog and digital instruments. In the figure, on the left, acceleration FAS of the Göynük Devlet Hastanesi E-W component record (analog) of the 17.08.1999 Kocaeli earthquake is plotted. Also shown in the figure is the subjectively fitted f^2 decay model (in green) intersecting the FAS where deviation from the decaying trend for FAS is observed; on the right, acceleration FAS, proposed f^2 decay model and noise FAS (red) of the Yarımca Petkim Tesisleri E-W component record (digital) of the 12.11.1999 Düzce earthquake is plotted. Notice that signal-to-noise ratio does not give an idea about low-cut filter frequency for the digital recording. As can be observed from the figures, subjective character of choosing a low-cut filter is limited but does not vanished.

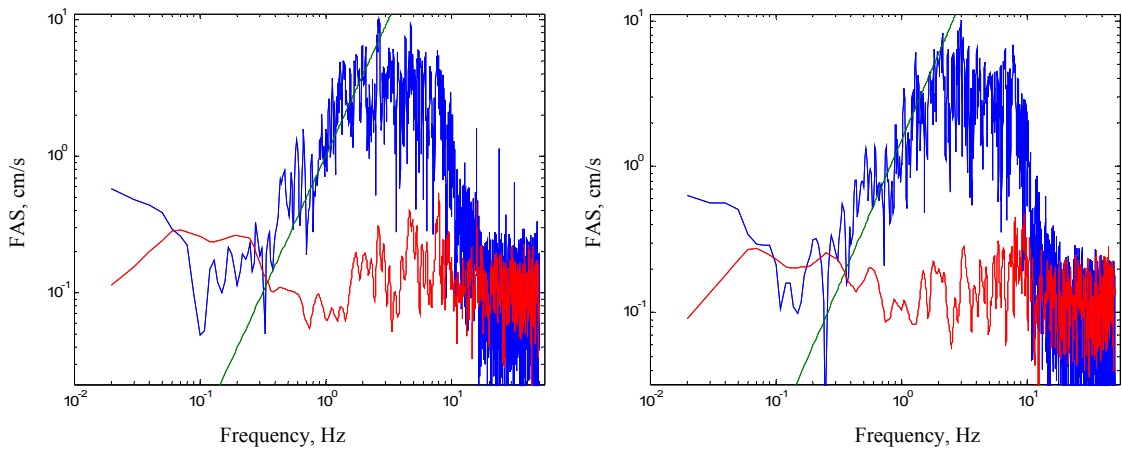


Figure 3.13 Acceleration FAS of the Malazgirt Meteoroloji İst. N-S (left) and E-W (right) components records of the 03.11.1997 Malazgirt earthquake.

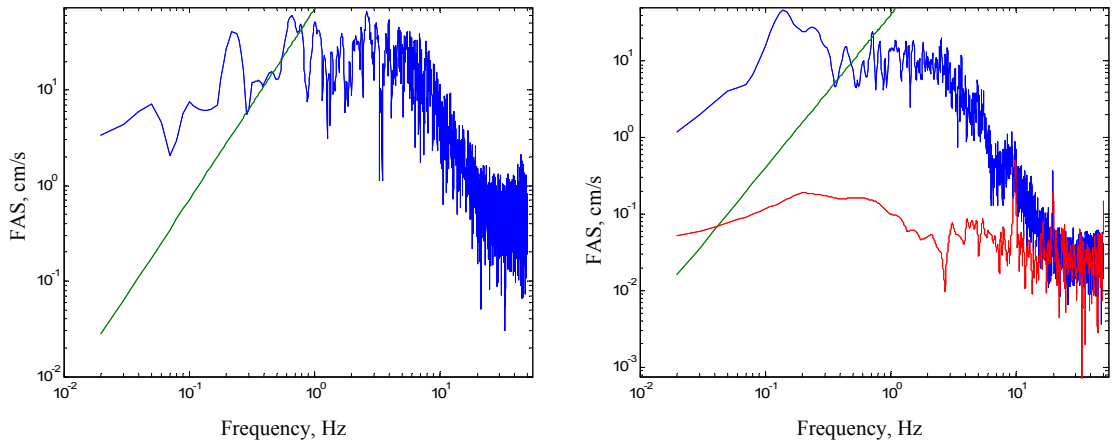


Figure 3.14 Use of f^2 decay model for analog (left) and digital instruments (right).

iii. Visual inspection of velocity and displacement time series can be used to judge whether used filter frequencies are appropriate. Since judgment does involve subjectivity as the meaning of the word, differences between researchers about appropriateness of the time series are unavoidable.

iv. Finally, appropriateness of selected low-cut frequency can be judged numerically according to the corner frequencies calculated from source theory. Based on Brune's single-corner source spectrum model from a stress drop of 100 bars, Joyner and Boore (1988) defined a relationship to estimate filter frequency as,

$$f_o = 10^{\frac{-(M-5)}{2}} \quad (3.5)$$

where f_o is the filter frequency and M is the moment magnitude. If a double-corner source spectrum model is used, then corners of the theoretical decaying of acceleration FAS are defined by Atkinson and Silva (2000) as,

$$f_a = 10^{2.181-0.496M} \quad (3.6)$$

$$f_b = 10^{2.410-0.408M} \quad (3.7)$$

Since none of the criteria can be based on physical evidences or mathematical proofs, the best way of deciding what the filter frequency should be, is to use all criteria simultaneously to make a sound decision.

Because of the sensitivity of obtained time series after processing to the selected low-cut filtering methodology and filter frequencies, acceptability of outcome become questionable beyond some pre-defined periods. For a detailed description of this debate, the reader can refer to the paper by Boore and Bommer (2005).

3.4.3. HIGH FREQUENCY NOISE AND TRANSDUCER ERRORS

Transducer errors, as mentioned in Chapter 3.2, occur due to the insufficient (small) natural frequencies of the accelerograph (Figure 3.2). Since sites with soft soil conditions filter the high frequency content of the motion, high frequency content in the acceleration traces are observed for recordings that have stiff site conditions. Therefore no correction for transducer error is required for digital instruments or analog instruments located on non-rocky sites. Transducer corrections simply amplify the amplitudes of acceleration traces for high frequency content where transducer natural frequency limits the instrument to evaluate the true behavior. Figure 3.15 shows examples of analog and digital instrument recordings and transducer effects. Analog instrument (left) is corrected for frequencies beyond its natural frequency. Digital instrument (right) do not need any correction since its response does not fluctuate within the frequency range investigated (Boore and Bommer, 2005).

On the other hand, high frequency noise affects the frequency content of the accelerograms contrary to transducer errors. Noisy content amplifies the high frequency portion of the Fourier spectra. On the right side in Figure 3.14, Fourier acceleration spectrum of the record and noise spectrum obtained from pre-event memory of the accelerograph are shown. As can be seen from the figure, noise overwhelms the record spectrum starting from frequencies 15 to 20 Hz. That is, what is seen as the Fourier spectrum of the record is actually noise spectrum. Moreover,

for high frequencies, acceleration FAS should decay inversely proportional to the square root of increase in frequencies in an opposite sense of low frequencies. So, flat portions at the end of the spectra are unreasonable. Therefore, it is convenient to filter the recording for frequencies where noise is considered to be effective or where the decaying of amplitudes flattens. The theory behind the necessity of using high-cut filters is to limit the noise content as it is for low-cut filters. Since filtering works on the contrary manner to the transducer correction, transducer correction will be useless where frequency ranges of the two applications counteracts.

Another limitation for the high frequency applications comes from the sampling rate. Nyquist frequency, the highest frequency at which characteristics of the motion can be correctly determined, is equal to $(1/2\Delta t)$ where Δt is the sampling interval. A high cut filter greater than Nyquist frequency will be useless.

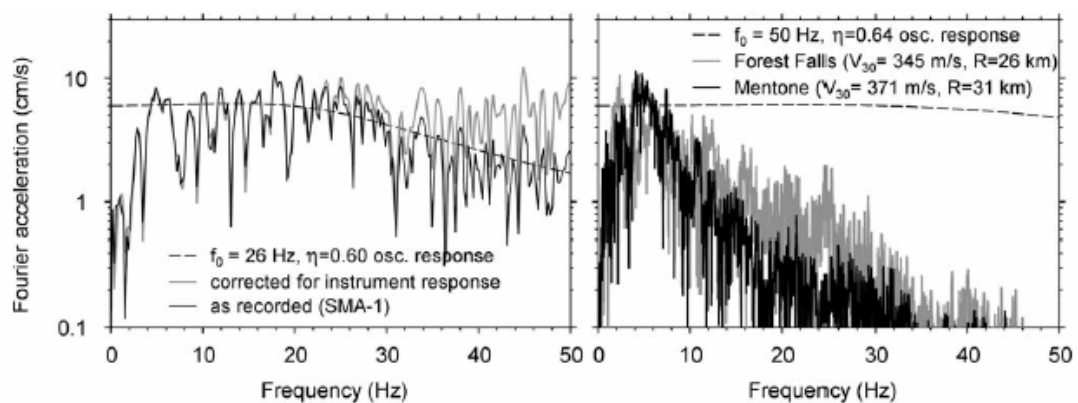


Figure 3.15 High frequency noise in Fourier acceleration spectra in analog and digital accelerograms (Boore and Bommer, 2005).

An important issue about data process is the compatibility of the time-series after processing. Either filtering or baseline corrections are applied, acceleration time-series are distorted or time lengths are changed because of padding. It should be keep in mind that after any process, all time series should have the same format and they should be compatible with each other. Researches have shown that pads that are

needed for acausal filtering, should not be removed after processing since removing distorts long period spectral ordinates (Converse and Brady, 1992).

3.5. DATA PROCESSING METHODOLOGY

There are various methodologies that are proposed or applied by the researchers or institutions for data processing. In this section, a brief summary of these methodologies are given. Then, methodology applied for this study will be given in detail.

For Dissemination of European Strong Motion Data, a correction for the instrument response, when the required characteristics are known, and high cut filtering, with a cosine transition from the roll-off frequency to the cut-off frequency; followed by low-cut acausal Butterworth filtering of the acceleration after padding has been applied to time series. Signal-to-noise ratios are used as the basis for estimating low-cut filter frequency (Internet Site for European Strong Motion Database).

PEER Center applied both baseline correction procedures and filtering together. After removing mean (simple baseline correction), high-cut and low-cut filter frequencies are determined from Fourier spectrum. Then, velocity and displacement time series are formed and baseline correction is made for acceleration trace. Again plotting time-series, displacement trace is controlled for its validity. If not problematic, data process is finished; if it is, new filter frequencies are selected (Darragh *et al.*, from http://www.cosmos_eq.org/recordProcessingPapers.html).

The methodology applied for USGS National Strong Motion Program contains a baseline correction based on fitting linear or low-order polynomials to the velocity trace after a simple mean removal, then an acausal band pass filtering of acceleration time series (Stephens and Boore, from http://www.cosmos_eq.org/recordProcessingPapers.html).

California Strong Motion Instrumentation Program (CSMIP) applied an instrument correction after a baseline correction followed by a high frequency filtering. Finally a low-cut filtering is made to the records considering a signal-to-noise ratio of 2 or 3 (Shakal *et al.*, from http://www.cosmos_eq.org/recordProcessingPapers.html).

Akkar and Bommer (2006b) suggested an iterative procedure to identify low-cut frequency based on source theory. After subtracting the mean from the record, observing the FAS of signal and noise, signal-to-noise ratio of 3 is checked as the frequency of filtering. If signal-to-noise ratio does not exist, or no consistent result is obtained, theoretical corner frequencies are checked to determine low-cut filter frequency. Starting with a filter frequency value that is lower than the theoretical FAS corner frequencies estimated from the theoretical models of Joyner and Boore (1988) and Atkinson and Silva (2000), low-cut filter frequencies are gradually increased until the displacement waveforms do not contain long-period fluctuations that run along the total record length or any other physically unjustifiable variation such as ending with very large displacements.

For this study, a simplified form of data processing scheme is applied. Logic tree of the applied procedure can be followed with Figure 3.16 where processing scheme is explained in the flowchart manner. First of all, as an initial baseline correction, mean of the pre-event portion of the recording for digital instruments or mean of the all raw acceleration record for analog instruments is subtracted from the accelerogram according to the type of instrument.

In order to eliminate noise, low-cut filter filters and high cut filters are applied together. A procedure called “band-pass” filtering is done. The above told procedure is applied with the help of commercial program called “MatLAB”. Original codes used are written by David Boore (Earthquake Effects Project, Western Earthquake Hazards Team, USGS) that can be obtained from his internet site (U.S. Geological Survey, Homepage). These codes were used within MatLAB to automate the procedure in a user friendly environment by Sinan Akkar (Earthquake Engineering Research Center, METU).

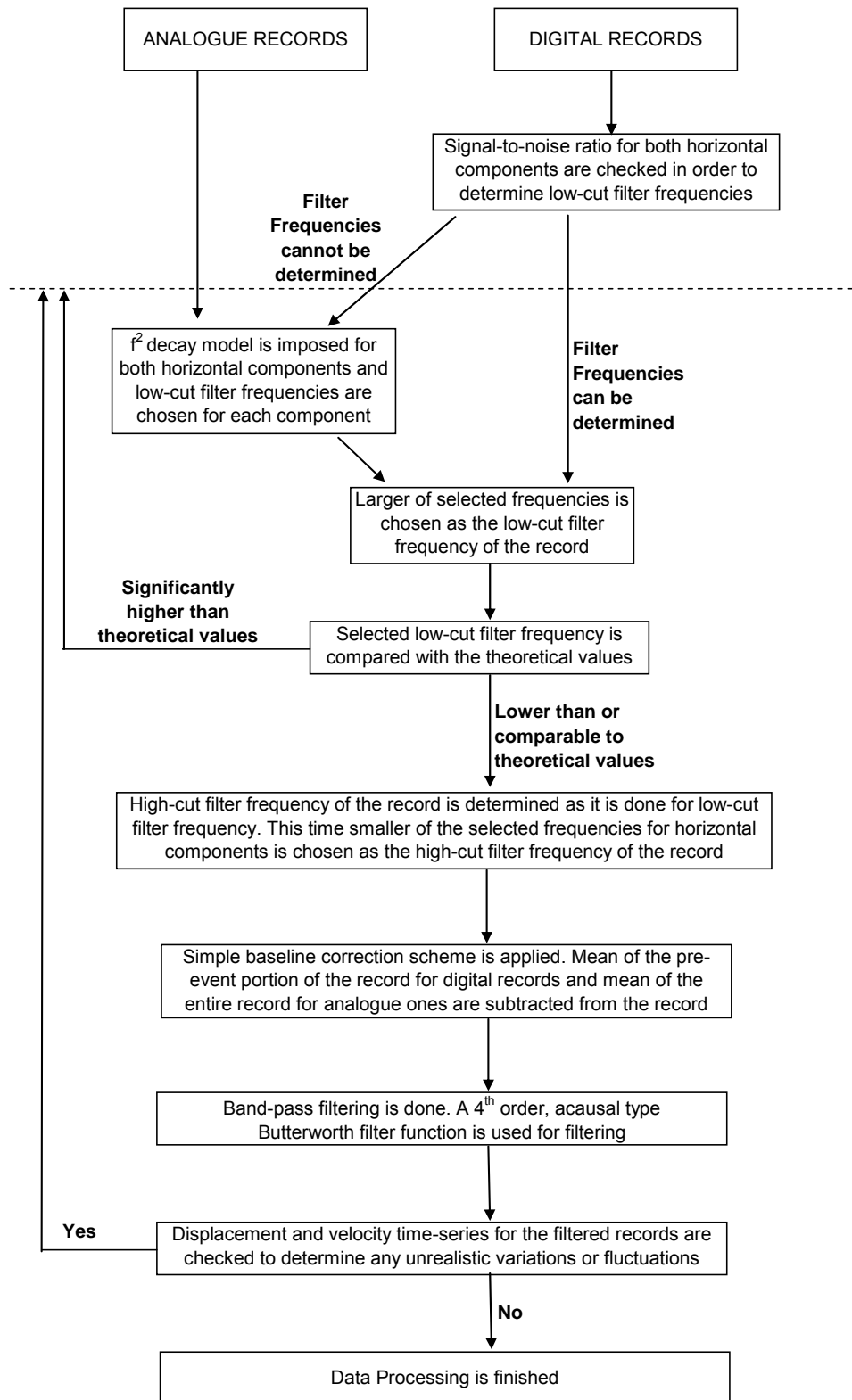


Figure 3.16 Data processing procedure applied for this study.

With some modifications, that automated procedure was applied for both analog and digital records. Since original codes dictate an embedded baseline correction scheme in the program, no baseline adjustment were made during the procedure because differences in time-series between filtering or filtering after a baseline adjustment were negligible. Unavoidably, use of this procedure exterminated residual displacements, i.e. residual displacements are all zero for the filtered records even if it is observed that the reverse is true. Since peak values are considered for this study, I believe that the outcomes are not severely distorted. In Figure 3.17, velocity and displacement time series for both baseline corrected and non-corrected applications after filtering with the same frequency cut-offs are drawn for Heybeliada Sanatoryumu N-S component record of the 17.08.1999 Kocaeli earthquake. Baseline is corrected for the time-series with sequential fits to velocity traces from 6.5 to 55 and 55 to 105 sec. Time-series obtained are quite the same especially for peak portions.

For low-cut filtering, a 4th order acausal Butterworth filter is preferred in order to have steep response curve for filter. In order to select filter frequencies, procedures described in Section 3.4.2 are applied. For digital recordings, signal-to-noise ratios are checked to see whether a filter frequency is applicable. If no filter frequency can be obtained from signal-to-noise ratio (and most of the cases did not) then an f^2 model is imposed to FAS in order to estimate the frequency where amplitude decay starts for decreasing frequencies. At the same time, theoretical filter frequencies are checked to provide the convenience. After these steps are applied for both orthogonal directions, a filter frequency for both directions is selected and applied. Generally, higher of two is selected as the filter frequency of the recording. In Appendix B.1, selected low-cut filter frequencies are given for each recording. In Figure 3.14, acceleration FAS and proposed f^2 decay models of the Göynük Devlet Hastanesi E-W component record of the 17.08.1999 Kocaeli earthquake and Yarımca Petkim Tesisleri E-W component record of the 12.11.1999 Düzce earthquake are shown. Acceleration FAS of these records and time-series after filtering are given from Figures 3.18 to 3.21. Note that, in Figures 3.19 and 3.21, dispersed lines at both end of the spectrum are the results of band-pass filtering with low and high cut filter values of 0.29 Hz - 20 Hz and 0.36 Hz - 18 Hz respectively. In Figure 3.22,

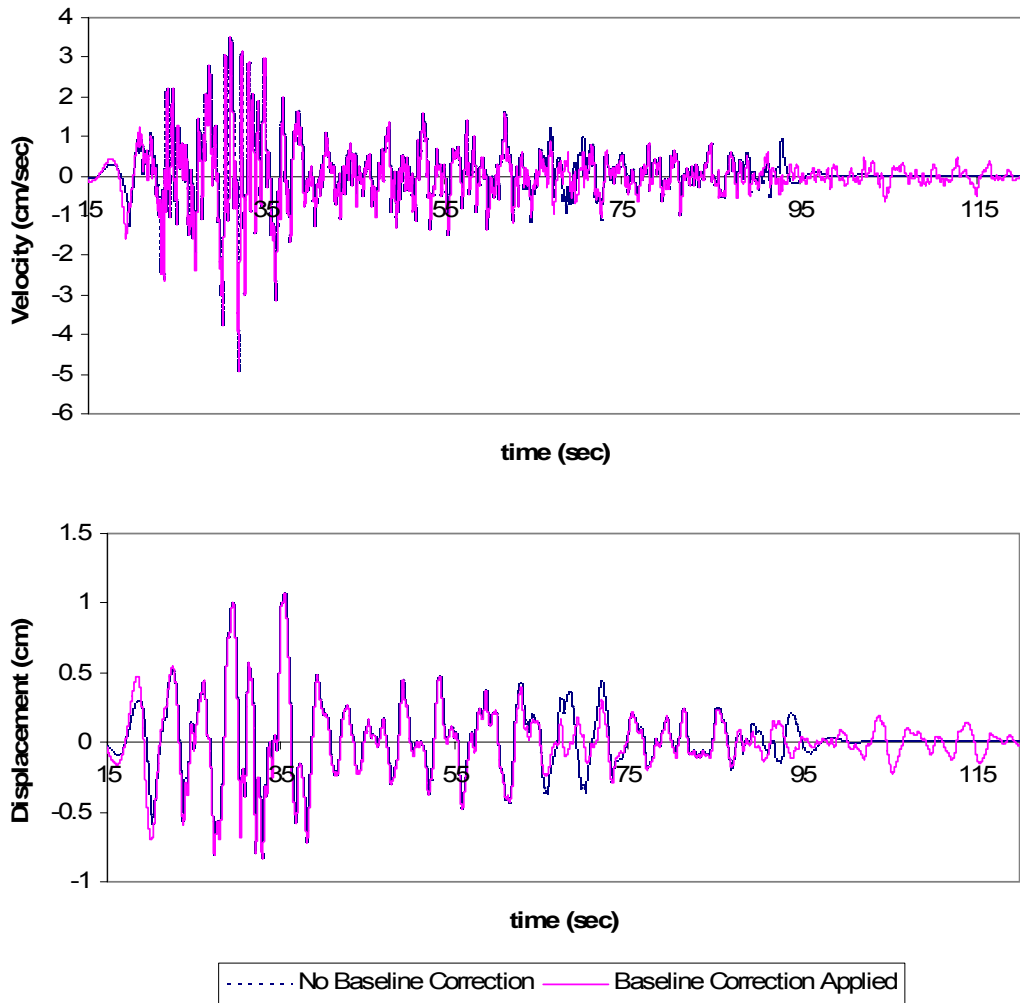


Figure 3.17 Velocity and displacement time-series of Heybeliada Sanatoryumu N-S component record of the 17.08.1999 Kocaeli earthquake after filtering for both baseline corrected and non-corrected data.

theoretical corner frequencies obtained from Joyner and Boore (1988) and Atkinson and Silva (2000) models compared with selected low-cut filter frequencies are displayed. Extracting 1999 Kocaeli and Düzce events that are large magnitude with low theoretical filter frequency earthquakes (filtering with that low frequencies are practically do not yield meaningful time-series), analog instruments are filtered by frequencies higher than theoretical Joyner and Boore (1988) frequencies, but they are within the limits of theoretical Atkinson and Silva (2000) double corner frequency model. On the contrary, digital instruments are generally filtered by frequencies that are smaller than theoretical single corner frequencies. Generally, filter frequencies are within acceptable limits considering theoretical filter frequencies.

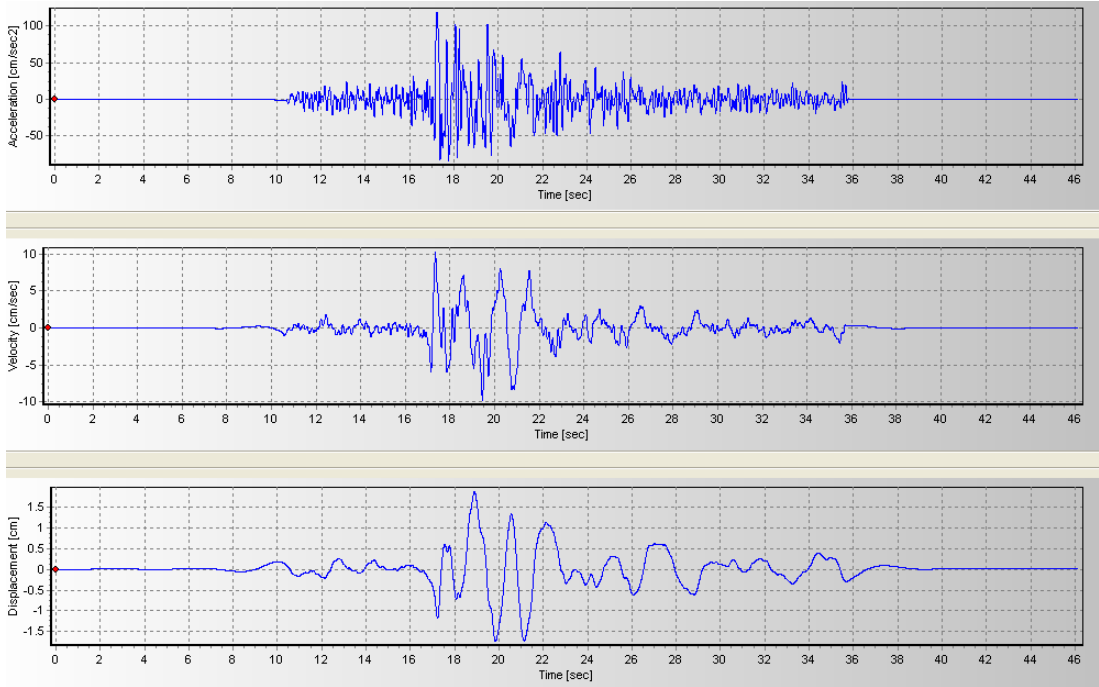


Figure 3.18 Corrected acceleration, velocity and displacement time series of Göynük Devlet Hastanesi E-W component record of the 17.08.1999 Kocaeli earthquake.

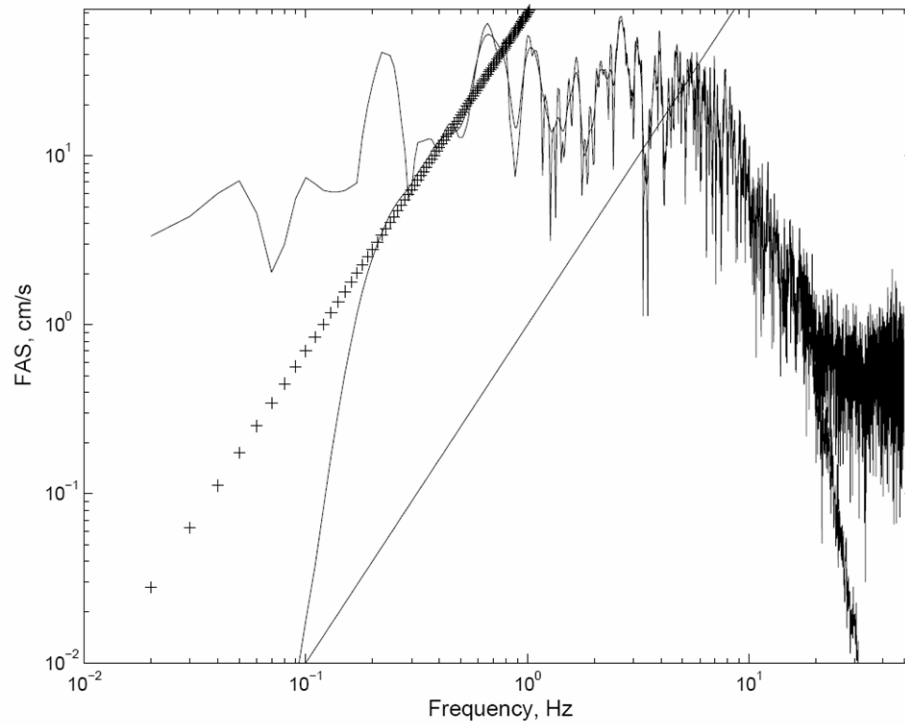


Figure 3.19 Corrected and uncorrected FAS of Göynük Devlet Hastanesi E-W component record of the 17.08.1999 Kocaeli earthquake.

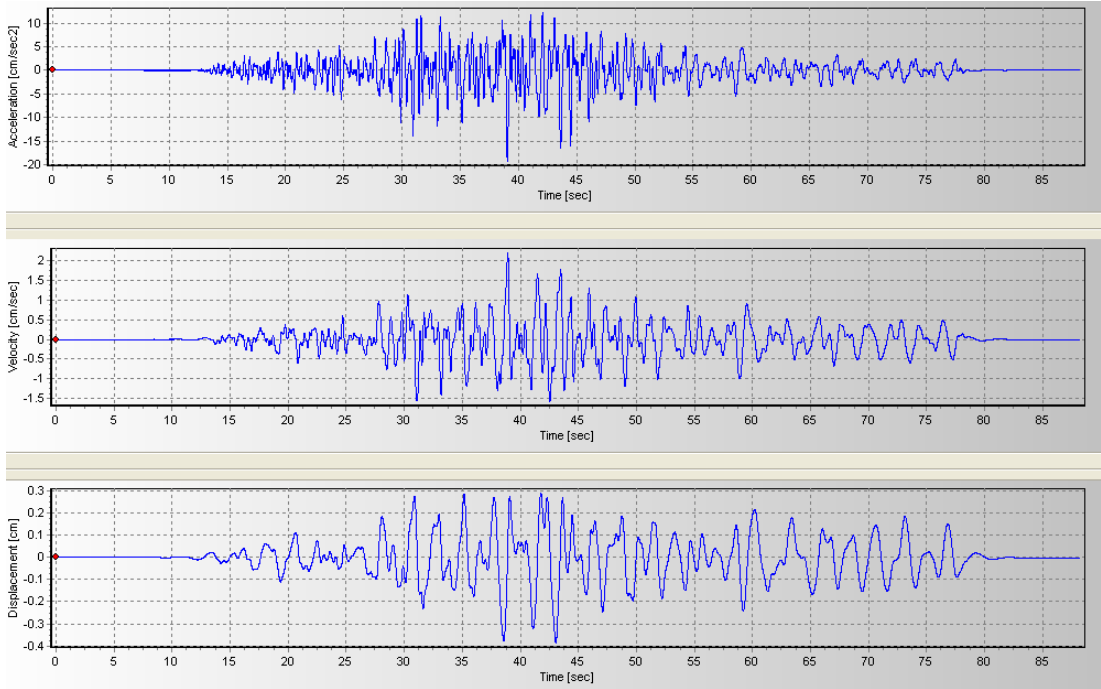


Figure 3.20 Corrected acceleration, velocity and displacement time series of Yarımca Petkim Tesisleri E-W component record of the 12.11.1999 Düzce earthquake.

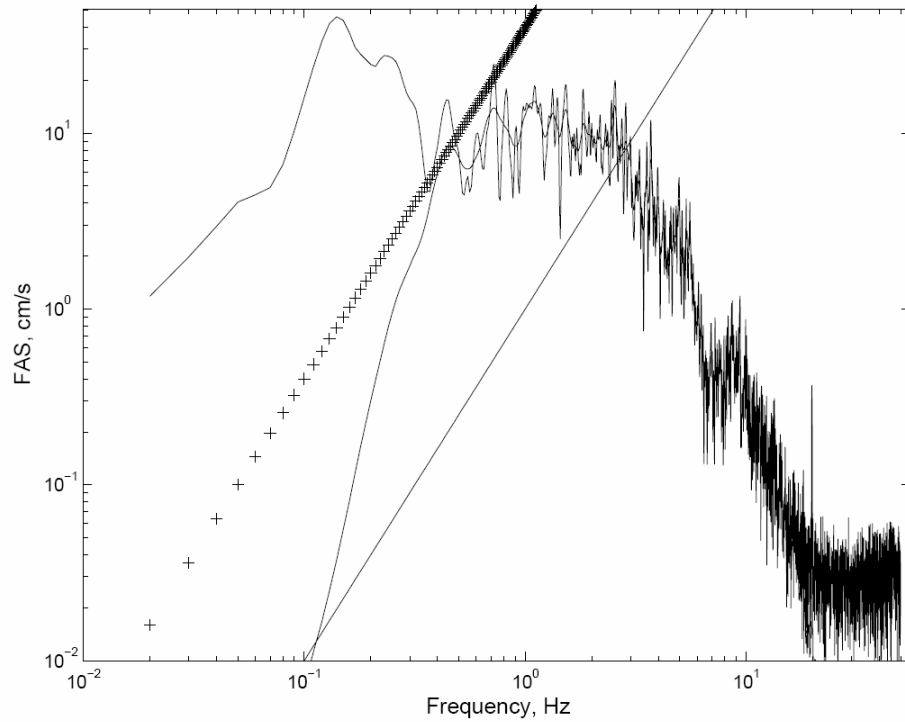


Figure 3.21 Corrected and uncorrected FAS of Yarımca Petkim Tesisleri E-W component record of the 12.11.1999 Düzce earthquake.

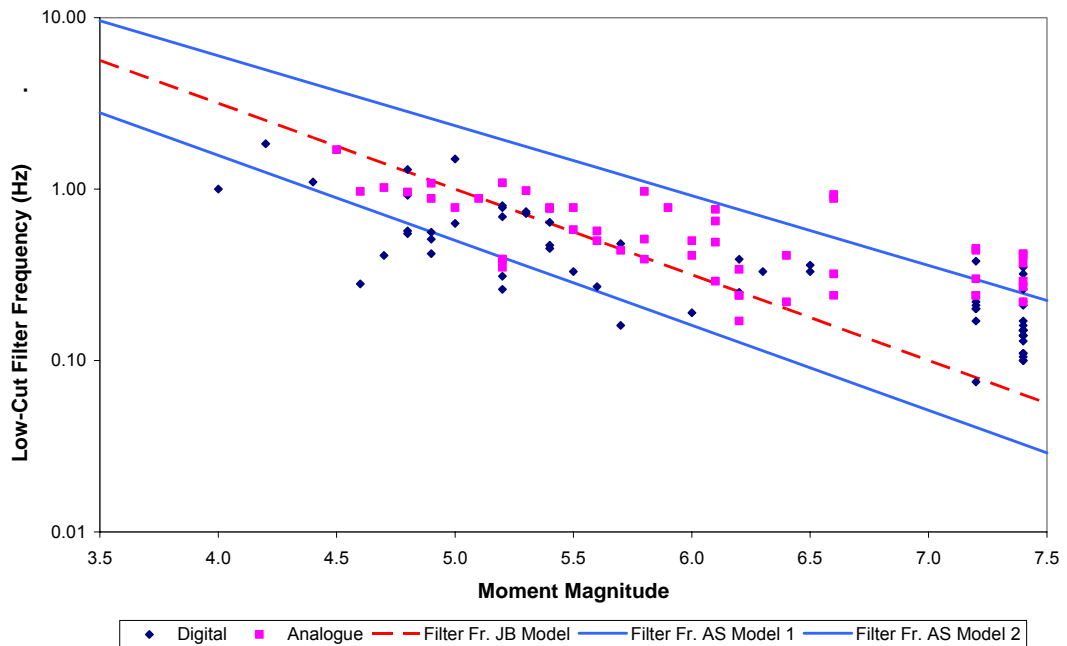


Figure 3.22 Theoretical and selected low-cut filter frequencies.

Unfortunately, subjectivity of criteria for selecting filter frequencies and application of different methodologies yield different choices for low-cut filter frequencies. In Figure 3.23, selected low-cut filter frequencies for different researches are shown for the 1999 Kocaeli earthquake. As a general trend, it can be said that PEER Center applied low filter frequencies compared to the other researches and harsh filters selected by Zare and Bard (2002) are noticeable. Inevitably, these differences are reflected to the PGV's obtained. In order to visualize the sensitivity of obtained results with respect to selected low-cut filter frequencies, Göynük Devlet Hastanesi E-W component record of the 17.08.1999 Kocaeli earthquake is also filtered with filter frequencies suggested by ESMD, PEER and Zare and Bard (2002). As mentioned before, this record is filtered by 0.29 Hz. Other filter frequencies are 0.45, 0.06 and 0.77 Hz for ESMD, PEER and Zare and Bard (2002) respectively. Obtained velocity and displacement traces are plotted in Figure 3.24. Peak values for velocity and displacement traces varies from 9.07 cm/s to 13.33 cm/s for velocity and 0.9 to 4.48 cm for displacement. Note that each trace has different pad lengths because of different filter frequencies. These pads are removed

from the traces while plotting for convenience. Researches have shown that digital records are less sensitive to deviations in filter frequencies considering differences in the outcome (Akkar and Bommer, 2006b).

For high-cut filtering, acceleration FAS of signal and noise (if it exists) are observed. Fluctuations within decaying character of amplitudes of FAS as frequency increased or dominance of noise content over signal are examined to identify the filter frequency. Selected high-cut filter frequencies are given for each recording in Appendix B.1. In Figure 3.14, acceleration FAS of both analog and digital accelerographs can be observed as an example. Both FAS has a flat plateau beyond a frequency level and for the digital accelerogram, noise dominates the signal FAS.

3.6. PEAK GROUND VELOCITY

Peak ground velocities of earthquakes commonly used as a measure of intensity of the ground motion and in energy related analysis of structures (Bommer and Alarcon, 2006). PGV for a given component of motion can not determined from the raw data of the records. To be able to use PGV data as a variable for further analysis, processing of the raw data must be done. Therefore, obeying the principles explained in the previous chapters, all data set of 223 components from 112 records obtained from main shocks of 57 earthquakes are processed. Selected cut-off frequencies for each component of the records and obtained corrected PGV dataset is given in Appendix B.1.

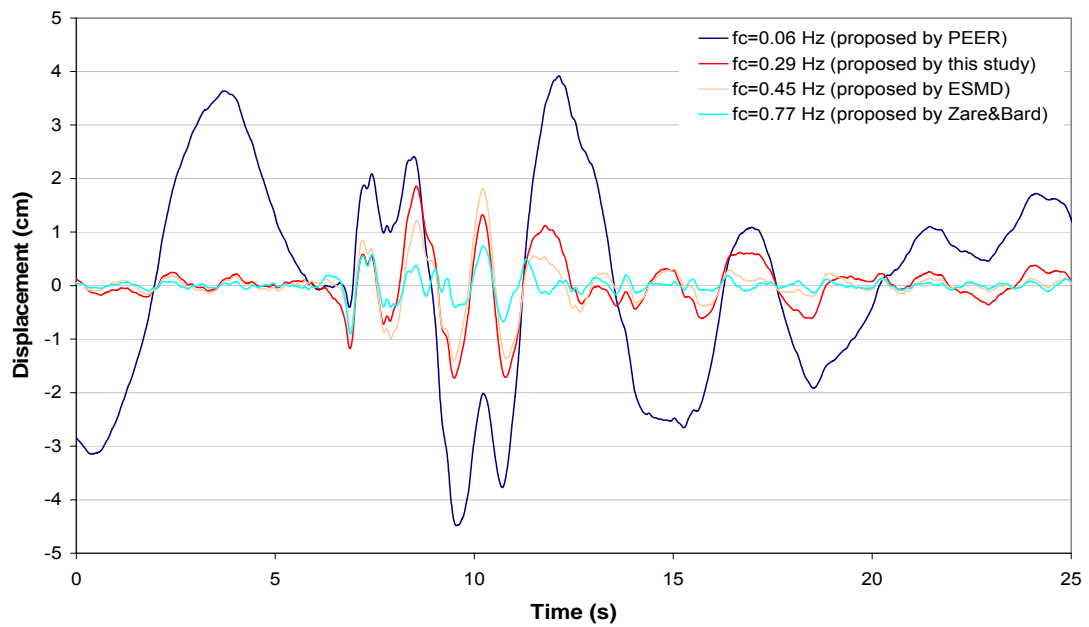
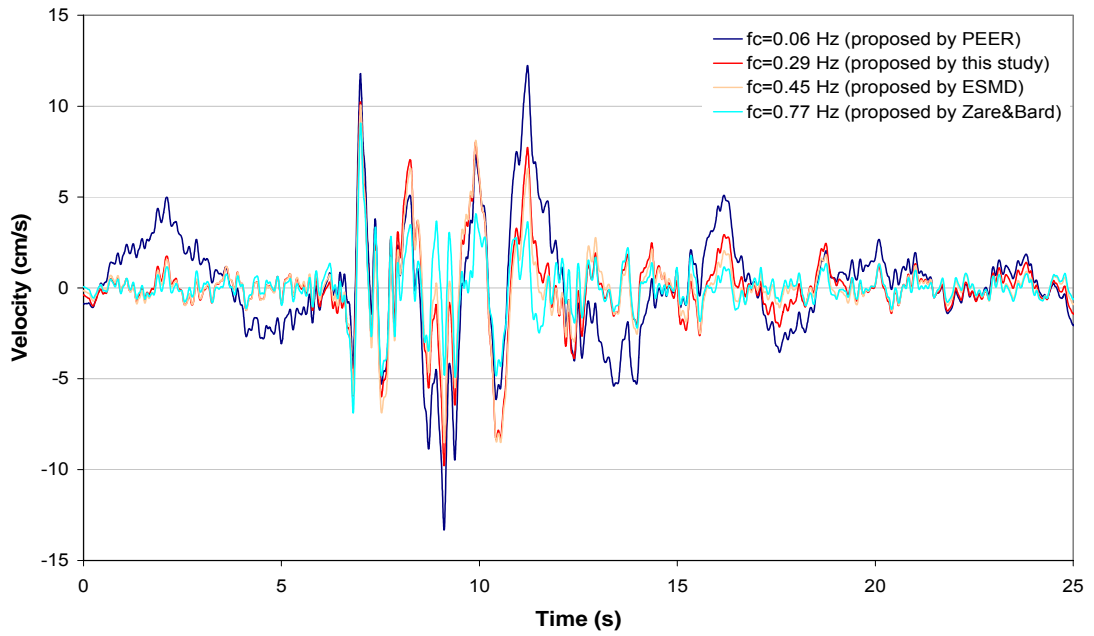


Figure 3.24 Velocity and displacement time series of Göynük Devlet Hastanesi E-W component record of the 17.08.1999 Kocaeli earthquake for different low-cut filter frequencies.

CHAPTER 4

DERIVATION OF GROUND MOTION PREDICTION EXPRESSION

4.1. GENERAL

Attenuation of peak values of ground motions has been studied extensively since 1970s. Since force methods are traditionally used to analyze structures in earthquake engineering, primarily desired characteristic of possible ground motion is the peak acceleration, which is easily converted to force terms. Therefore, attenuation relationships for PGA are by far the most studied objective. According to the worldwide summary of attenuation relationships, 141 attenuation relationships for PGA are developed within the period 1969-2002 (Douglas, 2001).

Attenuation relationships for PGV are scarce when compared to PGA. There are less than 30 relationship developed for PGV up to now (Bommer and Alarcon, 2006; Akkar and Bommer, 2006a) There are basically two reasons behind this fact. Firstly, using PGV as a tool for engineering purposes is a rather new subject when compared to PGA. Although limited now, using PGV in earthquake engineering seems to increase in near future. A number of areas where PGV can be used are given in Section 1.4. Second reason is the necessity of data processing for the used database before developing attenuation relationships. Besides data processing is a time consuming and laborious exercise, obtained results are questionable due to unavoidable subjectivity involved. Data processing is explained in detail in Chapter 3.

Either for PGA or PGV, to be able to construct the attenuation relationship, first of all, suitable model to analyze the data obtained has to be chosen. For all the attenuation relationships derived, regression analysis is used as the statistical tool since it provides a conceptually simple method for investigating functional relationships among variables. The standard approach in regression analysis is to use

a sample data to compute an estimate of the proposed relationship, and to evaluate the fit using terms as Coefficient of Determination, R^2 and Coefficient of Variation, σ^2 . The relationship is expressed in the form of an equation connecting the response or dependent variable y (in our case PGV), and one or more independent variables x_1, x_2, \dots, x_n (in our case magnitude, site geology, distance, etc.). Then regression equation, takes the form,

$$y = b_0 + b_1x_1 + b_2x_2 + \dots + b_nx_n \quad (4.1)$$

where $b_0, b_1, b_2, \dots, b_n$ are called regression coefficients and are determined from the analysis (Chatterjee, 1977). In statistics, numerous regression models exist for evaluating the relationship between any pair of variables, including models for linear and nonlinear relationships and normal or non-parametric distributions of data.

In this study, the coefficients in the equations for predicting ground motion were determined by least squares nonlinear regression procedure. Nonlinear regression is a method of finding a nonlinear model of the relationship between the dependent variable and a set of independent variables. Unlike traditional linear regression, which is restricted to estimating linear models, nonlinear regression can estimate models with arbitrary relationships between independent and dependent variables (SPSS Manual, 2004). This is accomplished using iterative estimation algorithms. When applying regression analysis, those parameters should be quantitative in the data set.

In this chapter, model adequacy and variance estimation, development of attenuation relationship for PGV, comparison of constructed relationship with other relationships and reliability of obtained results are presented and discussed in detail.

4.2. MODEL ADEQUACY CHECK

Although sum of the squares of the residuals does give an idea about how well the fit is for the developed equation on comparison basis, model adequacy check

is done to evaluate the goodness of fit in statistical fashion. A quantity, termed as the *coefficient of determination* (R^2) is used for checking of analysis results and shows quality of the curve fitting process. It can be determined by using the Equation (4.2) (Chatterjee, 1977);

$$R^2 = 1 - \frac{RSS}{CSS} = 1 - \frac{ResidualSumofSquares}{CorrectedSumofSquares} = 1 - \frac{\sum_{j=1}^n (\hat{y}_i - y)^2}{\sum_{j=1}^n (\hat{y}_i - \bar{y})^2} \quad (4.2)$$

where

$\hat{y}_i - y$ = Difference between i^{th} predicted value and observed value.

$\hat{y}_i - \bar{y}$ = Difference between i^{th} predicted value and mean value.

R^2 values are given for each attempt to improve the fit process in the development phase of attenuation relationship.

4.3. ESTIMATION OF VARIANCE

To be able to use the prediction equations with confidence, standard deviation of the models from mean values should be determined. The unbiased estimator, σ^2 , expresses variations in the residuals. The formula for σ^2 is given by Equation (4.3) (Kalkan, 2001).

$$\sigma^2 = \sum_{i=1}^n \frac{(y_i - \hat{y}_i)^2}{n - p} \quad (4.3)$$

In this formula, $y_i - \hat{y}_i$ denotes the difference between i^{th} observed value and predicted value, ‘n’ represents the number of data used in regression analysis and ‘p’ is the number of parameters estimated. The σ^2 values are given for each attempt to improve the fit process in the development phase of attenuation relationship.

4.4. DEVELOPING ATTENUATION RELATIONSHIP

4.4.1. CONSTITUTION OF THE METHODOLOGY

In order to develop an attenuation relationship, the form of the equation should be determined first. Instead of constructing a new form of relationship, modifying the proposed relationships that have been studied earlier is preferred since these forms reflect a virtue of the past experiences and studies.

Within the previous studies shown in Table 1.1, five equations are selected to be studied. These are Joyner and Boore (1981) (JB81), Sabetta and Pugliese (1996) (SP96), Tromans and Bommer (2002) (TB02), Pankow and Pechmann (2004) (PP04) and Akkar and Bommer (2006a) (AB06). The basic principle behind this choice is the terminology used for distance definitions. All of these equations use r_{jb} as the distance term that coincides with the terminology in the database used for this study. Functional forms of these equations are given in Table 4.1. Note that the original forms of these equations are modified to account for the properties of the dataset which will be explained in the following paragraphs where properties of the given studies are investigated.

In their study, Joyner and Boore (1981) restricted their dataset to California and shallow earthquakes. Their functional form uses a magnitude-independent shape based on geometric spreading and anelastic attenuation. Actually, Joyner and Boore (1981) expression is the only one that allows anelastic attenuation within the grouped studies examined here. Soil classification is made as rock and soil. Sites described by such terms as “granite,” “diorite,” “gneiss,” “chert,” “greywacke,” “limestone,” “sandstone,” or “siltstone” are grouped as rock and “alluvium,” “sand,” “gravel,” “clay,” “silt,” “mud,” “fill,” or “glacial outwash” as soil. For the regression analysis made, rock site are used as rock and soil and stiff soil sites are grouped as soil sites.

Sabetta and Pugliese (1996) used Italian strong-motion data with magnitude scale of M_s for M_s is greater than 5.5 and M_L for the rest. Maximum M_s value used for the analysis is 6.8, which is significantly lower than the maximum value of M_s

within the database used; M_s of the 1999 Kocaeli earthquake is 7.8. Note that with the usage of M_s to M_L conversion, the magnitude values do not vary from moment magnitude values significantly (see figure 2.2). Both epicentral and Joyner-Boore distances are used for the equation given. For the site classification, three categories are defined as stiff ($V_{s30} > 800$ m/sec), shallow alluvium (H is less or equal to 20 m) and deep alluvium (H is greater than 20 m) (400 m/sec $< V_{s30} < 800$ m/sec. for alluvium sites). Although it is not mentioned, use of the same coefficient for the alluvium sites depicts the unified alluvium site classes for PGV. For the regression analysis made, rock site are used as rock and soil and stiff soil sites are grouped as soil sites.

Tromans and Bommer (2002) used 51 European earthquakes to develop the relationship with surface-wave magnitudes between 5.5 and 7.9. Three site classes are defined based on average shear-wave velocity: $V_{s30} \geq 750$ m/sec for rock sites, $V_{s30} \leq 360$ m/sec for soft soil sites and soil sites between these levels. This classification is quite similar to the one suggested by this study: $V_{s30} \geq 700$ m/sec for rock sites, $V_{s30} \leq 300$ m/sec for soil sites and stiff soil sites between these levels.

Table 4.1 Functional forms of relationships considered.

Study	Functional Form
<i>JB81</i>	$\log PGV = C_1 + C_2M - \log\left(\sqrt{C_3^2 + r^2}\right) + C_4\sqrt{C_3^2 + r^2} + C_5S$
<i>SP96</i>	$\log PGV = C_1 + C_2M - \log\left(\sqrt{C_3^2 + r^2}\right) + C_4S$
<i>TB02</i>	$\log PGV = C_1 + C_2M + C_3 \log\left(\sqrt{C_4^2 + r^2}\right) + C_5S_1 + C_6S_2$
<i>PP04</i>	$\log PGV = C_1 + C_2(M - 6) + C_3 \log\left(\sqrt{C_4^2 + r^2}\right) + C_5S$
<i>AB06</i>	$\log PGV = C_1 + C_2M + C_3M^2 + (C_4 + C_5M) \log\left(\sqrt{C_6^2 + r^2}\right) + C_7S_1 + C_8S_2$

For their study based on worldwide records, Pankow and Pechmann (2004) used the database of Spudich *et al.* (1999) for extensional tectonic regions. The dataset includes many records from Europe, particularly Italy and Greece (Akkar and Bommer, 2006a). Their use of constrained magnitude scaling for the functional form is criticized for not being suitable for areas that are not extensional such as southern Europe, North Africa and Middle East Greece (Akkar and Bommer, 2006a). Site classification is made on two broad areas as rock and soil. V_{rock} is defined as 910 m/sec which is significantly higher than the value used for this study. On the other hand, V_{soil} is defined as 310 m/sec. Horizontal component is defined as geometric mean, which makes the comparison with other equations unreliable since other studies including this study, use larger component (Akkar and Bommer (2006a) used both terminologies). Note that, quadratic term in magnitude scaling is eliminated for PGV in the functional form (Pankow and Pechmann, 2004).

In their recent study, Akkar and Bommer (2006a) updated Tromans and Bommer (2002) due to its weaknesses as described in preceding part. 133 earthquakes from Europe and Middle East with 532 strong-motion accelerograms are used for the study. Same site classification of Tromans and Bommer (2002) is used for this study as well. Quadratic magnitude scaling and magnitude dependent spreading terms are added to the functional form. Anelastic attenuation term was examined but eliminated since it was understood that dataset is insufficient to simultaneously constrain this term and geometric spreading, yielding positive values of the coefficient for anelastic attenuation (Akkar and Bommer, 2006c). Original form does include influence of style-of-faulting. Since no such differentiation is made for this study, these terms are eliminated from the form and comparison is made accordingly.

In Figure 4.1, prediction curves for these equations are given for moment magnitudes 7.5, 6.5 and 5.5. Necessary conversions are made to plot the graphs: magnitude conversions for SP96 and TB02 are made obeying the equation given by Ambraseys and Free (1997) as

$$M_w = 4.749 - 0.337M_s + 0.093M_s^2 \quad (4.4)$$

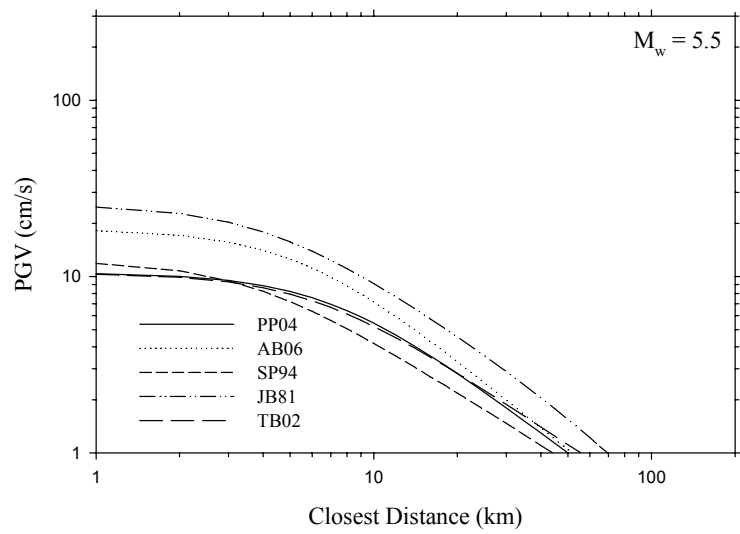
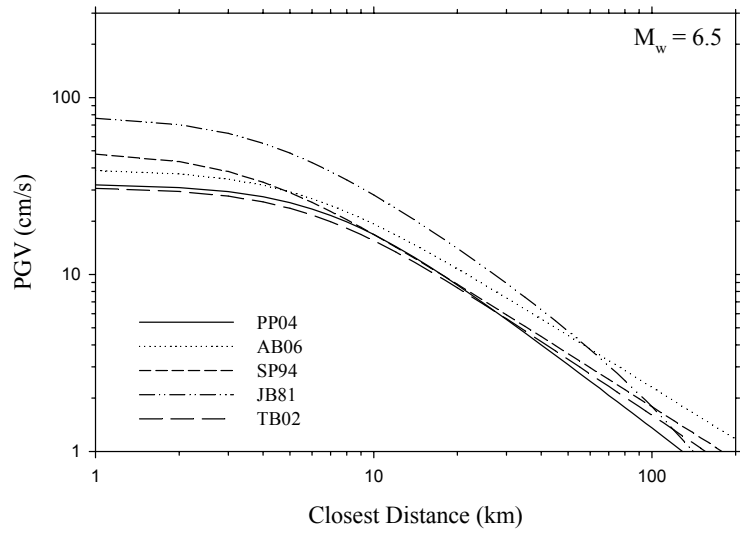
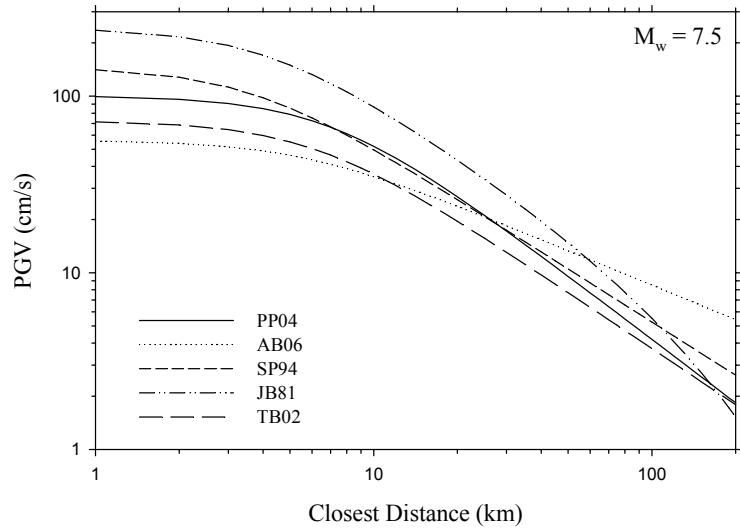


Figure 4.1 Predictive curves for 5 candidate equations for rock site conditions for $M_w = 7.5, 6.5$ and 5.5

Horizontal component conversion for PP04 is made according to the Bommer *et al.* (2005) using the 0.5 s spectral ordinate as a surrogate for PGV as proposed by Bommer and Alarcon (2006).

A striking observation made from these curves is the high values encountered for JB81, especially for earthquakes with greater magnitudes. Also SP96 exaggerate peak values when compared to the other 3 up to intermediate magnitudes. But it should be kept in mind that SP96 is not suitable for $M_w = 7.5$ since maximum magnitude covered with this study is $M_s = 6.8$ ($\approx M_w=6.76$).

Applicability of these equations for the database used is judged numerically. In Appendix C.1, goodness of fit values of the proposed relationships for their original forms can be seen. Best fit is observed for AB06 and worst fit is observed for JB81 which supports the observations that curves of JB81 seems to be unrealistic when compared to other equations. Also in Figure 4.2 residuals for the given equations are shown for mean of predicted values for five of them and for four of them excluding JB81 are displayed at the top and bottom graphs respectively. The aim of this attempt is to compare the worldwide PGV results with the database examined here. Obviously this is a debatable approach when common recordings used for different databases or different practices are considered, but it still gives an idea about the database correctness compared to their counterparts. When compared to the worldwide observations, it can be concluded that there are some inharmonious data conserved in the database. This issue will be considered in the following chapter in detail.

4.4.2. MODIFYING PROPOSED RELATIONSHIPS

After basics of the methodology are defined and proposed relationships are investigated, these relationships are modified for the database used. For statistical analysis, nonlinear least squares regression analysis is preferred which is based on the principle of minimizing sum of squares of residuals in an iterative manner.

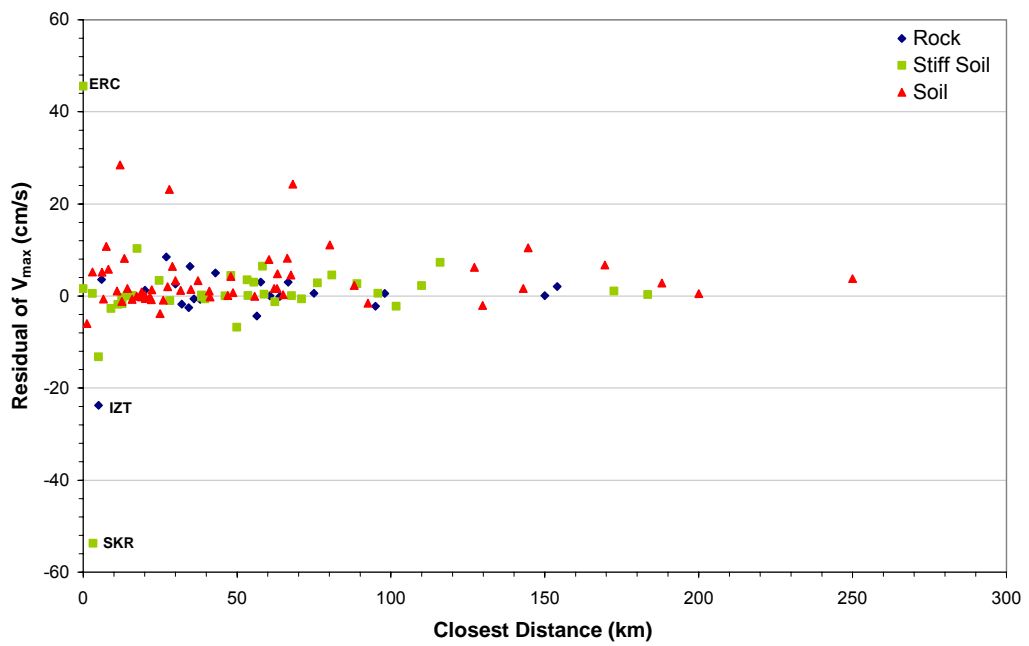
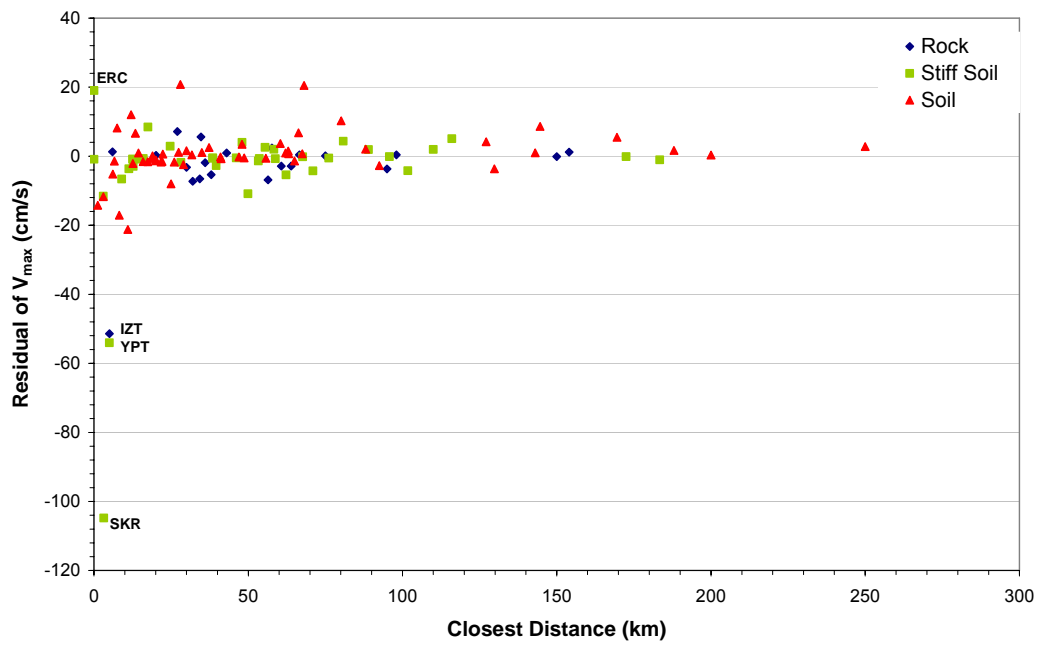


Figure 4.2 Residuals for the used database with respect to the mean of proposed relationships.

To compile the data set obtained using iterative estimation algorithm, SPSS statistical analysis software (Ver.13.0, 2004) is preferred. Among two iterative algorithms for estimating the parameters of nonlinear models, Sequential Quadratic Programming Algorithm (SQPA) and Levenberg-Marquardt Algorithm (LMA) (SPSS Manual, 2004), Levenberg-Marquardt algorithm is selected since SQPA is specifically used with constraint parameters or user defined loss functions. In the defined problem, no constraint parameters are used and default loss function (function to minimize sum of squares of residuals) is judged as adequate.

Results obtained from these analyses are given in Appendix C.1. Residuals are decreased rapidly (RSS from 6012 to 3415 for the best fitted form) and model adequacy increased significantly (R^2 from 0.75 to 0.86 for the best fitted form). Also in Figure 4.3 updated equations are plotted. In the figure, observed values are from the 1999 Kocaeli EQ with $M_w=7.4$ except (ERC) record of the 1992 Erzincan earthquake. Note that, these predictive equations are not related to their origins in any sense except for their form. As a notable feature of Figure 4.3, saturation of PGV for near-fault is lost for TB02, PP04 and AB06 formulations. When spreading is constrained as in JB81 and SP96 forms, this trend does not exist. This fact can be seen from the coefficients located inside the distance terms in Appendix C.1. The reason behind this fact is simply the scarcity of adequate data for the near-fault. The relatively simple applied algorithm has a tendency to approach the peaks of the database. Considering Figure 4.2 and 4.3 together, high PGV value of Erzincan record of the 1992 Erzincan Earthquake and unexpectedly low PGV values obtained from Sakarya and İzmit records of the 1999 Kocaeli earthquake affect the trustworthiness of the result obtained. Actually, the Sakarya record of 1999 Kocaeli earthquake is possibly defective since the N-S component of the record is lost during recording. As a result, studies done for this chapter are renewed after elimination of these three recordings.

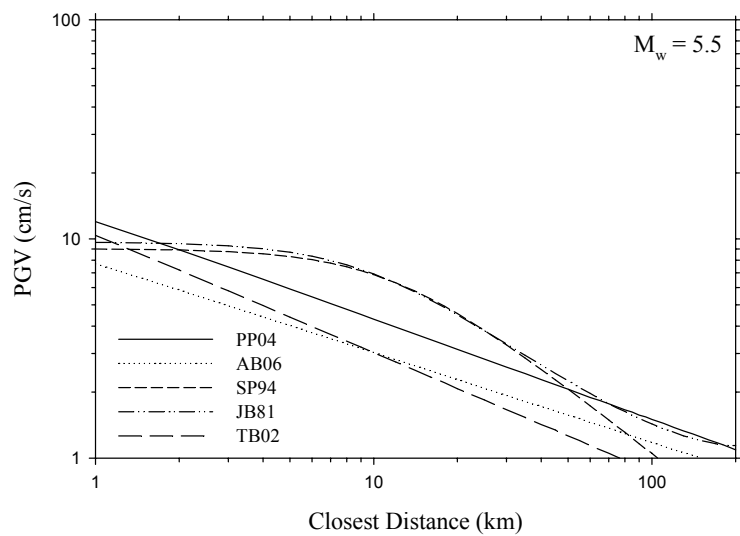
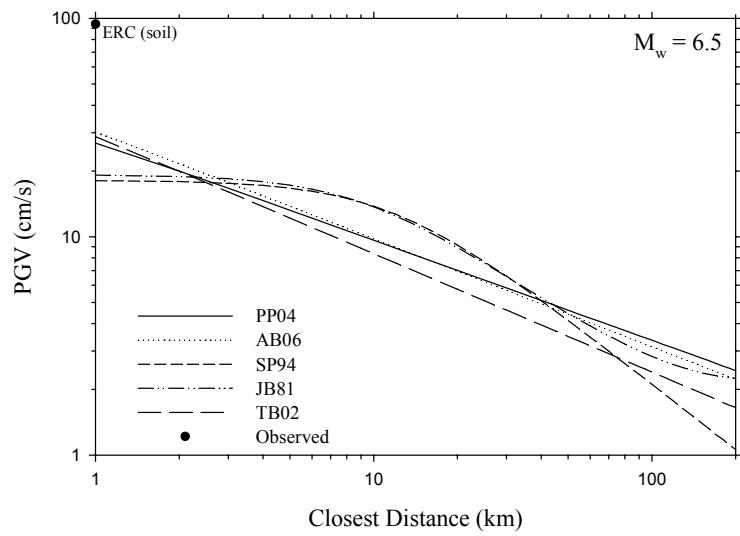
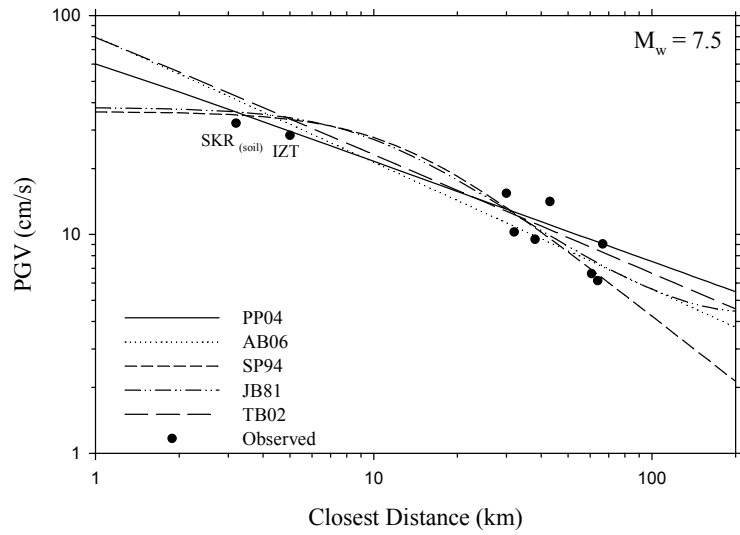


Figure 4.3 Predictive curves for five different forms of attenuation relationship for rock site conditions for $M_w = 7.5, 6.5$ and 5.5 .

4.4.3. FINALIZING THE ATTENUATION RELATIONSHIP

As a last attempt to finalize the regression analysis exercise, the reduced dataset is reanalyzed. The results obtained including finalized coefficients, sum of squares of residuals (RSS), model adequacy (R^2) and standard deviations ($\sigma_{\log PGV}$) for the expressions are given in Appendix C.1. A better fit to the database is obviously achieved. Also in Figures 4.4, 4.5 and 4.6, finalized forms of equations are plotted for rock, soil and stiff soil sites for $M_w=7.5$, 6.5 and 5.5. A number of observations can be made from numerical results and from the figures plotted:

- From adequacy checks and sum of squares of residuals, it can be concluded that equation forms of TB02 and AB06 fit analyzed dataset best. They fit the used dataset significantly better than other equations in terms of statistical values.
- Close agreement of JB81, SP96 and PP04 forms are verified by the graphical results of Figures 4.4 to 4.6. They are almost identical for all magnitudes and site classes. Limited effect of anelastic decay with positive constant for JB81 form indicates that the decaying term cannot be used for the database used here. Besides, constrained effect in the magnitude-scaling used for PP04 form does not affect the results. This can be explained in mathematical terms because the C_2 term in the PP04 relationship is multiplied by -6 summed with C_1 term is equal to C_1 term of SP96. The small difference between them is due to the C_3 term of PP04, which is close to but not equal to -1. Therefore, it can be concluded that whether or not constraints are used for magnitude scaling, same results would be obtained if a quadratic magnitude scaling term is not involved, at least for the type of analysis made here.
- In the light of above discussion above, TB02 and PP04 forms can be compared. The only difference between these two equations is the site classification. TB02 form has three classes whereas PP04 form has two. Since TB02 is one of the best fitted curves and PP04 is among other three, it can be concluded that better fits of TB02 and AB06 are basically due to their site class definitions.

- If Figures 4.4 to 4.6 are investigated for the effect of site class definitions, it can be seen that TB02 and AB06 forms have higher values for rock sites in a decreasing trend as the magnitude decreases. As expected for soil sites, these two forms have lower values than the ones with two site classes but for the soil sites the reverse hold. The reason behind this is that the two site classes forms are somewhere between the soil and stiff soil classes.
- In order to investigate the effect of quadratic magnitude scaling and magnitude spreading terms, TB02 and AB06 forms should be compared. Although their adequacies for the dataset are mathematically on the same level, significant differences can be observed in Figures 4.4 to 4.6. For high values of moment magnitudes, TB02 form seems to yield higher PGV values when compared to AB06 form. For the intermediate levels of magnitudes, reverse hold. For lower moment magnitudes, more or less the same results are obtained. Above comparison holds for distance range of up to 10 km. Above this limit, both equations yield quite similar results. Considering low value of magnitude dependent spreading term constant (C_5), it can be concluded that the reason for this difference is mainly from the quadratic magnitude scale of AB06.
- Although it is not easy to judge which equation fits better for the database used from the plotted figures, slightly lower RSS value of AB06 form and considering the fact that it is the most recent work in ground motion prediction that is applicable also to Turkey, AB06 form is concluded to be proposed as an outcome of this study.

The regression coefficients and standard deviations for AB06 prediction equation formulation that provides the best estimates for PGV for the selected database of Turkish strong ground motion are given in Table 4.2. Also in Equation 4.5 finalized form of attenuation relationship for PGV suggested by this study is given explicitly.

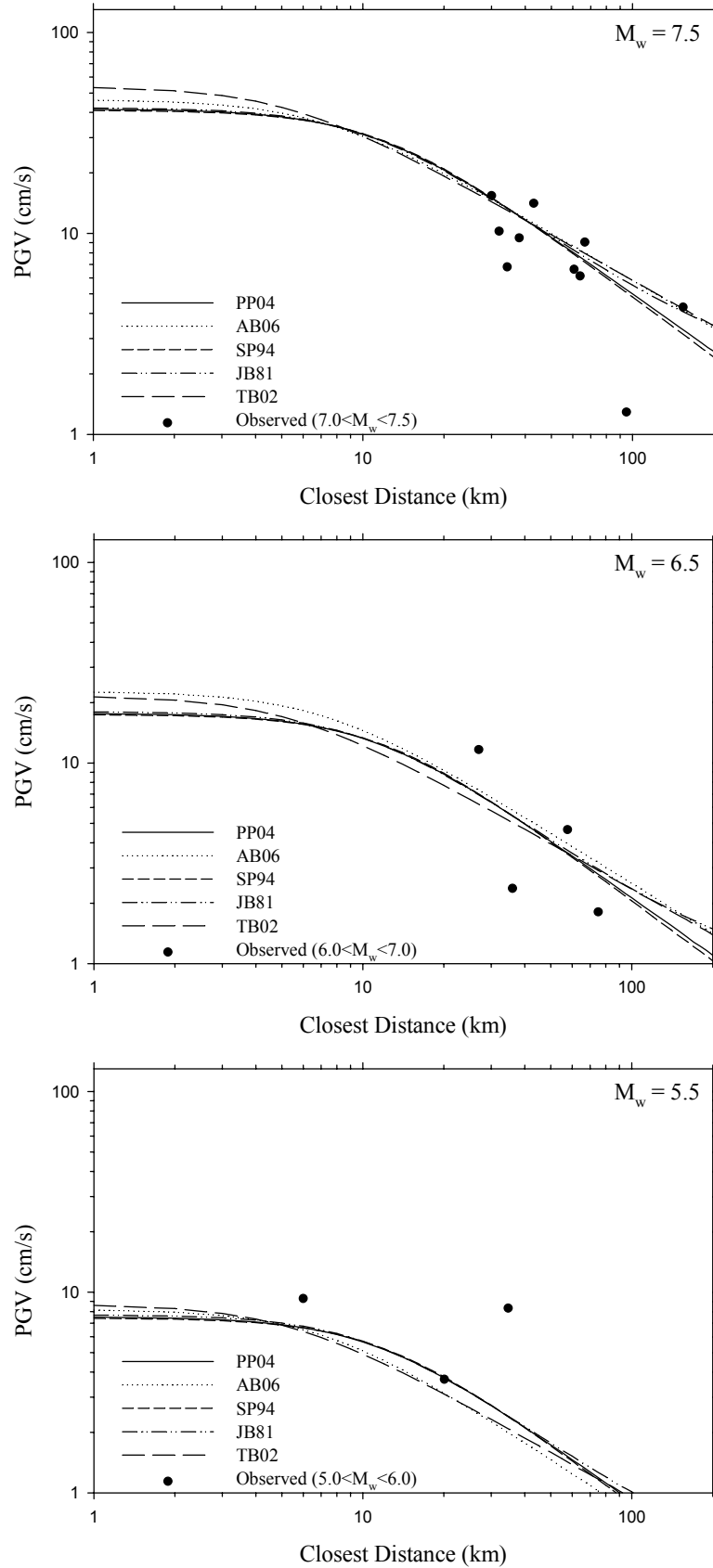


Figure 4.4 Ground motion prediction curves for five different expression forms obtained from the reduced database for rock site conditions for $M_w = 7.5$, 6.5 and 5.5.

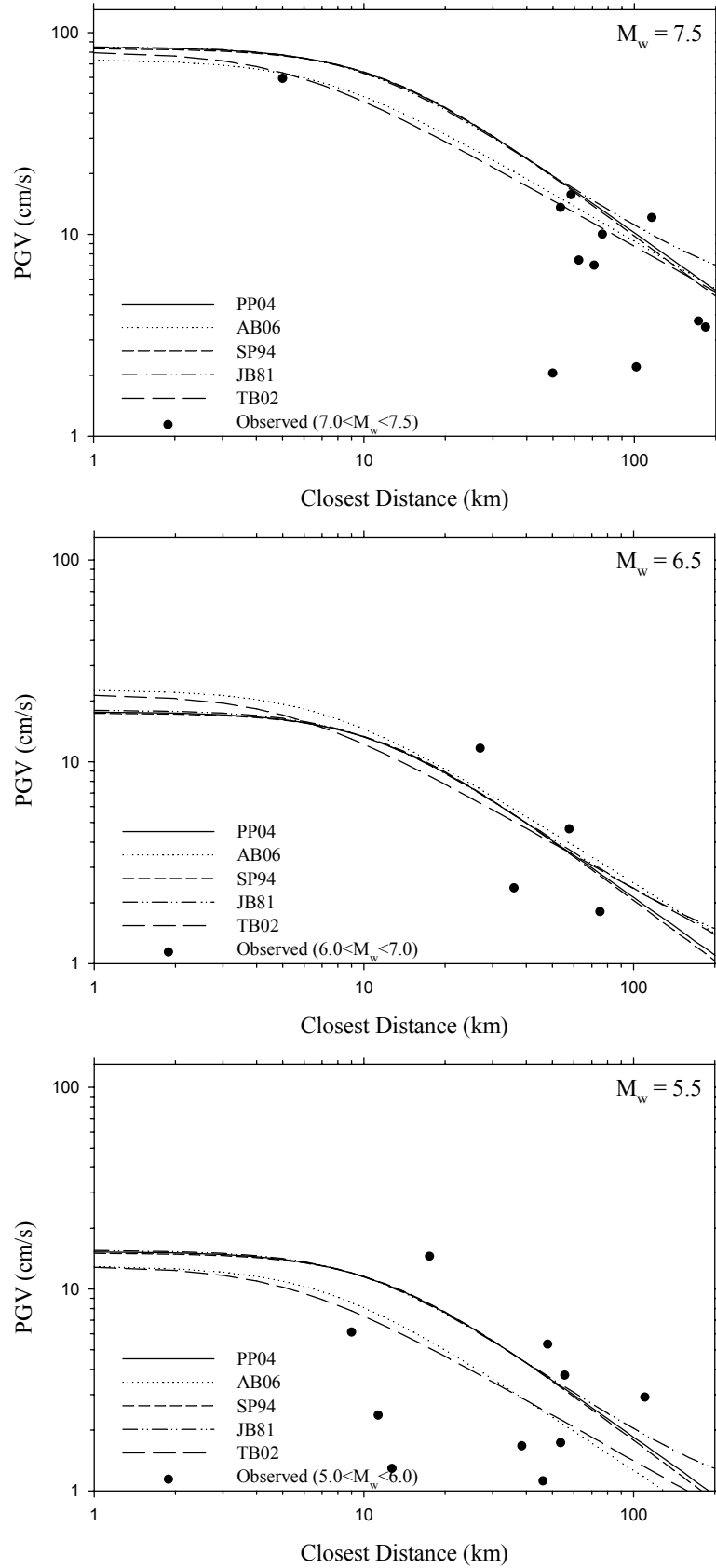


Figure 4.5 Ground motion prediction curves for five different expression forms obtained from the reduced database for stiff soil site conditions for $M_w = 7.5$, 6.5 and 5.5.

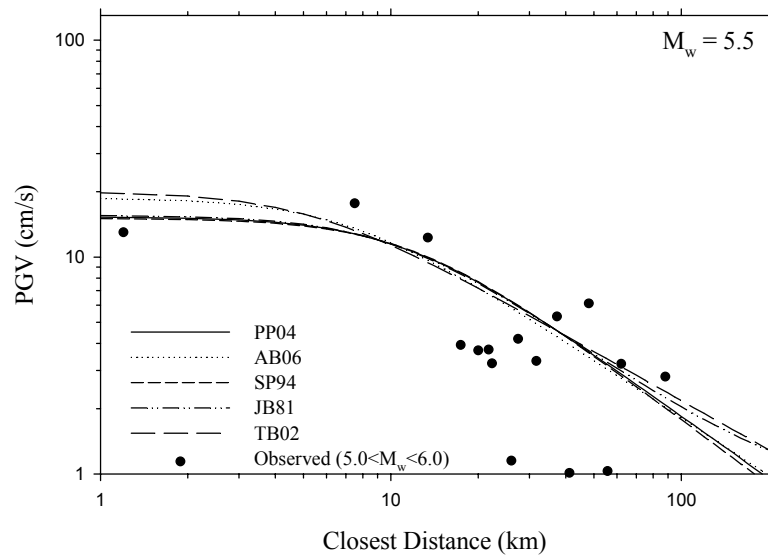
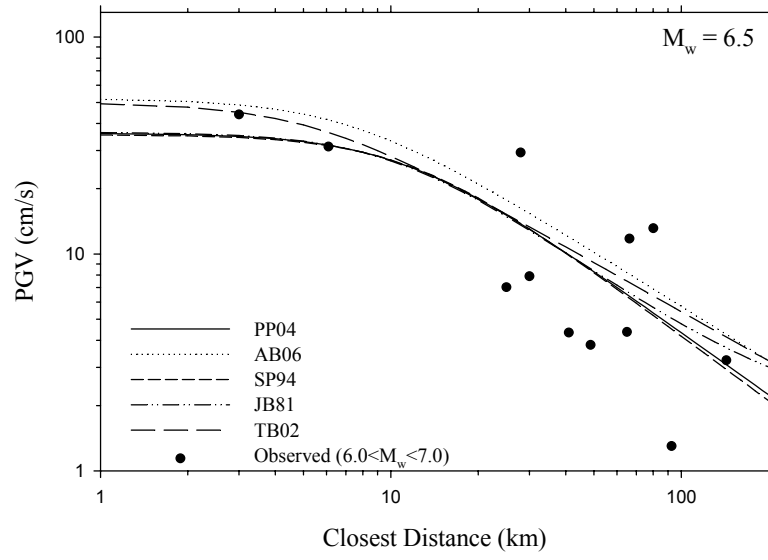
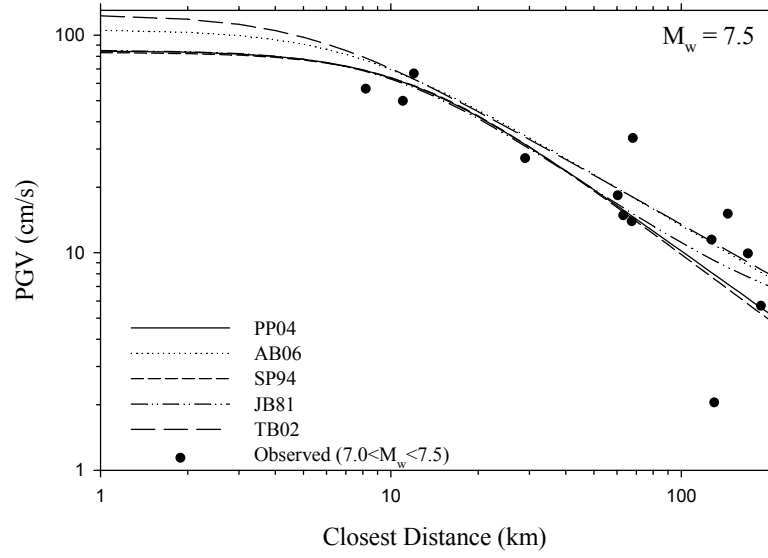


Figure 4.6 Ground motion prediction curves for five different expression forms obtained from the reduced database for soil site conditions for $M_w = 7.5, 6.5$ and 5.5 . Table 4.2 Regression coefficients and standard deviation for the prediction equation derived in this study

C1	C2	C3	C4	C5	C6	C7	C8	$\sigma_{\log PGV}$
-2.921	1.204	-0.067	-1.162	0.050	7.183	0.200	0.359	0.32

$$\log PGV = -2.921 + 1.204M - 0.067M^2 + (-1.162 + 0.05M) \log(\sqrt{7.183^2 + r^2}) + 0.2S_1 + 0.359S_2 + 0.32P \quad (4.5)$$

where M is the moment magnitude, r is the closest distance (or Joyner-Boore distance), S_1 and S_2 are the site terms where S_1 is equal to 1 for stiff soil sites and zero otherwise and S_2 is equal to 1 for soil sites and 0 otherwise. The standard deviation of this equation is encountered in this equation is $0.32P$ where 0.32 is the σ value with P being a variable that takes the value of 0 for the mean values of PGV and 1 for the 84-percentile values.

Residuals of this expression are plotted in Figure 4.7 for both distance and magnitude terms. Also shown are linear regression of residuals (LRR) of logarithm of PGV on distance and magnitude for three different site classes. Linear regression of the residuals depicts that the variation of residuals for rock sites are higher than the other two site classes. This can be committed to the range of distance and magnitude terms for rock site data that are shorter than the ones for other site classes. For the range of interest, no significant trends are observed for rock sites as well as the soil and stiff soil sites.

4.5. COMPARISON WITH OTHER GROUND MOTION PREDICTION EXPRESSIONS

Finalized form of the derived attenuation relationship (Eq. 4.5) is compared with original forms of JB81, SP96, TB02, PP04 and AB06 relationships. Necessary

arrangements for the differences in definitions of magnitude scale and distance terms are made for SP96, TB02 and PP04. Results and $\pm 1\sigma$ curves are plotted out in

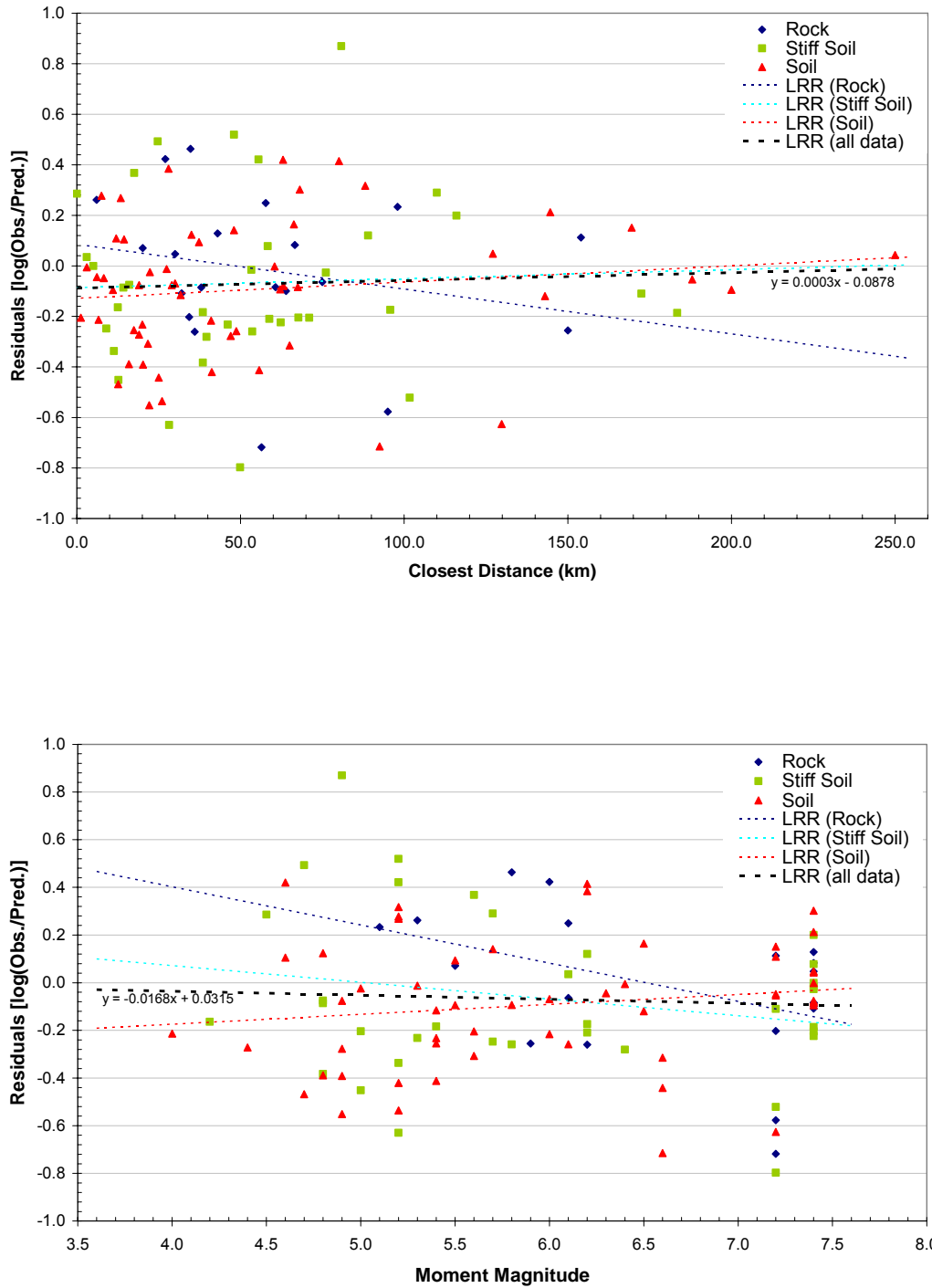


Figure 4.7 Residuals of logarithm of PGV as a function of closest distance and moment magnitude.

Figures 4.8 to 4.10. The following conclusions can be made from these figures:

- Attenuation of PGV with distance is limited when compared to the others with increasing distances. This trend is clearly observed for lower moment magnitudes. Considering soil and stiff soil sites for magnitudes 6.5 and 5.5, proposed expression overpredicts PGV for distances above 10 km when compared with the other relations (excluding JB81).
- For rock sites, the expression here underestimates the PGV to some distance and overestimates afterwards when compared to the others, which may be caused because of limited number of rock site recording. For example, rock sites contribute 33% (174/532) of all recordings for AB06 and 25% (62/249) for TB02 which is much higher than the ratio for this study (19%, 21/112).
- Very similar results are obtained for large moment magnitude ($M_w=7.5$) for this study and AB06. Dominance of Turkish recordings for $M_w>7$ for AB06 database and use of same mathematical form are the reasons for this.
- For soil and stiff soil sites with intermediate moment magnitudes ($M_w=6.5$), almost all curves (excluding JB81 and SP96) have the same peaks for near-fault distances, beyond this level relative over-prediction concerns arise as mentioned above.
- For lower moment magnitudes ($M_w=5.5$), TB02 and PP04 seem to have better agreement with the proposed relationship for near fault distances.
- High σ values can be better achieved with the help of figures. Significant differences for PGV are encountered when standard deviation is considered. Almost all curves are enveloped for a non-exceedance probability of 84.1%.

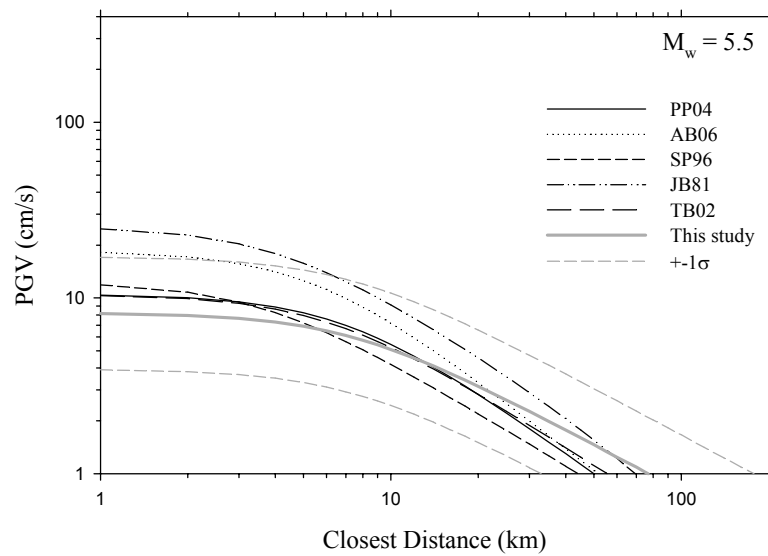
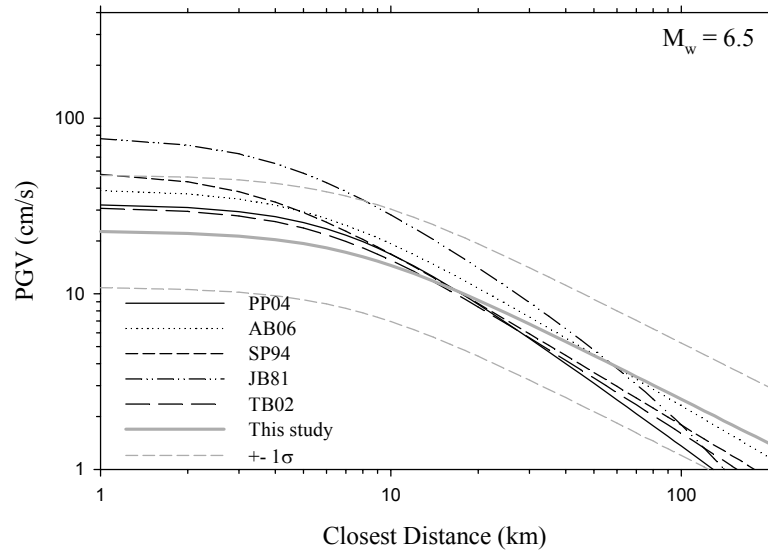
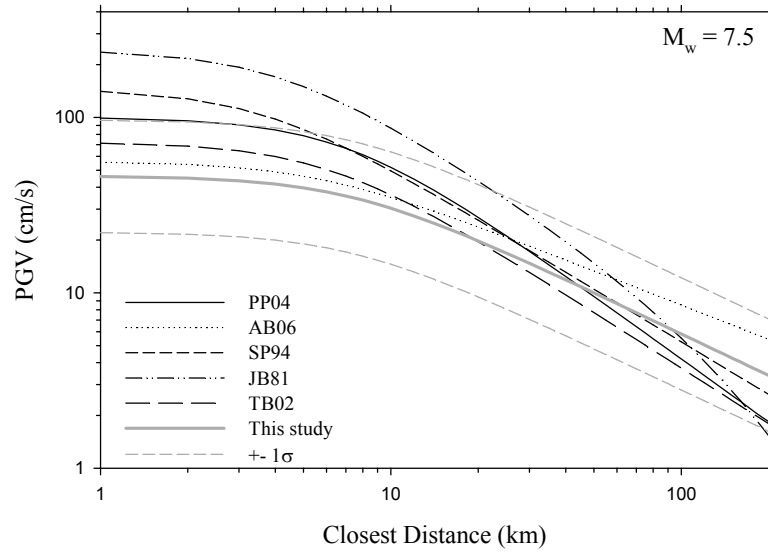


Figure 4.8 Comparison of PGV_{max} predictions of the new equation with other expressions for rock site conditions for $M_w=7.5, 6.5$ and 5.5 .

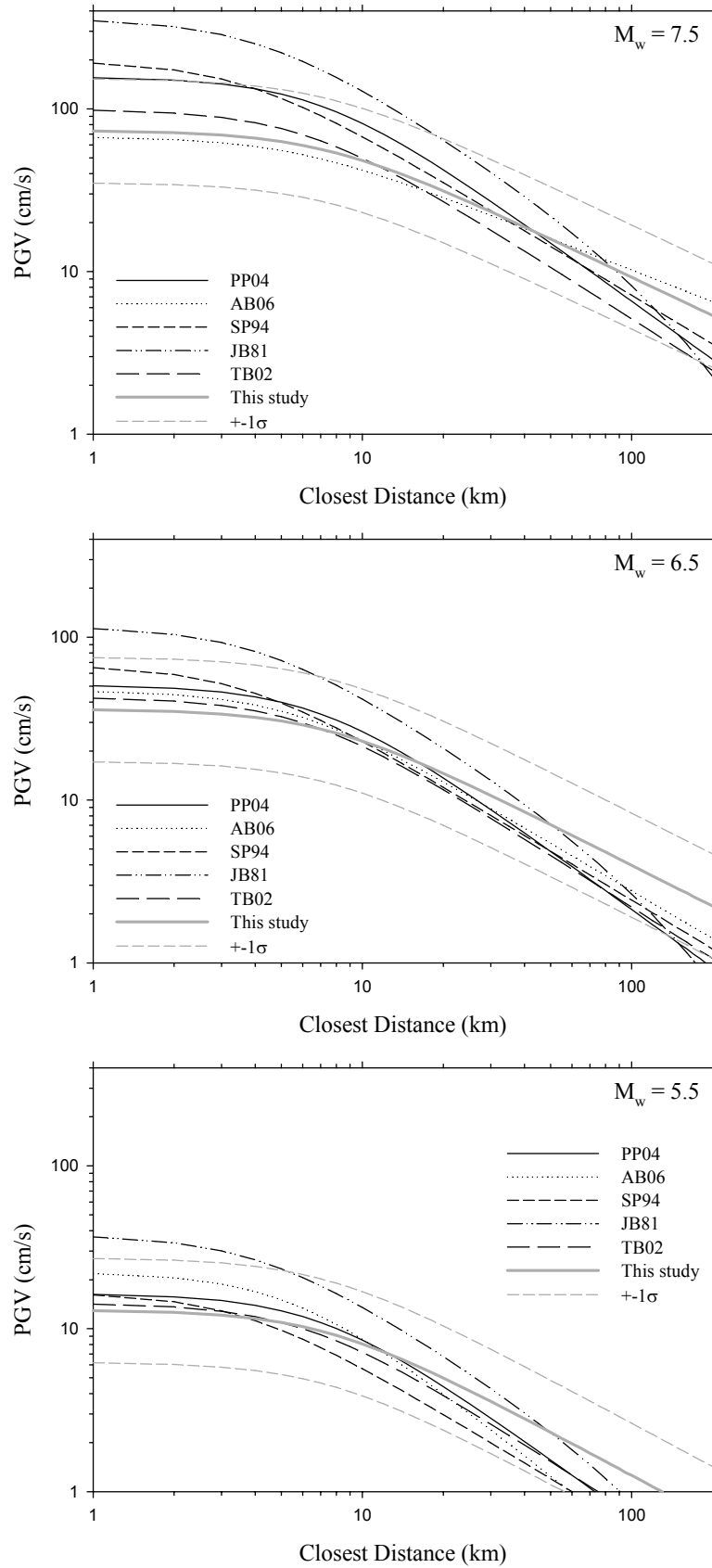


Figure 4.9 Comparison of PGV_{max} predictions from the new equation with other expressions for stiff soil site conditions for $M_w = 7.5, 6.5$ and 5.5 .

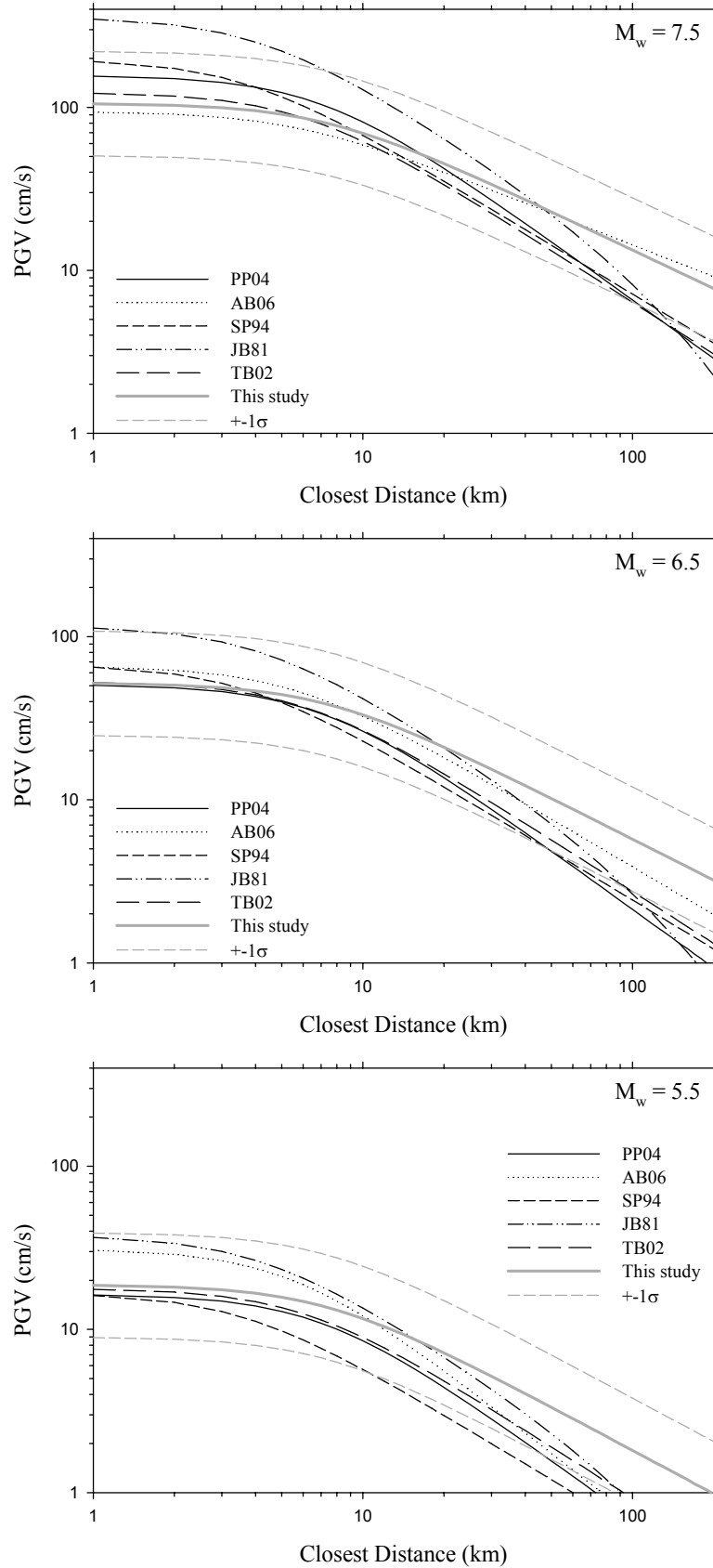


Figure 4.10 Comparison of PGV_{max} predictions from the new equation with other expressions for soil site conditions for $M_w = 7.5, 6.5$ and 5.5 .

4.6. A-POSTERIORI CHECK OF THE PROPOSED EQUATION

On 24th of October, 2006, a moderate size ($M_w=5.2$) earthquake occurred at the Gulf of Gemlik in the province of Bursa. Accuracy of the proposed prediction equation is checked for the strong ground motion records of this earthquake. In Appendix D, earthquake and station information together with the filter properties, observed and predicted peak ground velocities are given. Since closest distances can not be identified, epicentral distances either calculated from trigger time of stations or S-P wave arrival time differences are used. Although some assumptions are made to use predictive equation, a good agreement seems to be obtained. Also in Figure 4.11, predictive curves (lines) together with the observed results (dots) are plotted.

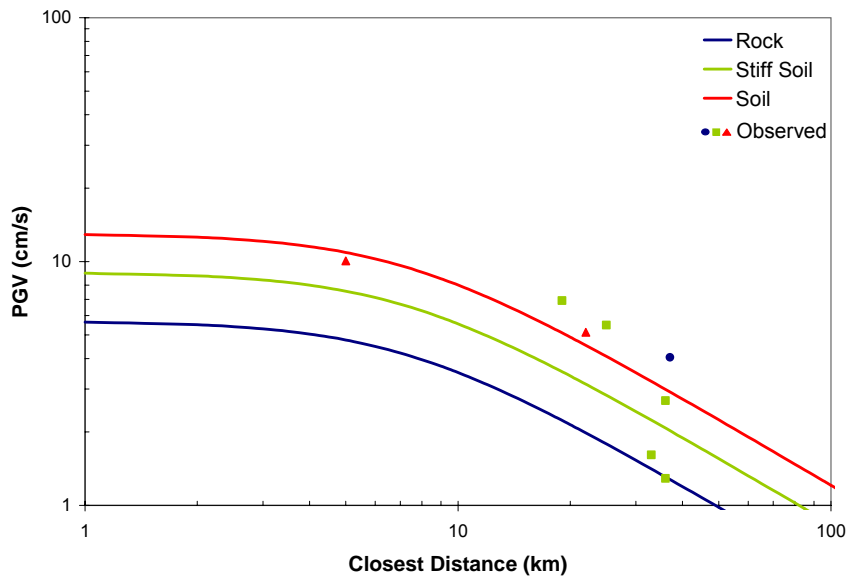


Figure 4.11 Comparison of PGV_{max} predictions of the proposed attenuation relationship with observed PGV values of the 24/10/2006 Gemlik earthquake.

CHAPTER 5

CONCLUSIONS AND RECOMMENDATIONS

A consistent set of strong ground motion data extracted from earthquakes that occurred in Turkey between 1976 and 2003 has been processed in order to develop an attenuation relationship for larger horizontal component of PGV. This may be viewed as a complementary study of Kalkan and Gülkan (2004) who used the same database to derive predictive expressions for PGA and spectral accelerations up to $T = 2$ s. The raw data is processed to eliminate noise and the corrected database is assembled. Then the filtered database is processed by using statistical methods to obtain an attenuation relationship for peak velocity that may be used in research and practical applications. The following observations, conclusions and recommendations can be proposed for the processing phase and from the results obtained.

One of the most important obstacles faced during the study was the lack of necessary local geological information about the stations. A number of attenuation relationships that may be useful to study are eliminated prematurely since they need extra information for the stations. The trustworthiness of the recordings used is also not fully assured for stations without a precise soil profile data since there is no measurable basis for the selection of their site classes. The public agency in Turkey in charge of the strong motion stations should address this drawback urgently.

Another disappointment for the author was that there is no reliable and broad database collection for strong motion records of Turkey or a classification that originated in Turkey. Unavoidably I was forced to search foreign sources to gain information about Turkish records, which is a disappointing exercise. As a result, expanding the strong motion station arrays, gaining operating information for

stations and constructing a serviceable database must be the main concerns of the people who make the decisions about these issues. Recent studies done for NSMP catalog are a milestone to overcome these deficiencies.

The difference between prediction curves before and after data elimination is consequential for near-fault where data is scarce. Near-fault records of the database are mostly obtained from two major events of 1999, i.e. Kocaeli and Düzce earthquakes, whose acceleration peak values are known to be low when compared with worldwide records. Therefore it should be kept in mind that at short distances, reliability of the prediction expression derived here appears to worsen.

The possible interdependence between moment magnitude and standard deviation has not been explored in this work because of the relatively small number of ground motion record. When future events enable this deficiency to be addressed, the records should be re-processed with this objective.

There are only few recordings in the database for distances greater than 150 km. Although peak values of velocity approach values that are not significantly damaging from the structural engineering point of view, from a strict statistical viewpoint, its use may not be appropriate for distances greater than 150 km.

The results obtained here can be progressively modified and improved and their uncertainties can be reduced as the number recordings used for the analysis are increased, station information is enriched, distance terms verified and data processing techniques are improved. Therefore, this study should be evaluated as an introduction to this area.

Attenuation formulas for peak ground velocities of the earthquakes have been used extensively in the recent years in many fields including as measures of intensity of the ground motion and liquefaction studies. A future debate may be energy related analysis of structures. Results of this study can be used as a guide for future research and other supplementary studies. It is believed that the processed database can be

attractive for future researchers not only in the field of deriving attenuation relationships but other circumstances where reliable input data is required.

REFERENCES

- 1 Akkar, S. and Bommer, J.J. (2006a), “Empirical Prediction Equations fro Peak Ground Velocity Derived from Strong-Motion Records from Europe and the Middle East,” *Bull Seismology Soc. Am*, Vol.97 (in press).
- 2 Akkar, S. and Bommer, J.J. (2006b), “Influence of long-period filter cut-off on elastic spectral displacements,” *Earthquake Engineering and Structural Dynamics*, Vol.35, pp. 1145-1165.
- 3 Akkar, S. and Bommer, J.J. (2006c), “Prediction of Peak Ground Velocity for Europe and Surrounding Countries,” *Proceedings of First European Conference on Earthquake Engineering and Seismology, Paper 631*.
- 4 Akkar, S. and Gülkan, P. (2002), “A Critical Examination of Near-Field accelerograms from the Sea of Marmara Region Earthquakes,” *Bulletin of Seismological Society of America*, Vol.92, No. 1, pp. 428-447, February.
- 5 Akkar S. and Özen, Ö. (2005), “Effect of peak ground velocity on deformation demands for SDOF systems,” *Earthquake Engineering and Structural Dynamics*, Vol.34, pp. 1551-1571.
- 6 Akkar S., Sucuoğlu, H., Yakut, A. (2005),” Displacement-based fragility functions for low- and mid-rise ordinary concrete buildings,” *Earthquake Spectra*, Vol.21, No. 2, pp. 901-927.
- 7 Ambraseys, N. N. and Free, M.W. (1997), “Surface-wave magnitude calibration for European region earthquakes,” *Journal of Earthquake Eng.*, Vol. 1, No. 1, pp. 1–22.

- 8 Ambraseys, N., Smit, P., Sigbjornsson, R., Suhadolc, P. and Margaris, B. (2002), "Internet-Site for European Strong-Motion Data," European Commission, Research-Directorate General, Environment and Climate Programme.
- 9 Atkinson, G. M. and Boore, D. M. (1995), "Ground-motion relations for eastern North America," *Bull Seismology Soc. Am.*, Vol. 85, No. 1, pp. 17–30.
- 10 Atkinson, G. M. and Boore, D. M. (1997), "Stochastic point-source modelling of ground motions in the Cascadian region," *Seismological Research Letter*, Vol. 68, No. 1, pp. 74–85.
- 11 Atkinson, G. M. and Boore, D. M. (2006), "Earthquake ground-motion prediction equations for Eastern North America," *Bull Seismology Soc. Am.*, Vol. 96 (in press).
- 12 Atkinson, G.M. and Silva, W. (2000), "Stochastic Modeling of California Ground Motions," *Bull Seismology Soc. Am.*, Vol.90, pp. 255-274.
- 13 Bolt, B.A. (2004), *Engineering Seismology*, in *Earthquake Engineering: From Engineering Seismology to Performance-Based Engineering*, Ed. V.V. Bertero and Y. Bozorgnia, CRC Press.
- 14 Bommer, J.J. and Alarcon, J.E. (2006), "The Prediction and Use of Peak Ground Velocity," *Journal of Earthquake Engineering*, Vol. 10, No. 1, pp. 1-31.
- 15 Bommer, J.J., Scherbaum, F., Bungum, H., Cotton F., Sabetta F. and Abrahamson, N.A. (2005), "On the Use of Logic Trees for Ground-Motion Prediction Equations in Seismic-Hazard Analysis," *Bull Seismology Soc. Am.*, Vol.95, No.2, pp. 377-389, April.
- 16 Boore, D. M. (2003), "Prediction of Ground Motion Using Stochastic Method," *Pure and Applied Geophysics*, Vol. 160., pp. 635-676.

- 17 Boore D. M. and G. M. Atkinson (2006), "Boore-Atkinson NGA empirical ground-motion model for the average horizontal component of PGA, PGV and SA at spectral periods of 0.1, 0.2, 1, 2 and 3 seconds: Interim report for USGS review (to be finalized for the PEER-NGA project)
- 18 Boore, D.M. and Bommer, J.J (2005), "Processing of Strong-Motion Accelerograms: needs, options, consequences," *Soil Dynamics and Earthquake Engineering*, Vol. 25, pp. 93-115.
- 19 Bozorgnia, Y. and Campbell, K.W. (2004), *Engineering Characterization of Ground Motion*, in *Earthquake Engineering: From Engineering Seismology to Performance-Based Engineering*, Ed. V.V. Bertero and Y. Bozorgnia, CRC Press.
- 20 Bragato, P. L. and D. Slejko (2005), "Empirical ground-motion attenuation relations for the Eastern Alps in magnitude range 2.5-6.3," *Bull. Seism. Soc. Am.*, Vol. 95, No. 1, pp. 252–276.
- 21 Bray, J. D. and Rodriguez-Marek, A. (2004), "Characterization of forward-directivity ground motions in the near-fault region," *Soil Dynamics and Earthquake Engineering*, Vol. 24, pp. 815–828.
- 22 Campbell, K.W. (1997), "Empirical Attenuation Relationships for Horizontal and Vertical Components of Peak Ground Acceleration, Peak Ground Velocity, and Pseudo-Absolute Acceleration Response Spectra," *Seismological Research Letters*, Vol. 68, No. 1, pp. 154-179, January/February.
- 23 Chatterjee, S. and Price, B. (1997), *Regression Analysis by Example*, John Wiley & Sons.
- 24 Converse, A.M. and Brady, A.G., "BAP – Strong-Motion Accelerogram Processing Software; Version 1.0.," *United States Geological Survey Open-File Report 1992*, p. 174. 92-296A.

- 25 Dost, B., T. Van Eck and H. Haak (2004), “Scaling of peak ground acceleration and peak ground velocity recorded in the Netherlands,” *Bollettino di Geofisica Teorica ed Applicata*, Vol. 45, No. 3, pp. 153-168.
- 26 Douglas, J. (2001), “A Comprehensive Worldwide Summary of Strong-Motion Attenuation Relationships for Peak Ground Acceleration and Spectral Ordinates (1969 to 2000),” ESEE Report No. 01-1, Imperial College of Science, Technology and Medicine, January.
- 27 Frisenda, M., Massa, M., Spallarossa, D., Ferretti, G. and Eva, C. (2005), “Attenuation relationships for low magnitude earthquakes using standard seismometric records,” *Journal of Earthquake Engineering*, Vol. 9, No. 1, pp. 23–40.
- 28 Gaull, B. A. (1988), “Attenuation of strong ground motion in space and time in South Westren Australia,” *Proceedings of Ninth World Conference on Earthquake Engineering*, Tokyo II, pp. 361-366.
- 29 Graizer, VM. (1979), “Determination of the true ground displacement by using strong motion records,” *Izvestiya, Phys. Solid Earth*, Vol.15, pp.875-85.
- 30 Gregor, N., Silva, W. and Darragh, B. (2002), “Development of attenuation relations for peak particle velocity and displacement,” *Pearl Report to PG&E/CEC/Caltrans—Pacific Engineering and Analysis*, <http://www.pacificengineering.org/rpts/page1.html>.
- 31 Gülkan, P. and Kalkan, E. (2002), “Attenuation Modeling of Recent Earthquakes in Turkey,” *Journal of Seismology*, Vol. 6, pp. 397-409.
- 32 Hao, H. and Gaull, B. A. (2004), “Prediction of seismic ground motion in Perth Western Australia for engineering application,” *Proceedings of the 13th World Conference on Earthquake Engineering*, Vancouver, Paper No. 1892.

- 33 Hudson, D.E. (1979), "Reading and Interpreting Strong Motion Accelerograms," Earthquake Engineering Research Institute.
- 34 Iwan, WD, Moser, MA and Peng, C-Y. (1985), "Some observations on strong motion earthquake measurement using a digital accelerograph," *Bull Seismology Soc. Am.*, Vol.75, pp. 1225-46.
- 35 Joyner, W.B., Warrick, R.E. and Fumal, T.E. (1981), "The Effect of Quaternary Alluvium on Strong Ground Motion in the Coyote Lake, California Earthquake of 1979," *Bulletin of Seismological Society of America*, Vol. 71., pp. 1333-1349.
- 36 Joyner, W.B. and Boore, D. M. (1981), "Peak Horizontal Acceleration and Velocity from Strong-Motion Records Including Records from the 1979 Imperial Valley, California, Earthquake," *Bulletin of Seismological Society of America*, Vol. 71., No. 6, pp. 2011-2038, December.
- 37 Joyner, W.B. and Boore D.M. (1988), "Measurement, Characterization, and Prediction of Strong Ground Motion," *Proceedings of Earthquake Engineering and Soil Dynamics II: Recent Advances in Ground-Motion Evaluation*, JL Von Thun (Editor), Geotechnical Special Publications 20, American Society of Civil Engineers, Park City Utah, 27-30 June, pp. 43-102.
- 38 Kamiyama, M., O'Rourke, M. J. and Flores-Berrones, R. (1992), "A semi-empirical analysis of strong-motion peaks in terms of seismic source, propagation path and local site conditions," *Technical Report NCEER-92-0023*, NCEER, Buffalo, New York.
- 39 Kalkan, E. (2001), "Attenuation Relationship Based on Strong Motion Data Recorded in Turkey," unpublished Master Thesis, METU, December.

- 40 Kalkan, E. and Gülkan, P. (2004), "Site Dependent Spectra Derived from Ground Motion Records in Turkey," *Earthquake Spectra*, No. 4, Vol. 20, pp. 1111-1138, November.
- 41 Kawashima, K., Aizama, K., and Takahashi, K. (1986), "Attenuation of peak ground acceleration, velocity and displacements based on multiple regression analysis of Japanese strong motion records," *Earthquake Engineering and Structural Dynamics*, Vol. 14, pp. 199-215.
- 42 Kostadinov, M. V., and Towhata, I. (2002), "Assessment of liquefaction-inducing peak ground velocity and frequency of ground shaking at onset of phenomenon," *Soil Dynamics & Earthquake Engineering*, Vol. 22, No. 4, pp. 309-322.
- 43 Kramer, S. L. (1996), *Geotechnical Earthquake Engineering*, Prentice Hall.
- 44 Margaris, B., Papazachos, C., Papaioannou, Ch., Theodulidis, N., Kalogeras, I. And Skarlatoudis, A. (2002), "Ground motion attenuation relations for shallow earthquakes in Greece," *Proceedings of the 12th European Conference on Earthquake Engineering*, London, Paper No. 385.
- 45 Marmara ve Düzce Depremleri Mühendislik Raporu, ODTÜ-TMMOB, Ankara, Nisan, 2000.
- 46 MatLAB, The MathWorks Inc., Ver.R2006a, 2006.
- 47 McGuire, R. K. (1978), "Seismic ground motion parameter relations," *Journal of the Geotechnical Division, ASCE*, Vol. 104, No. 4, pp. 481-490.
- 48 Midorikawa, S. and Ohtake, Y. (2004), "Variance of peak ground acceleration and velocity in attenuation relationships," *Proceedings of the 13th World Conference on Earthquake Engineering*, Vancouver, Paper No. 325.

- 49 Molas, G. L. and Yamazaki, F. (1995), "Attenuation of earthquake ground motion in Japan including deep focus events," *Bulletin of the Seismological Society of America*, Vol. 85, No. 5, pp. 1343–1358.
- 50 Orense, R. P. (2005), "Assessment of liquefaction potential based on peak ground parameters," *Soil Dynamics & Earthquake Engineering*, Vol.25, pp. 225-240.
- 51 Pankow, K.L and Pechmann, J.C. (2004), "The SEA99 Ground-Motion Predictive Relations for Extensional Tectonic Regimes: Revisions and a New Peak Ground Velocity Relation," *Bull Seismology Soc. Am.*, Vol.94, pp. 341-348, February.
- 52 Rinaldis, D., Berardi, R., Theodulidis, N. and Margaris, B. (1998), "Empirical predictive models based on a joint Italian and Greek strong-ground motion database: I, peak ground acceleration and velocity," *Proceedings of the 11th European Conference on Earthquake Engineering*, A. A. Balkema, Rotterdam.
- 53 Sabetta, F., Pugliese, A. (1996), "Estimation of Response Spectra and Simulations of Nonstationary Earthquake Ground Motions," *Bull Seismology Soc. Am.*, Vol.86, No.2, pp. 337-352, April.
- 54 Sadigh, R. K. and Egan, J. A. (1998), "Updated relationships for horizontal peak ground velocity and peak ground displacements for shallow crustal earthquakes," *Proceedings of the Sixth US National Conference on Earthquake Engineering*, Seattle, Paper No. 317.
- 55 Shabestari, K. T. and Yamazaki, F. (2002), "Attenuation relationships of the ground motion parameters considering directivity effects in the 1999 Chi-Chi, Taiwan earthquake," *Proceedings of the 7th US National Conference on Earthquake Engineering*, Boston.

- 56 Si, H. and Midorikawa, S. (2000), "New attenuation relations for peak ground acceleration and velocity considering effects of fault type and site condition," *Proceedings of the 12th World Conference on Earthquake Engineering*, Auckland, Paper No. 532.
- 57 Singh, S. K., Gansl, B. K., Bhattacharya, S. N., Pacheco, J. F., Dattatrayam, R. S., Ordaz, M., Kamal, G. S. and Hough, S. E. (2003), "Estimation of ground motion for Bhuj (26 January 2001; Mw 7.6) and for future earthquakes in India," *Bull. Seism. Soc. Am.*, Vol. 93, No. 1, pp. 353–370.
- 58 Skarlatoudis, A. A., B. N. Papazachos, N. Margaris, Ch. Theodulidis, I. Pappioannou, E. M. Kalogeras, E. M. Scordilis, and V. Karakostas (2003), "Empirical peak ground-motion predictive relations for shallow earthquakes in Greece," *Bull. Seism. Soc. Am.*, Vol. 93, No. 6, pp. 2591-2603.
- 59 SPSS Manual, SPSS Inc., SPSS Ver. 13.0, Chicago, IL, 2004.
- 60 Sucuoğlu, H., Yüçemen, S., Gezer, A., and Erberik, A., (1998), "Statistical evaluation of the damage potential of earthquake ground motions," *Structural Safety*, Vol.20, pp. 357-378.
- 61 Theodulidis, N. P. and Papazachos, B. C. (1992), "Dependence of strong ground motion on magnitude-distance, site geology and macroseismic intensity for shallow earthquakes in Greece: I, peak horizontal acceleration, velocity and displacement," *Soil Dynamics and Earthquake Engineering*, Vol. 11, pp. 387–402.
- 62 Trifunac, M. D. (1995), "Empirical Criteria for liquefaction in sands via standard penetration tests and seismic wave energy," *Soil Dynamics & Earthquake Engineering*, Vol.14, No.6, pp. 419-426.

- 63 Trifunac, M.D. and Brady, A.G. (1975), "On the correlation of seismic intensity scales with the peaks of recorded strong ground motion," *Bull Seismology Soc. Am.*, Vol.65, No.1, pp. 139-162.
- 64 Trifunac, M.D. and Brady, A.G. (1976), "Correlations of peak acceleration, velocity and displacement with earthquake magnitude, distance and site conditions," *Earthquake Engineering and Structural Dynamics*, Vol.4, No.5, pp. 455-471.
- 65 Trifunac, M.D. and Todorovska, M.I. (2001), "Evolution of accelerographs, data processing, strong motion arrays and amplitude and spatial resolution in recording strong earthquake motion," *Soil Dynamics and Earthquake Engineering*, Vol. 21, pp. 537-555.
- 66 Tromans, I.J. and Bommer J.J. (2002), "The Attenuation of Strong-Motion Peaks in Europe," in *Proc. of the Twelfth European Conference on Earthquake Engineering*, London, Paper no. 394.
- 67 Wald, D. J., Quitoriano, V., Heaton, T. H. and Kanamori, H. (1999), "Relationships between peak ground acceleration, peak ground velocity, and Modified Mercalli intensity in California," *Earthquake Spectra*, Vol.15, No.3, pp. 557-564.
- 68 Wu, Y., Teng, T., Shin, T and Hsiao, N. (2003), "Relationship between peak ground acceleration, peak ground velocity, and intensity in Taiwan," *Bull Seismology Soc. Am.*, Vol.93, No.1, pp. 386-396.
- 69 Zare, M. and Bard, P.Y. (2002), "Strong motion dataset of Turkey: data processing and site classification," *Soil Dynamics and Earthquake Engineering*, Vol.22, pp. 703-718.

- 70 Zhu, T. J., Tso, W. K. and Heidebrecht, A. C. (1987), "Ductility demand on structures designed based on NBCC 1985 base shear specifications," *Proc. of the Fifth Canadian Conference on Earthquake Engineering*, pp. 275-283.
- 71 Zhu, T. J., Tso, W. K. and Heidebrecht, A. C. (1988), "Effect of peak ground A/V ratio on structural damage," *Journal of Structural Engineering*, Vol. 114, No.5, pp. 1019-1037.

Internet Sources

- 72 Darragh, B., Silva W. and Gregor N., "Strong Motion Processing for the PEER Center," *Workshop on Record Processing Guidelines*, <http://www.cosmos-eq.org/recordProcessingPapers.html>, last accessed on 12/08/2006.
- 73 Earthquake Engineering Research Center, <http://eerc.ce.metu.edu.tr/nsmp/>, last accessed on 07/04/2006.
- 74 Earthquake Research Department of General Directorate of Disaster Affair, Turkey National Strong Ground Motion Program, <http://angora.deprem.gov.tr>, last accessed on 07/11/2006.
- 75 Imperial College of London Department of Civil and Environmental Engineering "Internet Site for European Strong Motion Database," <http://isesd.cv.ic.ac.uk>, last accessed on 22/07/2006.
- 76 Kandilli Observatory and Earthquake Research Institute, <http://www.koeri.boun.edu.tr>, last accessed on 05/11/2006.
- 77 Pacific Earthquake Engineering Research Center, PEER NGA Database, <http://peer.berkeley.edu/nga/>, last accessed on 15/07/2006.

- 78 Personal webpage of Dr. D. Boore, U.S. Geological Survey, Online Software, http://quake.wr.usgs.gov/~boore/software_online.htm, last accessed on 10/05/2006
- 79 Sayısal Grafik Sanayi ve Ticaret Ltd.Şti., “Earthquake Site of Turkey,” <http://sayisalgrafik.com.tr/deprem/>, last accessed on 20/08/2006.
- 80 Shakal, A.F., Huang, M.J. and Grazier V.M., “CSMIP Strong-Motion Data Processing,” *Workshop on Record Processing Guidelines*, <http://www.cosmos-eq.org/recordProcessingPapers.html>, last accessed on 12/08/2006.
- 81 Stephens, C.D. and Boore D.M., “ANSS/NSMP Strong-Motion Record Processing and Procedures,” *Workshop on Record Processing Guidelines*, <http://www.cosmos-eq.org/recordProcessingPapers.html>, last accessed on 12/08/2006.

APPENDIX A

Table A.1 Database of strong ground motion records in Turkey (August 1976 – July 2003)

Data No	Date (dd.mm.yy)	Earthquake Location	M _w *	Station Location	Station Structure	Station Code	Station Coordinates*	Owner	Epi. Dist. (km)**	r _{ci} ** (km)	V ₅₃₀ ** (cm/s)	Local Geology***	Peak Ground Acc. (g) NS	Peak Ground Acc. (g) EW	Ver.
1	19.08.1976	Merkez - DENİZLİ	6.1	DENİZLİ	Bayındırlık ve İskan Müd.	DNZ	37.8140 N - 29.1120 E	ERD	15.2	3.0		Stiff Soil	0.349	0.290	0.173
2	05.10.1977	Ilgaz - CANKIRI	5.8	CERKES	Meteoroloji İst.	GER	40.8800 N - 32.9100 E	ERD	57.6	62.1		Soil	0.036	0.039	0.016
3	16.12.1977	Bornova - IZMİR	5.6	IZMİR	Meteoroloji İst.	IZM	38.4000 N - 27.1900 E	ERD	1.1	1.2		Soil	0.391	0.125	0.094
4	11.04.1979	Caldiran - VAN	4.9	MURADIYE	Meteoroloji İst.	MUR	39.0300 N - 43.7000 E	ERD	19.0	19.0	250	Soil	0.046	0.045	0.025
5	28.05.1979	ANTALYA GULF	5.9	BUCAK	Kandıllı Gözlem Evi	BCK	37.4610 N - 30.5890 E	ERD	150.0	150.0		Rock	0.024	0.021	0.041
6	18.07.1979	Dursunbey - BALIKESİR	5.3	DURSUNBEY	Kandıllı Gözlem İstasyonu	DUR	39.6700 N - 28.5300 E	ERD	10.3	6.0		Rock	0.232	0.288	0.200
7	30.06.1981	Samandıra - HATAY	4.7	HATAY	Bayındırlık ve İskan Müd.	HTY	36.2500 N - 36.1100 E	ERD	21.6	24.7		Stiff Soil	0.154	0.136	0.144
8	05.07.1983	Biga - CANAKKALE	6.1	EDİNCİK	Kandıllı Gözlem İstasyonu	EDC	40.3600 N - 27.8900 E	ERD	57.7	57.7		Rock	0.053	0.047	0.032
9	05.07.1983	Biga - CANAKKALE	6.1	GONEN	Meteoroloji İst.	GNN	40.0800 N - 27.6800 E	ERD	48.6	48.7		Soil	0.050	0.047	0.038
10	05.07.1983	Biga - CANAKKALE	6.1	TEKIRDAG	Bayındırlık ve İskan Müd.	TKR	40.9600 N - 27.5300 E	ERD	75.1	75.0		Rock	0.030	0.035	0.017
11	31.10.1983	Senkaya - ERZURUM	6.6	ERZURUM	Bayındırlık ve İskan Müd.	HRZ	39.9060 N - 41.2560 E	ERD	92.8	92.5		Soil	0.035	0.025	0.032
12	31.10.1983	Merkez - BALIKESİR	4.5	HOROSAN	Meteoroloji İst.	HRS	40.0400 N - 42.1700 E	ERD	34.5	25.0		Soil	0.150	0.173	0.088
13	29.03.1984	Merkez - BALIKESİR	4.5	BALIKESİR	Huzur Evi	BLK	39.6600 N - 27.8600 E	ERD	2.4	0.0	339	Stiff Soil	0.224	0.129	0.297
14	17.06.1984	AEGEAN SEA	5.1	FOCA	Gümrük Müd.	FOC	38.6400 N - 26.7700 E	ERD	97.9	98.0		Rock	0.024	0.023	0.024
15	12.08.1985	Kelkit - GUMUSHANE	4.9	KIGI	Meteoroloji İst.	KIG	39.3400 N - 40.2800 E	ERD	80.7	80.8		Stiff Soil	0.163	0.089	0.043
16	16.12.1985	Koycegiz - MUĞLA	4.6	KOYCEGIZ	Meteoroloji İst.	KOY	36.9700 N - 28.6940 E	ERD	13.9	14.4		Soil	0.103	0.114	0.069
17	05.05.1986	Dogansehir - MALATYA	6.0	GOLBASI	Meteoroloji İst.	GOL	37.7810 N - 37.6410 E	ERD	29.6	27.0		Rock	0.115	0.076	0.039
18	06.06.1986	Dogansehir - MALATYA	5.8	GOLBASI	Meteoroloji İst.	GOL	37.7810 N - 37.6410 E	ERD	34.7	34.7		Rock	0.069	0.034	0.018
19	06.06.1986	Dogansehir - MALATYA	5.8	MALATYA	Bayındırlık ve İskan Müd.	MLT	38.3500 N - 38.3400 E	ERD	53.3	53.6		Stiff Soil	0.024	0.025	0.026
20	20.04.1988	Caldiran - VAN	5.5	MURADIYE	Meteoroloji İst.	MUR	39.0300 N - 43.7000 E	ERD	37.3	37.3	250	Soil	0.050	0.051	0.021
21	12.02.1991	MARMARA SEA	4.8	ISTANBUL	Kandıllı Gözlem Evi	IST	41.0800 N - 29.0900 E	ERD	38.5	38.5	425	Stiff Soil	0.028	0.018	0.010
22	13.03.1992	Uzunlu - ERZINCAN	6.6	ERZINCAN	Bayındırlık ve İskan Müd.	ERC	39.7520 N - 39.4870 E	ERD	12.7	0.0	421	Stiff Soil	0.405	0.471	0.239
23	13.03.1992	Uzunlu - ERZINCAN	6.6	REFAHIYE	Kaymakamlık Binası	REF	39.9010 N - 38.7690 E	ERD	76.2	65.0		Soil	0.067	0.086	0.032
24	16.11.1992	Menderes - IZMİR	6.0	KUSADASI	Meteoroloji İst.	KUS	37.8610 N - 27.2660 E	ERD	41.1	41.0		Soil	0.083	0.072	0.062
25	13.01.1994	Ceyhan - ADANA	5.0	ISLAHIYE	Meteoroloji İst.	ISL	37.0500 N - 36.6000 E	ERD	67.7	67.7		Stiff Soil	0.021	0.019	0.019
26	24.05.1994	IZMIR GULF	5.5	FOCA	Gümrük Müd.	FOC	38.6400 N - 26.7700 E	ERD	20.1	20.1		Rock	0.036	0.050	0.030
27	13.11.1994	Koycegiz - MUĞLA	5.4	KOYCEGIZ	Meteoroloji İst.	KOY	36.9700 N - 28.6940 E	ERD	17.4	17.4		Soil	0.073	0.097	0.058
28	29.01.1995	Illica - ERZURUM	5.2	TERCAN	Meteoroloji İst.	TER	39.7770 N - 40.3910 E	ERD	55.9	55.5		Stiff Soil	0.045	0.049	0.025
29	26.02.1995	Merkez - VAN	4.7	VAN	Bayındırlık ve İskan Müd.	VAN	38.4900 N - 43.3400 E	ERD	12.3	12.6		Soil	0.028	0.016	0.016
30	01.10.1995	Dinar - AFYON	6.4	CARDAK	Sağlık Ocağı	CRD	37.8250 N - 29.6680 E	ERD	46.1	39.6		Stiff Soil	0.065	0.061	0.098

Table A.1. Continued

Data No	Date (dd.mm.yy)	Earthquake Location	M _w *	Station Location	Station Structure	Station Code	Station Coordinates*	Owner	Epi. Dist. (km)**	r _{ci} ** (km)	V _{s30} ** (cm/s)	Local Geology***	Peak Ground Acc. (g) NS	Peak Ground Acc. (g) EW	Ver.
31	01.10.1995	Dinar - AFYON	6.4	DINAR	Meteoroloji İst.	DIN	38.0600 N - 30.1550 E	ERD	10.7	3.0	234	Soil	0.282	0.330	0.151
32	02.04.1996	AEGEAN SEA	5.4	KUSADASI	Meteoroloji İst.	KUS	37.8610 N - 27.2660 E	ERD	55.7	55.7		Soil	0.021	0.033	0.022
33	14.08.1996	Gumushacikoy - AMASYA	5.6	MERZIFON	Meteoroloji İst.	MRZ	40.8800 N - 35.4900 E	ERD	24.1	21.7		Soil	0.033	0.102	0.029
34	21.01.1997	Esmen - DENİZLİ	5.2	BULDAN	Kaymakamlık Binası	BLD	38.0450 N - 28.8340 E	ERD	11.2	11.3		Stiff Soil	0.039	0.024	0.028
35	22.01.1997	Merkez - HATAY	5.7	HATAY	Bayındırlık ve İskan Müd.	HTY	36.2500 N - 36.1100 E	ERD	12.3	9.0		Stiff Soil	0.136	0.151	0.089
36	22.01.1997	Merkez - HATAY	5.7	ISLAHIYE	Meteoroloji İst.	ISL	37.0500 N - 36.6000 E	ERD	109.9	110.0		Stiff Soil	0.028	0.030	0.023
37	28.02.1997	Merkez - CORUM	5.2	MERZIFON	Meteoroloji İst.	MRZ	40.8800 N - 35.4900 E	ERD	27.4	26.0		Soil	0.015	0.016	0.015
38	03.11.1997	Ahlat - BITLİS	4.9	MALAZGIRT	Meteoroloji İst.	MLZ	39.1700 N - 42.5400 E	ERD	47.2	47.0		Soil	0.018	0.018	0.011
39	04.04.1998	Dinar - AFYON	5.2	CARDAK	Sağlık Ocağı	CRD	37.8250 N - 29.6680 E	ERD	47.9	48.0		Stiff Soil	0.028	0.024	0.019
40	04.04.1998	Dinar - AFYON	5.2	DINAR	Meteoroloji İst.	DIN	38.0600 N - 30.1550 E	ERD	13.4	13.4	234	Soil	0.131	0.135	0.028
41	27.06.1998	Yuregir - ADANA	6.2	CEYHAN	PTT Müd.	CYH	37.0500 N - 35.8100 E	ERD	32.1	28.0		Soil	0.223	0.274	0.086
42	27.06.1998	Yuregir - ADANA	6.2	ISKENDERUN	Meteoroloji İst.	ISK	36.6300 N - 36.1500 E	ERD	58.8	58.8		Stiff Soil	0.015	0.015	0.012
43	27.06.1998	Yuregir - ADANA	6.2	ISLAHIYE	Meteoroloji İst.	ISL	37.0500 N - 36.6000 E	ERD	95.9	95.8		Stiff Soil	0.021	0.018	0.014
44	27.06.1998	Yuregir - ADANA	6.2	KARATAS	Meteoroloji İst.	KRT	36.5610 N - 35.3670 E	ERD	36.0	36.0		Rock	0.029	0.033	0.020
45	27.06.1998	Yuregir - ADANA	6.2	MERSİN	Meteoroloji İst.	MRS	36.8300 N - 34.6500 E	ERD	80.1	80.1		Soil	0.132	0.119	0.022
46	27.06.1998	Yuregir - ADANA	6.2	HATAY	Bayındırlık ve İskan Müd.	HTY	36.2130 N - 36.1600 E	ERD	89.4	89.0		Stiff Soil	0.027	0.026	0.012
47	09.07.1998	AEGEAN SEA	4.6	BORNOVA	Ziraat Fak.	BRN	38.4550 N - 27.2290 E	ERD	63.5	63.0		Soil	0.027	0.013	0.006
48	17.08.1999	Merkez - KOCAELİ	7.4	BURSA	Sivil Sav. Müd.	BRS	40.1830 N - 29.1310 E	ERD	87.5	66.6	660	Rock	0.054	0.046	0.026
49	17.08.1999	Merkez - KOCAELİ	7.4	CEKMECE	Nükleer Santral Binası	CEK	40.9700 N - 28.7000 E	ERD	106.1	76.1	382	Stiff Soil	0.118	0.090	0.050
50	17.08.1999	Merkez - KOCAELİ	7.4	DUZCE	Meteoroloji İst.	DZC	40.8500 N - 31.1700 E	ERD	107.4	11.0	276	Soil	0.315	0.374	0.480
51	17.08.1999	Merkez - KOCAELİ	7.4	EREGLİ	Kaymakamlık Binası	ERG	40.9800 N - 27.7900 E	ERD	181.0	116.0	660	Stiff Soil	0.090	0.101	0.057
52	17.08.1999	Merkez - KOCAELİ	7.4	GEBZE	Tıbbiye Hastanesi	GBZ	40.8200 N - 29.4400 E	ERD	41.8	30.0	750	Rock	0.265	0.141	0.198
53	17.08.1999	Merkez - KOCAELİ	7.4	GOYNUK	Devlet Hastanesi	GYN	40.3850 N - 30.7340 E	ERD	77.9	32.0		Rock	0.138	0.118	0.130
54	17.08.1999	Merkez - KOCAELİ	7.4	ISTANBUL	Bayındırlık ve İskan Müd.	IST	41.0580 N - 29.0130 E	ERD	85.3	71.0	425	Stiff Soil	0.061	0.043	0.036
55	17.08.1999	Merkez - KOCAELİ	7.4	IZNIK	Kaymakamlık Binası	IZN	40.4370 N - 29.6910 E	ERD	34.6	29.0	225	Soil	0.265	0.123	0.082
56	17.08.1999	Merkez - KOCAELİ	7.4	IZMIT	Meteoroloji İst.	IZT	40.7900 N - 29.9600 E	ERD	10.9	5.0	800	Rock	0.171	0.225	0.146
57	17.08.1999	Merkez - KOCAELİ	7.4	SAKARYA	Bayındırlık ve İskan Müd.	SKR	40.7370 N - 30.3840 E	ERD	40.2	3.2	471	Stiff Soil	N/A	0.407	0.259
58	17.08.1999	Merkez - KOCAELİ	7.4	BALIKESİR	Huzur Evi	BLK	39.6500 N - 27.8570 E	ERD	209.9	183.4	339	Stiff Soil	0.018	0.018	0.008
59	17.08.1999	Merkez - KOCAELİ	7.4	CANAKKALE	Meteoroloji İst.	CNK	40.1420 N - 26.4000 E	ERD	303.5	250.0	275	Soil	0.025	0.029	0.008
60	17.08.1999	Merkez - KOCAELİ	7.4	KUTAHYA	Sivil Sav. Müd.	KUT	39.4190 N - 29.9970 E	ERD	142.6	144.6	275	Soil	0.050	0.060	0.023

Table A.1. Continued

Data No	Date (dd.mm.yy)	Earthquake Location	M _w *	Station Location	Station Structure	Station Code	Station Coordinates*	Owner	Epi. Dist. (km)**	r _{ci} ** (km)	V _{s30} ** (cm/s)	Local Geology***	Peak Ground Acc. (g) NS	Peak Ground Acc. (g) EW	Ver.
61	17.08.1999	Merkez - KOCAELI	7.4	GEBZE	Arçelik ARGE Binası	ARC	40.8236 N - 29.3607 E	KOERI	55.0	38.0	380	Rock	0.211	0.134	0.083
62	17.08.1999	Merkez - KOCAELI	7.4	AMBARLI	Termik Santral	ATS	40.9860 N - 28.6926 E	KOERI	113.0	68.1	173	Soil	0.253	0.186	0.080
63	17.08.1999	Merkez - KOCAELI	7.4	BOTAŞ	Gaz Terminali	BTS	40.9919 N - 27.9795 E	KOERI	172.0	127.1	275	Soil	0.099	0.087	0.024
64	17.08.1999	Merkez - KOCAELI	7.4	YEŞİLKÖY	Havaimanı	DHM	40.9823 N - 28.8199 E	KOERI	103.0	58.3	425	Stiff Soil	0.090	0.084	0.055
65	17.08.1999	Merkez - KOCAELI	7.4	BURSA	Tofaş Fabrikası	BUR	40.2605 N - 29.0680 E	KOERI	92.0	60.4	275	Soil	0.101	0.100	0.048
66	17.08.1999	Merkez - KOCAELI	7.4	FATİH	Fatih Türbesi	FAT	41.0196 N - 28.9500 E	KOERI	94.0	53.3	339	Stiff Soil	0.189	0.162	0.132
67	17.08.1999	Merkez - KOCAELI	7.4	HEYBELİADA	Sanatonyum	HAS	40.8688 N - 29.0875 E	KOERI	78.0	43.0		Rock	0.057	0.110	0.143
68	17.08.1999	Merkez - KOCAELI	7.4	YARIMCA	Pekim Tesisleri	YPT	40.7639 N - 29.7620 E	KOERI	20.0	5.0	297	Stiff Soil	0.230	0.322	0.241
69	17.08.1999	Merkez - KOCAELI	7.4	LEVENT	Yapı Kredi Plaza	YKP	41.0811 N - 20.0111 E	KOERI	92.0	60.7		Rock	0.041	0.036	0.027
70	17.08.1999	Merkez - KOCAELI	7.4	MECİDİYEKÖY	Mecidiyeköy	MCD	41.0650 N - 28.9970 E	ITU	93.0	62.3	425	Stiff Soil	0.054	0.070	0.037
71	17.08.1999	Merkez - KOCAELI	7.4	MASLAK	Maslak	MSK	41.1040 N - 29.0190 E	ITU	93.0	63.9	660	Rock	0.054	0.038	0.031
72	17.08.1999	Merkez - KOCAELI	7.4	ZEYTİNBURNU	Zeytinburnu	ZYT	40.9860 N - 28.9080 E	ITU	96.0	63.1	230	Soil	0.120	0.109	0.051
73	17.08.1999	Merkez - KOCAELI	7.4	ATAKÖY	Ataköy	ATK	40.9890 N - 28.8490 E	ITU	101.0	67.5	275	Soil	0.102	0.168	0.068
74	11.11.1999	Merkez - KOCAELI	5.6	SAKARYA	Bayındırlık ve İskan Müd.	SKR	40.7370 N - 30.3840 E	ERD	18.0	17.5	471	Stiff Soil	0.207	0.345	0.133
75	12.11.1999	Merkez - DUZCE	7.2	BOLU	Bayındırlık ve İskan Müd.	BOL	40.7450 N - 31.6100 E	ERD	33.7	12.0	290	Soil	0.740	0.806	0.200
76	12.11.1999	Merkez - DUZCE	7.2	DUZCE	Meteoroloji İst.	DZC	40.8500 N - 31.1700 E	ERD	12.7	8.2	276	Soil	0.408	0.514	0.340
77	12.11.1999	Merkez - DUZCE	7.2	GOYNUK	Devlet Hastanesi	GYN	40.3850 N - 30.7340 E	ERD	56.3	56.4		Rock	0.028	0.025	0.025
78	12.11.1999	Merkez - DUZCE	7.2	IZNIK	Kaymakamlık Binası	IZN	40.4400 N - 29.7500 E	ERD	127.7	129.8	225	Soil	0.022	0.021	0.010
79	12.11.1999	Merkez - DUZCE	7.2	IZMIT	Meteoroloji İst.	IZT	40.7900 N - 29.9600 E	ERD	105.4	95.0	800	Rock	0.022	0.024	0.022
80	12.11.1999	Merkez - DUZCE	7.2	KUTAHA	Sivil Sav. Müd.	KUT	39.4190 N - 29.9970 E	ERD	179.5	169.5	275	Soil	0.017	0.021	0.009
81	12.11.1999	Merkez - DUZCE	7.2	MUDURNU	Kaymakamlık Binası	MDR	40.4630 N - 31.1820 E	ERD	30.9	34.3	660	Rock	0.121	0.058	0.063
82	12.11.1999	Merkez - DUZCE	7.2	SAKARYA	Bayındırlık ve İskan Müd.	SKR	40.7370 N - 30.3840 E	ERD	69.6	49.9	471	Stiff Soil	0.017	0.025	0.012
83	12.11.1999	Merkez - DUZCE	7.2	AMBARLI	Termik Santral	ATS	40.9860 N - 28.6926 E	KOERI	208.0	188.0	173	Soil	0.038	0.027	0.008
84	12.11.1999	Merkez - DUZCE	7.2	FATİH	Fatih Türbesi	FAT	41.0196 N - 28.9500 E	KOERI	187.0	172.5	339	Stiff Soil	0.036	0.025	0.008
85	12.11.1999	Merkez - DUZCE	7.2	HEYBELİADA	Sanatonyum	HAS	40.8688 N - 29.0875 E	KOERI	174.0	154.0		Rock	0.024	0.028	0.016
86	12.11.1999	Merkez - DUZCE	7.2	YARIMCA	Pekim Tesisleri	YPT	40.7639 N - 29.7620 E	KOERI	115.9	101.7	297	Stiff Soil	0.018	0.016	0.014
87	06.06.2000	Cerkes - CANKIRI	6.0	CERKES	Meteoroloji İst.	CER	40.8140 N - 32.8830 E	ERD	10.51	30.0		Soil	0.062	0.063	0.040
88	23.08.2000	Akyazı - SAKARYA	5.2	AKYAZI	Orman İşletme Müd.	AKY	40.6700 N - 30.6220 E	ERD	7.5	7.5		Soil	0.079	0.097	0.030
89	23.08.2000	Akyazı - SAKARYA	5.2	DUZCE	Meteoroloji İst.	DZC	40.8440 N - 31.1490 E	ERD	41.2	41.2	276	Soil	0.023	0.018	0.009
90	23.08.2000	Akyazı - SAKARYA	5.2	IZNIK	Kaymakamlık Binası	IZN	40.4400 N - 29.7500 E	ERD	85.4	88.1	225	Soil	0.022	0.016	0.008

Table A.1. Continued

Data No	Date (dd.mm.yy)	Earthquake Location	M _w *	Station Location	Station Structure	Station Code	Station Coordinates*	Owner	Epi. Dist. (km)**	r _{cl} ** (km)	V _{s30} ** (cm/s)	Local Geology***	Peak Ground Acc. NS	Peak Ground Acc. EW	Ver. (g)
91	23.08.2000	Akyazi - SAKARYA	5.2	SAKARYA	Bayındırlık ve İskan Müd.	SKR	40.7370 N - 30.3840 E	ERD	28.2	28.2	471	Stiff Soil	0.021	0.027	0.016
92	04.10.2000	Merkez - DENİZLİ	5.0	DENİZLİ	Bayındırlık ve İskan Müd.	DNZ	37.8120 N - 29.1140 E	ERD	12.7	12.7		Stiff Soil	0.049	0.066	0.049
93	15.11.2000	Tatvan-VAN	5.5	VAN	Bayındırlık ve İskan Müd.	VAN	38.5040 N - 43.4060 E	ERD	200.2	200.0		Soil	0.013	0.012	0.007
94	10.07.2001	Pasinler - ERZURUM	5.4	ERZURUM	Bayındırlık ve İskan Müd.	ERZ	39.9030 N - 41.2620 E	ERD	31.7	31.7		Soil	0.020	0.022	0.027
95	26.08.2001	Yığılca - DUZCE	5.0	BOLU	Bayındırlık ve İskan Müd.	BOL	40.7470 N - 31.6100 E	ERD	22.3	22.3	290	Soil	0.189	0.132	0.044
96	02.12.2001	Merkez - VAN	4.8	VAN	Bayındırlık ve İskan Müd.	VAN	38.5040 N - 43.4060 E	ERD	15.9	15.9		Soil	0.030	0.025	0.034
97	03.02.2002	Sultandagi - AFYON	6.5	AFYON	Bayındırlık ve İskan Müd.	AFY	38.7920 N - 30.5610 E	ERD	66.3	66.3		Soil	0.114	0.094	0.036
98	03.02.2002	Sultandagi - AFYON	6.5	KUTAHYA	Sivil Sav. Müd.	KUT	39.4190 N - 29.9970 E	ERD	144.8	143.0	275	Soil	0.023	0.021	0.014
99	03.04.2002	Basmakci - ISPARTA	4.2	BURDUR	Bayındırlık ve İskan Müd.	BRD	37.7040 N - 30.2210 E	ERD	12.5	12.5		Stiff Soil	0.029	0.021	0.031
100	14.12.2002	Sumbas - OSMANIYE	4.8	ANDIRIN	Tufan Paşa İlkokulu	AND	37.5800 N - 36.3400 E	ERD	15.9	16.0		Stiff Soil	0.077	0.050	0.032
101	10.03.2003	Akyazi - SAKARYA	4.0	AKYAZI	Orman İşletme Müd.	AKY	40.6700 N - 30.6220 E	ERD	6.6	6.6		Soil	0.023	0.035	0.012
102	10.04.2003	Seferhisar - IZMIR	5.7	BORNOVA	9 Eylül Üniv. Ziraat Fak.	BRN	38.4550 N - 27.2290 E	ERD	40.9	48.0		Soil	0.079	0.037	0.017
103	01.05.2003	Merkez - BINGOL	6.3	BINGOL	Bayındırlık ve İskan Müd.	BNG	38.8970 N - 40.5030 E	ERD	4.8	6.1		Soil	0.546	0.277	0.472
104	21.05.2003	Cumyeyri - DUZCE	4.4	DUZCE	Meteoroloji İst.	DZC	40.8440 N - 31.1490 E	ERD	14.5	19.0	276	Soil	0.018	0.032	0.017
105	09.06.2003	Bandirma - BALIKESİR	4.8	BANDIRMA	Bölge Trafik Den. Am.	BND	40.3410 N - 27.9420 E	ERD	15.9	14.2		Stiff Soil	0.036	0.023	0.015
106	06.07.2003	Bandirma - BALIKESİR	4.8	CANAKKALE	Meteoroloji İst.	CNK	40.1420 N - 26.4000 E	ERD	34.9	35.0	275	Soil	0.026	0.016	0.009
107	23.07.2003	Buldun - DENİZLİ	5.3	SARAYKÖY	Jeotermal İst. Müd.	DAT1	37.9320 N - 28.9230 E	ERD	27.4	27.4		Soil	0.090	0.123	0.061
108	23.07.2003	Buldun - DENİZLİ	5.3	DENİZLİ	Bayındırlık ve İskan Müd.	DNZ	37.8130 N - 29.1140 E	ERD	46.0	46.1		Stiff Soil	0.022	0.046	0.020
109	26.07.2003	Buldun - DENİZLİ	4.9	SARAYKÖY	Jeotermal İst. Müd.	DAT1	37.9320 N - 28.9230 E	ERD	20.1	20.2		Soil	0.048	0.034	0.036
110	26.07.2003	Buldun - DENİZLİ	5.4	SARAYKÖY	Jeotermal İst. Müd.	DAT1	37.9320 N - 28.9230 E	ERD	20.0	20.0		Soil	0.108	0.121	0.154
111	26.07.2003	Buldun - DENİZLİ	5.4	DENİZLİ	Bayındırlık ve İskan Müd.	DNZ	37.8130 N - 29.1140 E	ERD	38.4	38.5		Stiff Soil	0.024	0.026	0.022
112	26.07.2003	Buldun - DENİZLİ	4.9	SARAYKÖY	Jeotermal İst. Müd.	DAT1	37.9320 N - 28.9230 E	ERD	22.1	22.1		Soil	0.014	0.017	0.010

* Data updated according to NSMP database

** Data updated according to Ambraseys and Peer Catalogs

*** Data updated according to Ambraseys, PEER Catalogs and corrected V_{s30} values

APPENDIX B

Table B.1 Filter choices and PGV properties of chosen database.

Data No	Date (dd.mm.yy)	Earthquake Location	M _w *	Station Code	Uncorrected PGV (cm/s)		Corrected PGV (cm/s)		High-Cut Filter		Selected Low-Cut		Selected Low-Cut	
					N-S	E-W	N-S	E-W	High-Cut Filter Freq. (Hz)	Selected Low-Cut Filter Freq. (Hz)	Selected Low-Cut Filter Freq. (Hz)	Selected Low-Cut Filter Freq. (Hz)	Selected Low-Cut Filter Freq. (Hz)	Selected Low-Cut Filter Freq. (Hz)
1	19.08.1976	Merkez - DENIZLI	6.1	DNZ	40.16	484.81	25.22	16.53	30	0.35	0.65	0.650	0.970	
2	05.10.1977	Ilgaz - CANKIRI	5.8	CER	11.95	7.53	3.22	2.91	10	0.97	0.97	0.500	0.500	
3	16.12.1977	Bornova - IZMIR	5.6	IZM	28.27	25.71	13.00	4.74	10	0.50	0.50	0.880	0.880	
4	11.04.1979	Caldiran - VAN	4.9	MUR	4.72	4.31	2.84	2.55	20	0.88	0.88	0.780	0.780	
5	28.05.1979	ANTALYA GULF	5.9	BCK	1.55	1.77	0.45	0.51	21	0.56	0.78	0.980	0.980	
6	18.07.1979	Dursunbey - BALIKESIR	5.3	DUR	10.75	9.24	9.30	9.11	20	0.87	0.98	1.020	1.020	
7	30.06.1981	Samandagi - HATAY	4.7	HTY	51.35	46.91	4.40	3.10	25	1.02	0.97	0.490	0.490	
8	05.07.1983	Biga - CANAKKALE	6.1	EDC	25.22	31.99	4.65	2.14	20	0.30	0.49	0.760	0.760	
9	05.07.1983	Biga - CANAKKALE	6.1	GNN	45.69	53.93	3.81	2.39	20	0.29	0.29	0.880	0.880	
10	05.07.1983	Biga - CANAKKALE	6.1	TKR	15.24	6.11	1.81	1.68	20	0.76	0.76	0.930	0.930	
11	31.10.1983	Senkaya - ERZURUM	6.6	ERZ	7.50	2.70	1.30	0.59	13	0.78	0.88	1.700	1.700	
12	31.10.1983	Senkaya - ERZURUM	6.6	HRS	65.36	26.07	5.62	7.02	13	0.93	0.76	0.880	0.880	
13	29.03.1984	Merkez - BALIKESIR	4.5	BLK	11.72	6.86	6.66	4.01	20	1.70	1.00	0.970	0.970	
14	17.06.1984	AEGEAN SEA	5.1	FOC	8.85	4.78	0.66	0.80	10	0.59	0.88	1.080	1.080	
15	12.08.1985	Keikit - GUMUSHANE	4.9	KIG	7.68	3.89	4.89	2.83	13	1.08	1.16	0.500	0.500	
16	16.12.1985	Koycegiz - MUGLA	4.6	KOY	24.81	27.74	3.10	3.46	40	0.97	0.97	0.390	0.390	
17	05.05.1986	Dogansehir - MALATYA	6.0	GOL	26.60	27.80	11.67	4.06	15	0.50	0.50	0.510	0.510	
18	06.06.1986	Dogansehir - MALATYA	5.8	GOL	10.84	12.37	8.32	4.16	10	0.29	0.39	0.780	0.780	
19	06.06.1986	Dogansehir - MALATYA	5.8	MLT	56.79	17.33	1.73	1.49	30	0.51	0.34	0.960	0.960	
20	20.04.1988	Caldiran - VAN	5.5	MUR	8.00	10.47	3.46	5.32	5	0.78	0.70	0.320	0.320	
21	12.02.1991	MARMARA SEA	4.8	IST	2.36	1.35	0.46	0.24	11	0.90	0.96	0.240	0.240	
22	13.03.1992	Uzumlu - ERZINCAN	6.6	ERC	103.90	82.05	94.12	58.41	30	0.32	0.32	0.410	0.410	
23	13.03.1992	Uzumlu - ERZINCAN	6.6	REF	19.00	19.29	4.37	3.59	20	0.24	0.24	0.780	0.780	
24	16.11.1992	Menderes - IZMIR	6.0	KUS	13.23	14.60	4.34	3.40	35	0.41	0.41	0.580	0.580	
25	13.01.1994	Ceyhan - ADANA	5.0	ISL	1.88	1.68	0.56	0.47	15	0.78	0.58	0.770	0.770	
26	24.05.1994	IZMIR GULF	5.5	FOC	22.22	18.70	1.52	3.68	10	0.68	0.54	0.780	0.780	
27	13.11.1994	Koycegiz - MUGLA	5.4	KOY	3.88	4.40	3.93	3.71	20	0.77	0.77	0.410	0.410	
28	29.01.1995	Ilica - ERZURUM	5.2	TER	6.30	7.89	2.32	3.74	11	0.78	0.87	0.410	0.410	
29	26.02.1995	Merkez - VAN	4.7	VAN	1.24	2.32	1.18	0.59	12	0.35	0.41	0.410	0.410	
30	01.10.1995	Dinar - AFYON	6.4	CRD	19.64	7.09	3.12	4.06	13	0.32	0.41	0.410	0.410	

Table B.1 Continued.

Data No	Date (dd.mm.yy)	Earthquake Location	M _w *	Station Code	Uncorrected PGV (cm/s)		Corrected PGV (cm/s)		High-Cut Filter Freq. (Hz)	Selected Low-Cut Filter Freq. (Hz)	Selected Low-Cut Filter Freq. (Hz)	Selected Low-Cut Filter Freq. (Hz)	Selected Low-Cut Filter Freq. (Hz)
					N-S	E-W	N-S	E-W					
31	01.10.1995	Dinar - AFYON	6.4	DIN	180.20	161.78	29.70	43.95	12	0.17	0.22	0.220	
32	02.04.1996	AEGEAN SEA	5.4	KUS	1.84	2.10	1.03	0.80	15	0.49	0.78	0.780	
33	14.08.1996	Gumushacikoy - AMASYA	5.6	MRZ	7.16	7.26	2.07	3.74	13	0.49	0.57	0.570	
34	21.01.1997	Esmé - DENIZLI	5.2	BLD	2.55	2.42	2.37	2.13	11	0.39	0.39	0.390	
35	22.01.1997	Merkez - HATAY	5.7	HTY	16.56	5.80	5.55	6.12	40	0.16	0.12	0.160	
36	22.01.1997	Merkez - HATAY	5.7	ISL	3.34	2.99	2.91	1.76	15	0.44	0.49	0.440	
37	28.02.1997	Merkez - CORUM	5.2	MRZ	18.22	22.49	1.15	1.09	20	0.39	0.41	0.390	
38	03.11.1997	Ahlat - BITLIS	4.9	MLZ	35.98	14.19	0.82	0.65	13	0.56	0.55	0.560	
39	04.04.1998	Dinar - AFYON	5.2	CRD	6.61	2.32	0.78	5.33	20	1.16	1.09	1.090	
40	04.04.1998	Dinar - AFYON	5.2	DIN	18.99	6.26	23.32	13	12.28	0.35	0.27	0.350	
41	27.06.1998	Yuregir - ADANA	6.2	CYH	29.10	28.10	29.32	21.93	20	0.24	0.17	0.170	
42	27.06.1998	Yuregir - ADANA	6.2	ISK	2.75	4.61	1.66	2.81	11	0.33	0.34	0.340	
43	27.06.1998	Yuregir - ADANA	6.2	ISL	2.85	4.52	2.02	1.70	13	0.39	0.39	0.390	
44	27.06.1998	Yuregir - ADANA	6.2	KRT	20.00	15.81	1.88	2.37	20	0.24	0.24	0.240	
45	27.06.1998	Yuregir - ADANA	6.2	MRS	27.44	25.02	8.15	13.13	10	0.24	0.32	0.240	
46	27.06.1998	Yuregir - ADANA	6.2	HTY	2.68	4.78	2.55	4.23	30	0.25	0.21	0.250	
47	09.07.1998	AEGEAN SEA	4.6	BRN	2.25	1.43	1.99	1.11	20	0.27	0.28	0.280	
48	17.08.1999	Merkez - KOCAELI	7.4	BRS	9.50	71.64	9.04	8.57	20	0.08	0.10	0.100	
49	17.08.1999	Merkez - KOCAELI	7.4	CEK	14.99	16.59	10.03	7.17	15	0.43	0.40	0.420	
50	17.08.1999	Merkez - KOCAELI	7.4	DZC	52.64	59.53	49.86	36.55	17	0.30	0.35	0.350	
51	17.08.1999	Merkez - KOCAELI	7.4	ERG	20.67	12.80	12.12	8.87	20	0.37	0.37	0.370	
52	17.08.1999	Merkez - KOCAELI	7.4	GBZ	97.09	127.9	15.40	14.20	20	0.39	0.44	0.410	
53	17.08.1999	Merkez - KOCAELI	7.4	GYN	33.92	25.03	10.25	9.05	20	0.29	0.29	0.290	
54	17.08.1999	Merkez - KOCAELI	7.4	IST	9.58	8.59	7.03	5.80	40	0.12	0.11	0.110	
55	17.08.1999	Merkez - KOCAELI	7.4	IZN	17.97	31.68	17.04	27.16	15	0.22	0.27	0.270	
56	17.08.1999	Merkez - KOCAELI	7.4	IZT	92.79	76.22	19.82	28.34	25	0.21	0.22	0.220	
57	17.08.1999	Merkez - KOCAELI	7.4	SKR	-	82.27	-	32.20	40	-	0.26	0.260	
58	17.08.1999	Merkez - KOCAELI	7.4	BLK	6.18	5.63	3.04	3.47	20	0.15	0.13	0.140	
59	17.08.1999	Merkez - KOCAELI	7.4	CNK	10.52	6.39	6.64	5.26	20	0.15	0.15	0.150	
60	17.08.1999	Merkez - KOCAELI	7.4	KUT	9.41	17.15	9.34	15.11	12.5	0.09	0.12	0.105	

Table B.1 Continued.

Data No	Date (dd.mm.yy)	Earthquake Location	M _w *	Station Code	Uncorrected PGV (cm/s)		Corrected PGV (cm/s)		High-Cut Filter Freq. (Hz)		Selected Low-Cut Filter Freq. (Hz)		Selected Low-Cut Filter Freq. (Hz)	
					N-S	E-W	N-S	E-W	40	20	N-S	E-W	N-S	E-W
61	17.08.1999	Merkez - KOCAELI	7.4	ARC	17.43	44.93	8.83	9.49	40	0.17	0.32	0.320		
62	17.08.1999	Merkez - KOCAELI	7.4	ATS	39.92	34.34	28.36	33.64	20	0.15	0.13	0.150		
63	17.08.1999	Merkez - KOCAELI	7.4	BTS	11.81	12.76	11.08	11.47	20	0.10	0.15	0.150		
64	17.08.1999	Merkez - KOCAELI	7.4	DHM	25.33	15.07	15.73	12.04	30	0.14	0.10	0.140		
65	17.08.1999	Merkez - KOCAELI	7.4	BUR	17.87	18.24	16.39	18.35	20	0.12	0.14	0.130		
66	17.08.1999	Merkez - KOCAELI	7.4	FAT	21.00	16.94	13.59	10.24	40	0.17	0.22	0.220		
67	17.08.1999	Merkez - KOCAELI	7.4	HAS	282	397	4.94	14.12	15	0.20	0.23	0.210		
68	17.08.1999	Merkez - KOCAELI	7.4	YPT	88.83	88.71	59.26	55.89	20	0.20	0.15	0.170		
69	17.08.1999	Merkez - KOCAELI	7.4	YKP	8.39	7.51	6.62	3.63	30	0.11	0.17	0.140		
70	17.08.1999	Merkez - KOCAELI	7.4	MCD	7.07	9.97	5.19	7.45	30	0.09	0.11	0.110		
71	17.08.1999	Merkez - KOCAELI	7.4	MSK	7.40	6.54	6.14	5.65	13	0.08	0.12	0.100		
72	17.08.1999	Merkez - KOCAELI	7.4	ZYT	16.96	16.46	14.83	11.73	40	0.16	0.15	0.160		
73	17.08.1999	Merkez - KOCAELI	7.4	ATK	18.89	17.60	11.37	13.94	30	0.15	0.15	0.150		
74	11.11.1999	Merkez - KOCAELI	5.6	SKR	14.72	11.20	14.53	9.66	20	0.27	0.27	0.270		
75	12.11.1999	Merkez - DUZCE	7.2	BOL	57.78	66.60	52.57	66.56	30	0.23	0.15	0.200		
76	12.11.1999	Merkez - DUZCE	7.2	DZC	66.47	90.78	35.99	56.64	30	0.30	0.29	0.300		
77	12.11.1999	Merkez - DUZCE	7.2	GYN	9.84	8.68	1.33	1.41	20	0.43	0.47	0.450		
78	12.11.1999	Merkez - DUZCE	7.2	IZN	4.74	11.07	2.05	1.64	30	0.24	0.24	0.240		
79	12.11.1999	Merkez - DUZCE	7.2	IZT	16.31	11.89	1.29	1.26	30	0.19	0.24	0.240		
80	12.11.1999	Merkez - DUZCE	7.2	KUT	5.69	10.21	5.09	9.92	12.5	0.050	0.100	0.075		
81	12.11.1999	Merkez - DUZCE	7.2	MDR	17.68	32.09	6.81	3.98	15	0.44	0.34	0.440		
82	12.11.1999	Merkez - DUZCE	7.2	SKR	4.81	5.17	1.70	2.05	25	0.20	0.20	0.200		
83	12.11.1999	Merkez - DUZCE	7.2	ATS	9.45	7.53	5.70	5.15	11	0.17	0.17	0.170		
84	12.11.1999	Merkez - DUZCE	7.2	FAT	4.46	3.63	3.72	2.19	20	0.20	0.21	0.210		
85	12.11.1999	Merkez - DUZCE	7.2	HAS	161.25	50.54	4.29	2.23	20	0.20	0.22	0.220		
86	12.11.1999	Merkez - DUZCE	7.2	YPT	4.22	9.13	2.20	1.67	18	0.36	0.38	0.380		
87	06.06.2000	Cerkes - CANKIRI	6.0	CER	8.50	7.09	7.89	5.73	30	0.16	0.19	0.190		
88	23.08.2000	Akyazi - SAKARYA	5.2	AKY	16.87	18.41	15.76	17.69	13	0.26	0.26	0.260		
89	23.08.2000	Akyazi - SAKARYA	5.2	DZC	1.41	1.99	1.01	0.90	23	0.59	0.69	0.690		
90	23.08.2000	Akyazi - SAKARYA	5.2	IZN	2.93	1.91	2.81	1.98	13	0.31	0.29	0.310		

Table B.1 Continued.

Data No	Date (dd.mm.yy)	Earthquake Location	M _w *	Station Code	Uncorrected PGV (cm/s)		Corrected PGV (cm/s)		High-Cut Filter Freq. (Hz)	Selected Low-Cut Filter Freq. (Hz)		Selected Low-Cut Filter Freq. (Hz)	Selected Low-Cut Filter Freq. (Hz)	
					N-S	E-W	N-S	E-W		N-S	E-W		N-S	E-W
91	23.08.2000	Akyazi - SAKARYA	5.2	SKR	1.57	1.56	0.60	0.60	25	0.74	0.85	0.800	0.800	
92	04.10.2000	Merkez - DENIZLI	5.0	DNZ	1.64	2.45	1.29	1.23	25	0.42	0.63	0.630	0.630	
93	15.11.2000	Tatvan-VAN	5.5	VAN	1.53	1.05	0.79	0.75	13	0.14	0.33	0.330	0.330	
94	10.07.2001	Pasinler - ERZURUM	5.4	ERZ	2.38	2.34	3.32	1.77	20	0.27	0.45	0.450	0.450	
95	26.08.2001	Yigilca - DUZCE	5.0	BOL	3.47	1.85	3.23	2.02	20	1.49	1.51	1.500	1.500	
96	02.12.2001	Merkez - VAN	4.8	VAN	1.89	1.20	1.38	0.95	25	0.92	1.03	0.920	0.920	
97	03.02.2002	Sultandagi - AFYON	6.5	AFY	25.93	42.04	11.77	7.82	13	0.22	0.36	0.360	0.360	
98	03.02.2002	Sultandagi - AFYON	6.5	KUT	3.02	4.34	2.52	3.23	20	0.17	0.33	0.330	0.330	
99	03.04.2002	Basmakci - ISPARTA	4.2	BRD	1.12	0.84	0.77	0.51	30	1.40	1.84	1.840	1.840	
100	14.12.2002	Sumbas - OSMANIYE	4.8	AND	2.27	1.30	1.96	1.29	25	1.16	1.30	1.300	1.300	
101	10.03.2003	Akyazi - SAKARYA	4.0	AKY	0.94	0.91	0.67	1.04	30	0.93	1.12	1.000	1.000	
102	10.04.2003	Seferhisar - IZMIR	5.7	BRN	6.21	3.98	6.11	3.14	20	0.34	0.48	0.480	0.480	
103	01.05.2003	Merkez - BINGOL	6.3	BNG	37.04	21.73	31.22	17.97	40	0.33	0.19	0.330	0.330	
104	21.05.2003	Cumayeri - DUZCE	4.4	DZC	1.12	0.97	0.61	0.86	25	0.78	1.10	1.100	1.100	
105	09.06.2003	Bandirma - BALIKESIR	4.8	BND	2.55	2.48	2.09	1.61	30	0.46	0.55	0.550	0.550	
106	06.07.2003	Bandirma - BALIKESIR	4.8	CNK	2.82	3.16	2.32	1.82	25	0.57	0.56	0.570	0.570	
107	23.07.2003	Buldani - DENIZLI	5.3	DAT1	5.16	4.69	4.19	3.69	40	0.55	0.74	0.740	0.740	
108	23.07.2003	Buldani - DENIZLI	5.3	DNZ	1.89	2.26	0.63	1.12	35	0.50	0.72	0.720	0.720	
109	26.07.2003	Buldani - DENIZLI	4.9	DAT1	1.56	1.12	1.31	1.27	40	0.42	0.45	0.420	0.420	
110	26.07.2003	Buldani - DENIZLI	5.4	DAT1	5.32	4.13	3.71	3.48	40	0.64	0.64	0.640	0.640	
111	26.07.2003	Buldani - DENIZLI	5.4	DNZ	1.76	1.65	1.17	1.67	40	0.47	0.44	0.470	0.470	
112	26.07.2003	Buldani - DENIZLI	4.9	DAT1	2.21	1.40	0.81	0.84	20	0.51	0.45	0.510	0.510	

APPENDIX C

Table C.1 Coefficients for the studied prediction equations and comparison of model adequacy and unbiased estimator.

Joyner & Boore (1981)	Original Form					RSS 1E+05	R² -3.08	σ_{logPGV} 0.39			
	C1	C2	C3	C4	C5						
	-0.670	0.489	4.000	-0.0026	0.170						
Sabetta & Pugliese (1996)	Original Form				RSS 25634	R² -0.05	σ_{logPGV} 0.34				
	C1	C2	C3	C4							
	-0.710	0.455	3.600	0.133							
Tromans & Bommer (2002)	Original Form						RSS 9234	R² 0.62	σ_{logPGV} 0.32		
	C1	C2	C3	C4	C5	C6					
	0.003	0.356	-1.058	6.060	0.138	0.280					
Pankow & Pechmann (2004)	Original Form					RSS 17694	R² 0.28	σ_{logPGV} 0.36			
	C1	C2	C3	C4	C5						
	2.252	0.490	-1.196	7.060	0.195						
Akkar & Bommer (2006)	Original Form								RSS 6012	R² 0.75	σ_{logPGV} 0.36
	C1	C2	C3	C4	C5	C6	C7	C8			
	-1.260	1.103	-0.085	-3.103	0.327	5.504	0.079	0.226			
Joyner & Boore (1981)	Modified Form According to the Database					RSS 7615	R² 0.69	σ_{logPGV} 0.38			
	C1	C2	C3	C4	C5						
	0.323	0.297	9.752	0.00200	0.316						
Sabetta & Pugliese (1996)	Modified Form According to the Database				RSS 7464	R² 0.69	σ_{logPGV} 0.39				
	C1	C2	C3	C4							
	0.357	0.303	11.696	0.320							
Tromans & Bommer (2002)	Modified Form According to the Database						RSS 3624	R² 0.85	σ_{logPGV} 0.32		
	C1	C2	C3	C4	C5	C6					
	-1.409	0.442	-0.542	0.234	0.121	0.454					
Pankow & Pechmann (2004)	Final Form After Database Elimination					RSS 2320	R² 0.86	σ_{logPGV} 0.32			
	C1	C2	C3	C4	C5						
	-0.691	0.396	-0.756	5.299	0.174						
Akkar & Bommer (2006)	Final Form After Database Elimination								RSS 2988	R² 0.82	σ_{logPGV} 0.35
	C1	C2	C3	C4	C5	C6	C7	C8			
	2.061	0.371	-0.958	11.019	0.309						
Akkar & Bommer (2006)	Modified Form According to the Database								RSS 3415	R² 0.86	σ_{logPGV} 0.33
	C1	C2	C3	C4	C5	C6	C7	C8			
	-5.415	1.614	-0.085	0.058	-0.085	0.238	0.111	0.443			
Joyner & Boore (1981)	Final Form After Database Elimination								RSS 2299	R² 0.86	σ_{logPGV} 0.32
	C1	C2	C3	C4	C5	C6	C7	C8			
	-2.921	1.204	-0.067	-1.162	0.05	7.183	0.2	0.359			

RSS : Residual sum of squares

R² : Coefficient of determination

σ_{logPGV} : Standard deviation for the expression

APPENDIX D

Table D.1 Earthquake information for the Gemlik earthquake

Date (dd.mm.yy)	Event	Earthquake Location	Faulting Type	Seismic M. M ₀ (dyne.cm)	M _w	Depth (km)	Epicenter Coordinates	Number of Recordings Rock Stiff Soil
24.10.2006	GEMLIK	Gulf of Gemlik	Strike-Slip	N/A	5.2	15.1	40.4200 N - 29.0400 E	1 5 2

Table D.2 Station information for the Gemlik earthquake

Data No	Station Location	Station Structure	Station Coordinates	Owner	Epi. Dist. (km)	r _{cl} (km)	V _{s30} (cm/s)	Local Geology	Peak Ground Acc. (g) NS EW Ver.
1	BURSA	Köy Hizmetleri	40.1820 N - 29.1300 E	ERD	36.0	36.0	366	Stiff Soil	0.037 0.028 0.014
2	BURSA	Afet Yön. Mer.	40.2260 N - 29.0750 E	ERD	37.0	37.0		Rock	0.077 0.037 0.034
3	BURSA	Kurtul Koyu	40.3630 N - 29.1220 E	ERD	19.0	19.0	339	Stiff Soil	0.159 0.180 0.086
4	BURSA	Gemlik Askeri Vet. Okulu	40.3940 N - 29.0980 E	ERD	5.0	5.0	279	Soil	0.177 0.206 0.089
5	BURSA	Umurbey	40.4100 N - 29.1800 E	ERD	25.0	25.0	300	Stiff Soil	0.070 0.100 0.033
6	BURSA	Gemlik End. Mes. Lis.	40.4250 N - 29.1670 E	ERD	22.0	22.0	274	Soil	0.066 0.095 0.036
7	BURSA	Cargil Fabrikası	40.4220 N - 20.2910 E	ERD	36.0	36.0	462	Stiff Soil	0.030 0.045 0.016
8	YALOVA	Doğuş Et Fabrikası	40.5640 N - 29.3060 E	ERD	33.0	33.0		Stiff Soil	0.028 0.029 0.016

Table D.3 Filter choices and PGV properties of the Gemlik earthquake

Data No	Station Code	Uncorrected PGV (cm/s) E-W	Selected High-Cut Filter Freq. (Hz) N-S	Selected Low-Cut Filter Freq. (Hz) E-W	Selected Low-Cut Filter Freq. (Hz) for both comp.	Corrected PGV (cm/s) N-S	PGV (observed) (cm/s) E-W	PGV (predicted) (cm/s)
1	BYT01	1.33	25.00	0.13	0.19	1.29	1.29	2.06
2	BYT02	4.29	25.00	0.20	0.31	4.05	4.05	1.28
3	BYT04	7.24	25.00	0.69	0.69	6.92	6.92	3.54
4	BYT05	8.72	40.00	0.10	0.10	8.79	10.06	11.03
5	BYT06	3.62	35.00	0.22	0.22	3.62	5.49	2.85
6	BYT07	3.35	35.00	0.44	0.44	3.31	5.13	4.55
7	BYT08	1.81	35.00	0.50	0.50	1.84	2.69	2.07
8	BYT11	1.00	35.00	0.51	0.51	0.95	1.61	2.23